Revised greenhouse scenarios for exposure of aquatic organisms to plant protection products

Soil-bound crops in greenhouses

F. van den Berg, R.F.A. Hendriks, J.J.T.I. Boesten, W. Voogt, A. Tiktak, M. Mandryk and M. Braakhekke

WAGENINGEN
UNIVERSITY & RESEARCH

Revised greenhouse scenarios for exposure of aquatic organisms to plant protection products

Soil-bound crops in greenhouses

F. van den Berg[1], R.F.A. Hendriks[1], J.J.T.I. Boesten[1], W. Voogt[2], A. Tiktak[3], M. Mandryk[4] and M. Braakhekke[1]

1 WENR, Wageningen Environmental Research
2 Wageningen UR, Greenhouse Horticulture
3 PBL, Netherlands Environmental Assessment Agency
4 Ctgb, Board for the Authorisation of Plant Protection Products and Biocides

This research was conducted by Wageningen Environmental Research (WENR) and funded by the Dutch Ministry of Economic Affairs (or name a different financial source) (project number BO-43-102.01-006).

Wageningen Environmental Research
Wageningen, February 2022

Reviewed by:
Dr E.L. Wipfler (WENR), senior research scientist

Approved for publication:
Dr W.B. Buddendorf (ERA)

Report 3151
ISSN 1566-7197

WAGENINGEN
UNIVERSITY & RESEARCH

F. van den Berg, R.F.A. Hendriks, J.J.T.I. Boesten, W. Voogt, A. Tiktak, M. Mandryk and M. Braakhekke, 2022. *Revised greenhouse scenarios for exposure of aquatic organisms to plant protection products; Soil-bound crops in greenhouses.* Wageningen, Wageningen Environmental Research, Report 3151. 96 pp.; 63 fig.; 16 tab.; 21 ref.

In 2016 a greenhouse scenario for soil-bound crops has been adopted in the Dutch authorisation procedure for plant protection products to assess the exposure of aquatic organisms. However, two important shortcomings resulting from the parameterisation of the surface water scenario were discovered. These were due to the assumption of an exact repetition of the irrigation scheme for a fully-grown chrysanthemum crop and that of a top layer with a well-developed macropore system. The first assumption resulted in an extreme sensitivity of the exposure concentration to the application date and the second assumptions was considered unrealistic, because the soil in the greenhouse is frequently ploughed. The above two issues were addressed in the revised exposure scenario presented in this report. The first important improvement was the division of the greenhouse into 24 cultivation sections with a description of the sequence and growth development of all crop cycles in each cultivation section. The second shortcoming was remedied by the change of the topsoil layer with a well-developed macropore system into a topsoil layer without macropores. The target concentration for the assessment of the exposure in surface water strongly depends on the half-life of the substance in the greenhouse soil. Should data on the DegT50 obtained from measurements in greenhouse soils not be available, we recommend to apply provisionally the same factor as included in the tiered assessment scheme proposed by Wipfler et al. (2014), i.e. multiplying the DegT50 value derived from measurements in field soils by a factor 10. The new version of the Greenhouse Emission model (GEM) contains the option to specify an application day relative to the date of planting or harvest. If the GAP (Good Agricultural Practice) of a plant protection product specifies a number of applications per crop cycle, this option should be used. If the GAP specifies a number of applications per year, the application option to specify an absolute date should be selected. For the selection of the application date resulting in the required percentile of the PEC90 in surface water, we recommend an update of the SAFE (Select Application For Evaluation) tool. Suggestions are made to increase the validation status of the model and for the further development and use of the GEM model within the EU.

Keywords: chrysanthemum, cut-flowers, exposure scenario, greenhouse, groundwater, macropores, pesticide fate model, plant protection product, surface water, soil-bound crops

The pdf file is free of charge and can be downloaded at https://doi.org/10.18174/564926 or via the website www.wur.nl/environmental-research (scroll down to Publications – Wageningen Environmental Research reports). Wageningen Environmental Research does not deliver printed versions of the Wageningen Environmental Research reports.

Wageningen Environmental Research Report 3151 | ISSN 1566-7197

Photo cover: J.J.T.I. Boesten

Contents

Verification

Report: 3151
Project number: BO-43-011-01-006

Wageningen Environmental Research (WENR) values the quality of our end products greatly. A review of the reports on scientific quality by a reviewer is a standard part of our quality policy.

Approved reviewer who stated the appraisal,

position: senior research scientist (WENR)

name: Dr E.L. Wipfler

date: 21 January 2022

Approved team leader responsible for the contents,

name: Dr W.B. Buddendorf (ERA)

date: 14 February 2022

Preface

In 2016 the GEM model has been adopted to assess the risks of leaching to groundwater and to assess the exposure of aquatic organisms to plant protection products as a result of discharge of drain water containing plant protection products from greenhouses with soil-bound cultivations. For these assessments a surface water scenario and a groundwater scenario were developed. Unfortunately, some shortcomings in these scenarios were discovered about a year after the introduction of the GEM model. The Ministry of Agriculture, Nature and Food Quality decided to ask for a repair of these shortcomings in the scenarios and deliver a new version of the GEM model facilitating the application of these revised scenarios.

This report describes the modifications in the surface water and groundwater scenarios. These modifications are related to the irrigation management, the description of the crop development and the description of the macroporous system in the greenhouse soil. These new scenarios are implemented in the new version of the GEM model, i.e. version 4.4.3.

Samenvatting

In 2014 hebben Wipfler et al. een kasscenario geselecteerd en geparameteriseerd voor de beoordeling van de blootstelling van waterorganismen. Sinds 2016 wordt dit scenario gebruikt in de toelatingsprocedure voor de beoordeling van gewasbeschermingsmiddelen in Nederland. Dit kasscenario was geselecteerd op basis van simulaties voor relevante kassen met grondgebonden teelten in Nederland. In totaal werden 12 kastypen in beschouwing genomen. Er waren echter tekortkomingen in de parameterisatie van dit scenario. Ten eerste was de blootstellingsconcentratie extreem gevoelig voor de toedieningsdatum. Dit was het gevolg van de herhaling van precies hetzelfde irrigatieschema voor elk jaar met een volledig ontwikkeld chrysantgewas gedurende het gehele jaar, zoals dat was aangenomen in het scenario. Een ander belangrijk punt was de aanname dat in de toplaag een goed-ontwikkeld macroporiesysteem aanwezig was. Dit werd later als niet-realistisch beoordeeld, aangezien de grond in de kas vaak geploegd wordt.

De bovenstaande items werden aangepakt in het herziene scenario dat in dit rapport wordt beschreven. De eerste belangrijke verbetering was de verdeling van de kas in 24 teeltvakken. Voor de simulatie van elk teeltvak werd de opeenvolgende reeks van chrysantteelten beschreven, zodat de teeltcycli in een teeltvak een verschillende plantdatum hadden, die daardoor beter bij de realiteit aansluiten dan het volledig ontwikkeld gewas zoals dat in het eerdere scenario was aangenomen. In het herziene scenario is de irrigatie voor elke teelt gekoppeld aan het groeistadium van het gewas. Daarmee was het probleem van de extreme gevoeligheid van de blootstellingsconcentratie voor de toedieningsdatum opgelost. Berekeningen met het herziene scenario lieten zien dat de blootstellingsconcentratie nog wel gevoelig is voor de toedieningsdatum, maar het is beter voorspelbaar en het is voornamelijk gekoppeld aan het seizoensgebonden patroon van de drainage fluxen.

De tweede belangrijke verbetering was de wijziging van de toplaag van de kasgrond met een goed-ontwikkeld macroporie-systeem in een laag zonder macroporiën. In de herziene beschrijving van de kasgrond heeft alleen de ondergrond macroporiën, d.w.z. de grond beneden een diepte van 0.25 m.

Het blootstellingsscenario was geselecteerd op basis van alle 12 relevante kastypen in Nederland. Zoals gebruikelijk in de toelatingsprocedure werd een realistisch worst-case scenario geselecteerd die resulteert in het 90-percentiel van de blootstellingsconcentratie (PEC90) in het oppervlaktewater. De verandering van de bovengrond met macroporiën in een bovengrond zonder macroporiën zou de selectie van de kas voor het scenario beïnvloedt kunnen hebben, aangezien de relatieve kwetsbaarheid van elke kas anders zou kunnen zijn geworden. De selectie van de kas voor het oppervlaktewater scenario werd daarom opnieuw uitgevoerd. Echter, de uitkomst van de selectieprocedure resulteerde niet in een andere keuze voor de kas. De kas met een zware kleigrond met een fluctuerende grondwaterspiegel rond een diepte van 80 cm werd wederom geselecteerd.

Het rapport van Wipfler et al. (2014) beschrijft ook een grondwaterscenario. In het rapport van Wipfler et al. (2014) werd een kas in de Venlo regio geselecteerd. Ook voor het herziene grondwaterscenario werd de procedure voor de selectie van de kas herhaald. Dit keer werd een kas in het Westland gebied geselecteerd. Beide kastypen hebben een licht-zandige grond, maar de fluctuatie van het grondwaterniveau is iets minder voor de kas in het Westland.

Ten einde de juistheid van het herziene oppervlaktewater scenario te kunnen verifiëren zou een kasexperiment nodig zijn om de modelresultaten te kunnen vergelijken met metingen met betrekking tot de hydrologie van de kasgrond en met metingen van concentraties in de bodem en het drainagewater van de toegediende middelen. Aangezien een dergelijke studie niet beschikbaar was, heeft de werkgroep de plausibiliteit van het geselecteerde oppervlaktewater scenario aan de hand van monitoring gegevens over concentraties van tolclophos-methyl in het Bommelerwaard gebied. Bij deze controle werd duidelijk dat, als gebruik gemaakt werd van de waarde voor de DegT50 verkregen in omzettingsstudies met veldgronden, de berekende PEC90 waarden van deze stof veel lager waren dan de gemeten concentraties in de

monitoringsstudie. Wanneer gebruik gemaakt werd van de DegT50 waarde gemeten in kasgronden werd een PEC90 berekend die van dezelfde orde van grootte was als de hoogst gemeten waarden in de monitoringsstudie. Als vervolgstap voor de controle van de juistheid van het herziene oppervlaktewater scenario, bevelen we aan om een protocol uit te werken voor een onderzoek in de kas met een specificatie van de opzet van het experiment en van de uit te voeren metingen.

De doelconcentratie voor de beoordeling van de blootstelling in het oppervlaktewater hangt sterk af van de halfwaardetijd van het middel in de kasgrond. Het is daarom belangrijk om gegevens voor de stof te gebruiken die representatief zijn voor kasgronden. Mochten deze gegevens niet beschikbaar zijn, dan bevelen we aan om vooralsnog dezelfde factor te gebruiken die onderdeel is van het door Wipfler et al. (2014) voorgestelde getrapte beoordelingssysteem. Dat is een vermenigvuldiging met een factor 10 van de DegT50 waarde gemeten in veldgronden. Deze factor zou gebruikt kunnen worden voor de beoordeling van de blootstelling in oppervlaktewater en grondwater voor stoffen waarvoor alleen een DegT50 waarde in veldgronden beschikbaar is. Het meten van de halfwaardetijd in kasgronden zou deel uit kunnen maken van de beoordeling van de blootstelling in een hogere Tier.

Deze nieuwe versie van het Greenhouse Emission model (GEM) heeft de optie om een toedieningsdatum te kiezen relatief ten opzichte van de datum van planten of oogst. Als de GAP (Good Agricultural Practice) van een gewasbeschermingsmiddel het aantal toedieningen aangeeft per teelt, dan dient deze optie te worden gebruikt. Als de GAP het aantal toedieningen per jaar aangeeft, dan dient de optie gekozen te worden waarmee een absolute datum kan worden gespecificeerd. Gezien het seizoensgebonden patroon, kan voor de datum van de laatste toediening in het toedieningsschema het beste een datum rond 1 juli gekozen worden. Dat resulteert dan in een redelijke worst-case schatting van de blootstellingsconcentratie.

Voor een meer nauwkeurige keuze van de toedieningsdatum die resulteert in het gevraagde percentiel van de PEC90 in oppervlaktewater, bevelen wij een update aan van het SAFE (Select Application For Evaluation) instrument. Dit instrument werd ontwikkeld ter ondersteuning van het gebruik van het grondwaterscenario in GEM versie 3.3.2. Het maakt het de gebruiker mogelijk om met het model berekeningen te doen voor een reeks toedieningsdata om vervolgens de toedieningsdatum te kunnen kiezen die de hoogste uitspoelconcentraties geeft. Een vernieuwde versie van dit instrument zou het makkelijker maken om de toedieningsdatum te kiezen die resulteert in een redelijke worst-case schatting van de blootstellingsconcentratie in het oppervlaktewater.

Alhoewel de herziene scenario's ontwikkeld en getest zijn voor chrysant (snijbloemen), kunnen deze gebruikt worden voor alle grondgebonden gewassen die geteeld worden in Nederlandse kassen. Desalniettemin, in het geval van radijs (een ander belangrijk grondgebonden gewas in de kas in Nederland), zou de mate van bescherming van de scenario's ter discussie gesteld kunnen worden. De reden is dat radijs geteeld wordt in kasgronden met een veel lager organisch-stofgehalte. Aan de andere kant zijn de irrigatiegiften bij radijs lager. Wij bevelen daarom aan om gegevens te verzamelen over de praktijk bij de teelt van radijs en om de mate van bescherming van het kasscenario ook voor radijs te verifiëren.

Het kasscenario in dit rapport werd ontwikkeld om milieurisico's als gevolg van het gebruik van gewasbeschermingsmiddelen in Nederlandse kassen te kunnen beoordelen. Echter, het GEM model zou een nuttig instrument kunnen zijn voor de risicobeoordeling van de toediening van gewasbeschermingsmiddelen in andere kassystemen in de EU. Aanbevolen wordt om te onderzoeken wat de omvang van de teelt en karakteristieken zijn van grondgebonden gewassen als ook teeltpraktijken in andere EU landen. Dergelijke informatie zou helpen in het identificeren van gebieden waarvoor additionele blootstellingsscenario's ontwikkeld dienen te worden.

Summary

In 2014, Wipfler et al. selected and parameterised a greenhouse scenario for the exposure assessment of aquatic organisms. Since 2016 the scenario has been used in the authorisation procedure of plant protection products in the Netherlands. This greenhouse scenario was selected based on results of simulations for relevant greenhouses with soil-bound crops in the Netherlands. In total 12 greenhouse types were considered. There were, however, shortcomings resulting from the parameterisation of this scenario. Firstly, there was an extreme sensitivity of the exposure concentration to the application date. This was due to the exact repetition of the irrigation scheme for a fully-grown chrysanthemum crop throughout the year as assumed in the scenario. Another important issue was the assumption that the top layer contained a well-developed macropore system. This was later considered unrealistic, because the soil in the greenhouse is frequently ploughed.

The above two issues were addressed in the revised exposure scenario presented in this report. The first important improvement was the division of the greenhouse into 24 cultivation sections. The sequence of chrysanthemum crops in the simulation of each cultivation section was described, so the crop cycles in a cultivation section have different planting dates, which is closer to reality than the fully-grown crop assumed in the earlier scenario. In the revised scenario, irrigation is linked to the crop development stage of the crop in each crop cycle. This resolved the problem of the extreme sensitivity of the exposure concentration to the application date. Calculations with the revised irrigation scheme showed that the exposure concentration is still sensitive to the application date, but it has become more predictable and is primarily linked to the seasonal pattern of drainage fluxes.

The second important improvement was the change of the topsoil layer with a well-developed macropore system into a layer without macropores. In the revised description of the greenhouse soil, only the subsoil, so the soil below a depth of 0.25 m, contains macropores.

The exposure scenario was selected from simulations for all 12 relevant greenhouse types in the Netherlands. As usual in regulatory practice, a realistic worst-case scenario corresponding to the 90th-percentile exposure concentration (PEC90) in surface water was selected. The change of the topsoil with macropores into a topsoil without macropores could have affected the greenhouse selection for the scenario, because the relative vulnerability of each greenhouse might have changed. The selection of the greenhouse for the surface water scenario was therefore redone. However, the outcome of this selection procedure did not result in a change of the selected greenhouse. The greenhouse with a heavy clay soil and fluctuating groundwater level at around 80 cm depth was selected again.

The report by Wipfler et al. (2014) also presents a groundwater scenario. In the report of Wipfler et al. (2014), a greenhouse in the Venlo area was selected. For the revised groundwater scenario too, the selection procedure was redone. This time the greenhouse in the Westland area was selected. Both greenhouses have a light sandy soil, but the fluctuation in groundwater level is somewhat less in the Westland greenhouse.

To check the validity of the revised surface water scenario, a greenhouse experiment would be needed to check the model output against measurements on the soil hydrology and concentrations of the substances applied in the soil and in the drainage water. In the absence of such a study, the working group tested the plausibility of the selected surface water scenario using monitoring data on surface water concentrations of tolclophos-methyl in the Bommelerwaard area. From this check, it became clear that when using the DegT50 value obtained from studies with field soils, the PEC90 concentrations calculated were much lower than those measured in the monitoring study. When using the value for the DegT50 obtained from studies with greenhouse soils, the resulting PEC90 concentrations were of the same order as the highest values measured in the monitoring study. As a next step to check the validity of the revised surface water scenario, we recommend to develop a protocol for a greenhouse study with a specification of the experimental design and a specification of the measurements to be made.

The target concentration for the assessment of the exposure in surface water strongly depends on the half-life of the substance in the greenhouse soil. Therefore, it is important to use data on substance properties that are representative for greenhouse soils. Should this data not be available, we recommend to apply provisionally the same factor as included in the tiered assessment scheme proposed by Wipfler et al. (2014), i.e. multiplying the DegT50 value derived from measurements in field soils by a factor 10. This factor could be used in the surface water and groundwater exposure assessments for substances for which only DegT50 values for field soils are available. The measurement of the half-life in greenhouse soils could be part of the exposure assessment at a higher tier.

This new version of the Greenhouse Emission model (GEM) contains the option to specify an application day relative to the date of planting or harvest. If the GAP (Good Agricultural Practice) of a plant protection product specifies a number of applications per crop cycle, this option should be used. If the GAP specifies a number of applications per year, the application option to specify an absolute date should be selected. Given the seasonal pattern, the date of the last application in the application scheme can best be set at around the 1st of July. This would result in a reasonable worst-case estimate of the exposure concentration.

For a more accurate selection of the application date resulting in the required percentile of the PEC90 in surface water, we recommend an update of the SAFE (Select Application For Evaluation) tool. This tool has been developed to support the use of the groundwater scenario in GEM version 3.3.2. It enables the user to run the model for a range of application dates and then select the application date with the highest leaching concentration. An update of this tool would make it easier to select the application date resulting in a reasonable worst-case estimate of the exposure concentration in surface water.

Although developed and tested for chrysanthemum (cut flowers), the revised scenarios can be used for all soil-bound crops that are grown in Dutch greenhouses. However, in the case of radish (another important soil-bound greenhouse crop in the Netherlands), the protectiveness of the scenarios can be questioned. The reason is that radish is grown in soil with a much lower organic matter content. On the other hand, irrigation amounts in radish are lower. We therefore recommend to collect data on cultivation practices in radish and to check the protectiveness of the greenhouse scenario also for radish.

The greenhouse scenarios presented in this report have been developed to assess the environmental risks due to the use of pesticides in Dutch greenhouses. However, the GEM model could be a useful tool for the risk assessment of the application of plant protection products in other greenhouse systems in the EU. Therefore, it is recommended to investigate the extent and characteristics of soil-bound crops as well as the cultivation practices in other EU countries. Such information would assist in identifying areas where additional exposure scenarios need to be developed.

1 Introduction

In protected cropping systems in the Netherlands plant protection products are used to safeguard the crop yield. Since 2016, the software tool GEM is used to evaluate the exposure of aquatic organisms and groundwater to plant protection products. Unfortunately, some shortcomings have been discovered in the surface water scenario (chrysanthemums) which is used in the risk assessment for soil-bound crops. The outcome of the surface water assessment was found to be very sensitive to the date of application. Detailed analysis of this problem has shown that the irrigation regime in the scenario was too simple. It was assumed that the irrigation regime was repeated every year, so drain flow events occurred on the same day every year. Moreover, the assumption of permanent macropores in the topsoil turned out to be incorrect, since soil cultivation events such as ploughing the topsoil occur several times a year. Furthermore, it was assumed that the soil cover of the crop (and thus plant interception of the plant protection product) was constant in time which is not realistic as the chrysanthemums start as tiny plants. It was therefore concluded that the scenario to assess the drainage to surface water via drains needed to be improved by taking differences in irrigation amounts over the years and the absence of macropores in the topsoil into account and describe the development of the crop more accurately.

More data on irrigation and crop cycles were collected from greenhouses with a chrysanthemum cropping system. The modifications in the cropping system are described in Chapter 2 and the new irrigation scenario is described in Chapter 3. The parameterisation of the soil in the greenhouse cropping system was improved by considering the topsoil to be no longer containing a macropores system. These improvements as well as the modifications required in the hydrological model SWAP are described in Chapter 4. The changes in the PEARL model as required by these changes are described in Chapter 5. Because these changes in the description of the hydrology in the greenhouse soil and those related to the processes describing the transport of substance in the soil could result in a different vulnerability compared to the other representative greenhouses as defined by Wipfler et al. (2014), the procedure to select the greenhouse generating the 90^{th} percentile target concentration in surface water and groundwater was repeated. The set-up and results of the selection procedure is presented in Chapter 6. The results of assessments for example compounds as well as those on the effect of the changes in the scenario on the target output as obtained for the revised surface water scenario as well as a comparison of the outcome of calculations for tolclofos-methyl with monitoring data is presented in Chapter 7. In Chapter 8 the results of computations to assess the sensitivity of the target peak surface water concentration to changes in the application day are presented. In Chapter 9 issues are discussed in relation to selection of the application date as well as the use of the new application option for the revised scenario to specify a date relative to the day of planting or the day of harvest. In Chapter 10, the conclusions are listed and recommendations are proposed for a follow-up.

2 Revised description of cropping system

2.1 Introduction

In the current scenario it is assumed that a fully grown crop is present in the greenhouse throughout the year (Wipfler et al., 2014). The consequence of this assumption is that the interception of substance by the crop is no longer a parameter that depends on the crop development, but has a fixed value. The interception percentage for all applications to the crop is set to 50% in GEM version 3.2.2.

In practice, crop cultivation sections with crops in different stages of development are present at any time during the year. In the next paragraph a description is given of the method to take these differences in the crop stage into account.

2.2 Revised description of cropping system

In the greenhouse that has been selected to be representative for the scenario, the length of each chrysanthemum crop cycle has been set at 65 days. This implies that between 5 to 6 crops can be grown in a single year. If a crop cycle starts on Jan 1st, then the 6th crop cycle begins somewhere in November and the plants are harvested in the following year. Furthermore, there are 24 cropping sections in the greenhouse with a shift of two-three days in planting day between two adjacent sections. Right after the harvest of each cultivation section, the next crop will be planted, sometimes the same day, but with a maximum of two days of bare soil. Consequently, the greenhouse surface is continuously fully covered with chrysanthemum plants in all 24 cultivation sections with different cropping stages. As there are 24 different sequences of chrysanthemum crops, with corresponding water and nutrient demands in the greenhouse, there are also 24 different irrigation schemes. Typically greenhouse grown chrysanthemum is characterized by a continuous sequence of crops, so the irrigation amounts and irrigation patterns differ from year to year.

In the greenhouse scenario a warming-up period of 6 years has been adopted, which is followed by an evaluation period of 7 years. Based on outdoor measurements of global radiation, the air temperature, air humidity, both the irrigation amounts and the timing of these amounts for the chrysanthemum cultivations in the greenhouse were calculated using the KASPRO model (Swinkels, 2006). In these calculations a surplus irrigation of 25% was selected as a realistic choice of a conservative irrigation management scenario. This is somewhat lower than the irrigation surplus selected in the scenario developed by Wipfler et al. (2014), where a surplus of 30% was assumed. This decrease is the result of the improvement of the irrigation practised since then. More detailed information on the irrigation scheme is given in Chapter 3. Hourly meteorological data on global radiation were taken from the Rotterdam weather station for the evaluation period of 2000 to 2006. As no hourly data on global radiation were available for the Rotterdam weather station for the warming-up period (1994-1999), hourly data on global radiation were taken from the De Bilt weather station. Although differences in the global radiation between the two weather stations occur, the impact of these differences on the irrigation amounts calculated can be expected to be small. Moreover, these differences occur only during the warming-up period, so they will not have an effect on the hydrology for the evaluation period. Because it was not possible to assess the evapotranspiration (ET_c) for each cultivation section, an average value of the ET_c in the greenhouse was derived. Moreover, according to De Graaf (1981) and Voogt et al. (2000) it can be assumed that the total daily ET_c at all individual cropping stages is equal. Calculated irrigation and derived ETc were used to prepare the input on daily meteorological parameters as required by SWAP and PEARL.

Because an irrigation amount of 3 mm occurs on the first day after the planting day, the crop calendar for chrysanthemum for the whole simulation period (warming-up and evaluation period) for each cultivation

section could be established. The total number of crop cycles in a cultivation section in this period is 70. The development of the crop is assumed to be the same for each crop cycle.

The Leaf Area Index (LAI) as a function of the development stage of the crop is shown in Figure 2.1 (Wageningen UR Greenhouse Horticulture, unpublished measurements). It should be noted that at planting (crop stage = 0) the LAI is 0.3.

In the SWAP version used for GEM 3.2.2, the fraction covered by plants, $f_{c,s}$, was calculated as follows:

$$f_{c,s} = LAI / 3 \qquad \text{Eq 2.1}$$

This simple calculation procedure has been replaced by a more accurate description:

$$f_{c,s} = 1 - \exp(-k_{dif}\ k_{dir}\ LAI) \qquad \text{Eq 2.2}$$

with:
k_{dif} = extinction coefficient for diffuse visible light (-)
k_{dir} = extinction coefficient for direct visible light (-)

The value for k_{dif} is set to 0.6 and that for k_{dir} to 0.75, so the product is 0.45. Based on the LAI data for chrysanthemum, the course with time for the soil cover as calculated with Eq. 2.2 is shown in Figure 2.2.

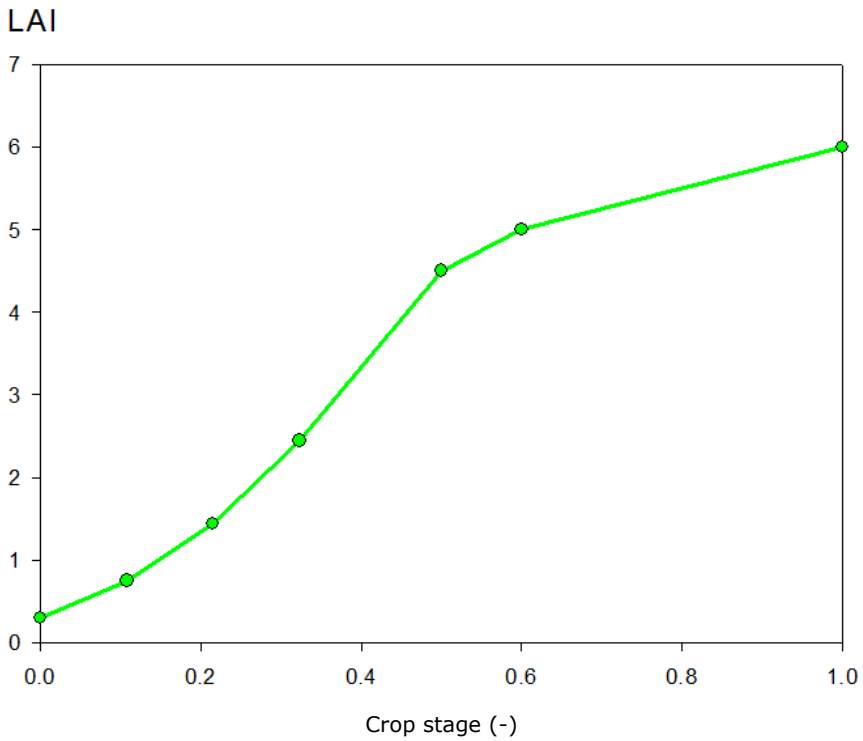

Figure 2.1 *The relation between LAI and crop stage for chrysanthemum*

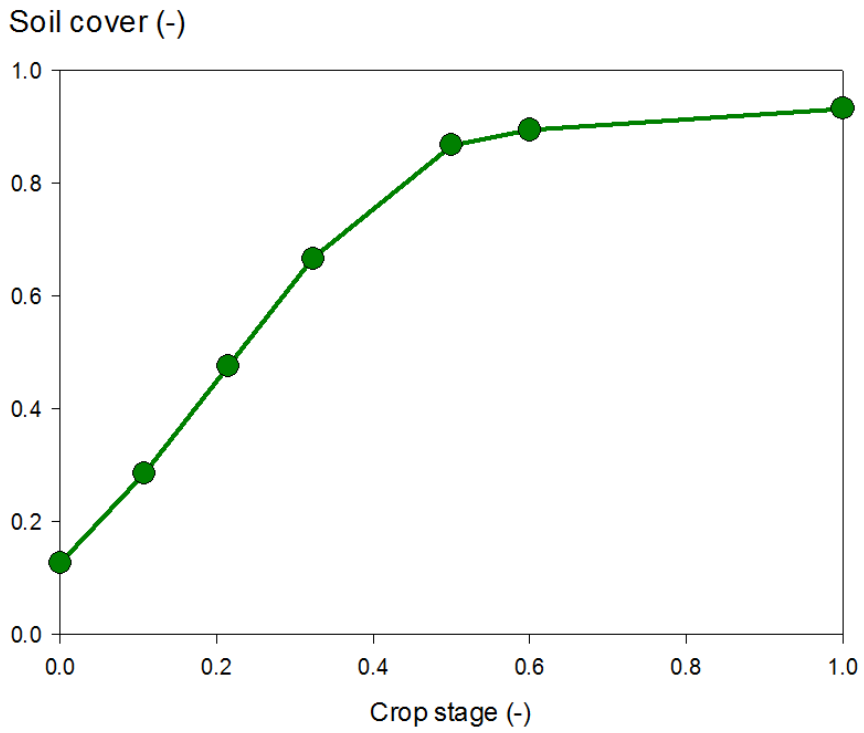

Figure 2.2 *The relation between soil cover and crop stage for chrysanthemum*

The data presented in these figures have been used to describe the crop development. The parameterisation of the crop development is given in Table 2.1. More detailed information on the handling of these crop properties in the SWAP model is given in Kroes et al. (2017)

Table 2.1 *Characteristics of the chrysanthemum crop in the greenhouse*

Crop stage	LAI	Soil cover	Rooting depth (m)	Crop height (m)
0	0.3	0.13	0.04	0.12
0.108	0.75	0.29	0.05	0.18
0.215	1.44	0.48	0.06	0.25
0.323	2.44	0.67	0.09	0.35
0.5	4.5	0.87	0.17	0.55
0.6	5	0.89	0.20	0.64
1	6	0.93	0.30	0.86

2.3 Soil management

For the cultivation of chrysanthemum in the greenhouse, the soil is ploughed by rototillage before each crop cycle over a depth of 15 cm. During the summer months July – August the top soil is disinfected yearly by steam sterilisation. Before disinfection, the soil is ploughed by rototillage over a depth of 25 cm.

2.4 Application of plant protection products in chrysanthemum

The cultivation of chrysanthemum is very intensive, with a relatively short cropping cycle of approximately 65 days and the waiting period between the harvest of a crop and the planting of the next crop that can be as short as a few hours. The sequence is interrupted only by the yearly sterilisation (by steaming) of the soil, then the time between two crops is extended to a few days. On a weekly basis there are five consecutive

plantings carried out. The planted surface within a period of two to three days is grouped together by the grower and considered as a cultivation section, which is controlled individually for all crop management actions (e.g. irrigation, pest control, day-length). Since the whole cropping cycle takes on average 65 days (±3), or 9.2 weeks, the greenhouse is subdivided into 24 distinguishable cultivation sections. As a consequence the crop development stages differ between cultivation sections in the greenhouse. The execution of tasks during the crop cycle, such as fertilisation, irrigation and spraying with plant protection products requires therefore an efficient and well-defined management process. Spraying with plant protection products is limited to periods when the crop surface is dry, a few hours after the last irrigation event. Furthermore, no irrigation will be applied immediately after the application with plant protection products, hence the waiting time between an application and the next irrigation event is at least 24 to 48 hours.

Examples of commonly-used plant protection products in soil-bound cultivations that have been approved or are being evaluated for approval is given in Table 2.2

Table 2.2 *Relevant plant protection products in chrysanthemum, tomatoes, radish and lettuce*

Product	Active Substance (as)	Plague	Crops	Number of applications and interval	g as/ha	Application time
Oberon	Spiromesifen	Greenhouse whitefly (Trialeurodes vaporariorum); Greenhouse red spider mite (Tetranychus urticae)	Ornamental crops	2 per 12 months/ 10 d	120	BBCH 13-89 Jan –Dec
Sanmite 10 SC	Pyridaben	mites	Floriculture crops	1 per 12 months	196	BBCH 11-89 Jan-Dec
			Tree nursery crops	1 per 12 months	140	BBCH 11-89 Jan-Dec
			Perennial cops	1 per 12 months	140	BBCH 11-89 Jan-Dec
Rizolex vloeibaar	Tolclofos-methyl	Rhizoctonia solani /	Head/flowering cabbage, Brussels sprouts, Chinese cabbage, Kohlrabi	1 per crop cycle	2000	BBCH 0 Jan-Dec
			Floriculture (cut flowers)	1 per crop cycle	16000	BBCH 14 Jan-Dec
			Floriculture (pot plants)	1 per crop cycle	250 ml/m^3 soil mixing;100 ml/hL soil drench	BBCH 14-71 Jan-Dec
Vydate 10G	Oxamyl	Nematodes	Floriculture crops, perennials, tree nursery (soil bound)	1 per 12 months	4000	BBCH 0 Jan-Dec
			Floriculture - Pot plants	1 per crop cycle	4 kg /m^3	BBCH 0 Jan-Dec
			Floriculture crops, perennials, tree nursery (hydroponic)	1	4000	Post planting drilling

3 Revised irrigation schemes

3.1 Introduction

The scenario for soil-bound crops in greenhouses as implemented in GEM 3.3.2 is based on the average irrigation for all cultivation sections in the greenhouse. Further, it is assumed that a fully-developed crop is present in the greenhouse throughout the year. In reality crops are grown throughout the year with a length of a crop cycle of about 65 days, so the development stage of the crop changes with time. As the irrigation amount to be applied depends on the greenhouse climate, the soil moisture conditions and the crop development stage, the irrigation scheme for the chrysanthemum crop had to be revised. The approach that has been developed to revise the irrigations scheme is presented in the next paragraph.

3.2 New approach for irrigation schemes

The greenhouse selected for the scenario contains 24 cultivation sections. As the irrigation strategy follows a defined pattern, which is related to the cropping stage, and the irrigation amount depends on the climatic conditions and global radiation level, a procedure was developed to calculate the irrigation amount as a function of the level of global radiation level and the crop growth stage.

3.2.1 Irrigation scheme for the chrysanthemum crop

The irrigation strategy of chrysanthemums follows a certain pattern. At the start of each crop cycle a fixed 3 mm irrigation is applied in combination with a tolclofos-methyl application, except for the first planting right after the steam sterilisation, when no tolclofos-methyl is applied. After this irrigation, irrigation is applied on a regular base, i.e. every second or third day, with irrigation amounts ranging from 5 mm to 16 mm. During the last phase of the crop cycle there is no irrigation to avoid quality depreciation of the flowers.

For the regular irrigation period the irrigation amount applied depends on the cropping stage and environmental factors, such as solar radiation, heating and ventilation. The target irrigation I^*_{std} (mm) amount of chrysanthemum is given by:

$$I^*_{std} = R \cdot I_{std} \qquad \text{Eq. 3.1}$$

in which:
I_{std} = standard irrigation amount (mm per event). Value set to 5.0 mm.
R = radiation and greenhouse climate-dependent factor

The standard irrigation amount is the average irrigation amount per event for the chrysanthemum cultivation. The factor R has been introduced to correct the standard irrigation amount to meet the cumulative calculated crop water demand. This demand is derived from the ET_c, (crop evapotranspiration) and is calculated according to Voogt et al., (2000). R can have three values that are listed in Table 3.1 The value of R on each day is based on the average radiation for the period starting from the preceding day until the 6th day, resulting in a weekly average.

Table 3.1 *Values for the radiation correction factor R for different daily radiation levels*

Level	Radiation (J/cm^2/day)	R (-)
1	< 900	0.8
2	900 – 1500	2.0
3	> 1500	3.2

From day 1 to 54 the actual irrigation amount is equal to the target irrigation amount:

$$I_{act} = I^*_{std}$$ Eq. 3.3

In which:
I_{act}= actual irrigation amount applied (mm)

After each irrigation event, the cumulative crop water demand is reset to zero. The irrigation occurs as soon as the cumulative crop water demand has surpassed $I_{act.}$

From day 53 onwards, no irrigation is applied.

At the end of the crop cycle irrigation is applied to bring the moisture content back to field capacity.

This amount is calculated from:

$$I_{act} = f_{i,s} \cdot I^*_{std}$$ Eq. 3.4

In which:
$f_{i,s}$ = factor for irrigation surplus (-)

In the current parameterisation an irrigation surplus of 25% is assumed, which is equivalent to a value of 1.25 for the parameter $f_{i,s}$.

4 Revised soil hydrology

The soil system in the greenhouse scenario for surface water consists of a clayey soil with a high organic matter content of 13.7% in the top 0.25 m layer. The clay fraction in this soil is 0.225 kg kg^{-1} for the top layer and 0.635 for the subsoil. In this heavy clay soil, a macropore domain has been defined containing permanent macropores down to the depth of the drainage system. More details on the soil system have been given by Wipfler et al. (2014).

During the analysis of the problems in the current parameterisation of the scenario, additional data on the management practices became available. In the cultivation of chrysanthemum in greenhouses the topsoil is ploughed by shallow rototillage (approx. 15 cm) after the harvest of each crop, except for the steam-sterilisation event, when prior to the steaming, deep rototillage is carried out, up to 25 cm. Under such management practices, the existence of permanent macropores can no longer be assumed. Therefore, a study was started to identify an alternative method to describe the hydrology in this soil. An alternative for the current soil profile description could be a topsoil layer without macropores (covering layer cl) and a subsoil with macropores. The description of this alternative is given in the next section.

4.1 Revised description of the soil system

The presence of a covering top layer without macropores can be described using the current concept for macropore geometry. In order to achieve this, one additional parameter is required: the depth in soil corresponding to the top level of the macropore system Z_{top} (cm below soil surface). By introducing Z_{top} the procedure implemented in the hydrological model SWAP sets the upper boundary of the macropore system at that depth. This is visualised in Figure 4.1 that shows the transition from current to revised macropore geometry. In the revised geometry, water can enter the macropores by vertical flow from the saturated matrix covering the macroporous soil layers or by lateral flow from the saturated matrix of these soil layers (see Figure 4.7). The vertical inflow of water into crack-shaped macropores is calculated using an approach from the drainage theory of flow to tile drains:

$$h_{z=\mathrm{bot,cl}} < 0 \quad \rightarrow \quad q_{\mathrm{top,mp}} = 0$$
$$h_{z=\mathrm{bot,cl}} \geq 0 \quad \rightarrow \quad q_{\mathrm{top,mp}} = -\omega_{\mathrm{cl}} \cdot K_{\mathrm{s,top}} \cdot \left[\frac{\partial(h+z)}{\partial z}\right]_{z=\mathrm{bot,cl}} \qquad \text{Eq. 4.1}$$

where:
$q_{top,mp}$ = inflow from the covering layer into the top of macropores (cm d^{-1});
$K_{s,top}$ = isotropic saturated hydraulic conductivity of the covering layer (cm d^{-1});
h_z = soil water pressure head in the soil matrix at depth z (cm);
z = soil depth (negative is downward; cm from soil surface);
$z_{bot,cl}$ = bottom of the covering layer (cm d^{-1});
ω_{cl} = geometry coefficient for flow from covering layer into macroporous layer (-).

This approach assumes an isotropic saturated hydraulic conductivity in the covering layer. The geometry coefficient ω expresses the influence of flow contraction at the interface of the covering layer and the macroporous layer. It is derived from an analogy with the flow of water in soil to tile drains. The relation between the water flux to tile drains and the groundwater heads is expressed by a resistance to flow. For unidirectional vertical water flow, the resistance equals the ratio between the thickness of the layer and the conductivity at saturation. When the water flow converges to point sinks or line sinks, an additional resistance should be accounted for. Following Ernst (1962) in his derivation of a drainage equation that accounts for vertical, horizontal and radial flow components, the coefficient ω can be denoted as (see Annex 2, A2.1 for derivation of geometry factor ω_{cl}):

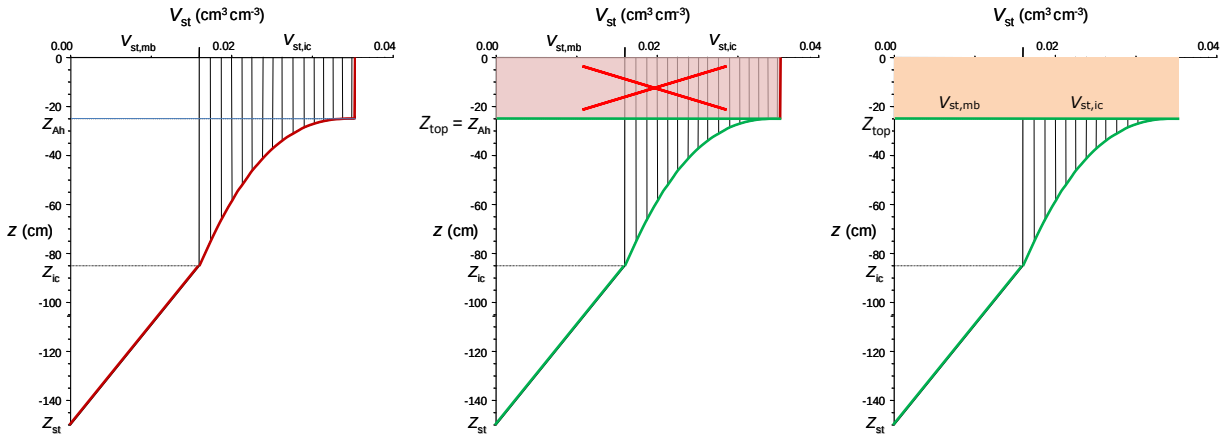

Figure 4.1 *Schematic view of the transition of the macropore geometry from current version to the version with a covering soil layer without macropores in three steps. Left: geometry of a system of static macropores (V_{st}) starting at the soil surface. Centre: removal of the macropore volume between Z_{top} and the soil surface. Right: the revised geometry with a top layer without macropores and below Z_{top} a macropore geometry equal to the original macropore geometry of the soil system. Subscripts mb and ic denote macropores of the Main Bypass and Internal Catchment domains respectively.*

$$\omega = \frac{1}{1+\frac{D_{\mathrm{pol}}}{\pi\frac{1}{2}\Delta z_i} ln\left(\frac{D_{\mathrm{pol}}}{\pi\frac{1}{2}w_{\mathrm{cr}}}\right)+\frac{\left(D_{\mathrm{pol}}\right)^2}{6{\Delta z_i}^2}} \qquad \text{Eq. 4.2a}$$

and

$$w_{\mathrm{cr}} = D_{\mathrm{pol}} \cdot \left(1-\sqrt{1-V_{\mathrm{st}}}\right) \qquad \text{Eq. 4.2b}$$

with:

D_{pol} = diameter of soil polygons in the topsoil layer with macropores (cm);
w_{cr} = width of the macropore cracks in the topsoil layer with macropores (cm);
V_{st} = volume fraction of static macropores in the top layer with macropores in Figure 4.1 (cm³ cm⁻³).

The numerical implementation of equation 4.1 reads:

$$\begin{aligned} &h_{\mathrm{b}} + \tfrac{1}{2}\Delta z_{\mathrm{b}} \leq 0 \;\rightarrow\; q_{\mathrm{top,mp}} = 0 \\ &h_{\mathrm{b}} + \tfrac{1}{2}\Delta z_{\mathrm{b}} > 0 \rightarrow\; q_{\mathrm{top,mp}} = -\omega_{\mathrm{cl}} \cdot K_{\mathrm{s,top}} \cdot \left(\frac{h_{\mathrm{b}}}{\tfrac{1}{2}\Delta z_{\mathrm{b}}}+1\right) \end{aligned} \qquad \text{Eq. 4.3}$$

where h_{b} (cm) and Δz_{b} (cm) are pressure head and thickness of the deepest model compartment of the covering layer, respectively.

If a value for Z_{top} less than zero is put in, then it overrules any input value for parameter Z_{Ah} (ZAHor), because this latter parameter is used in the description of a macroporous soil profile starting at the soil surface (see Figure 4.1, left graph). The volume of static macropores at $z = Z_{\mathrm{top}}$ is set to the value of input parameter VolStaTop (V_{st}) which is in the originally version the static macropore volume at z = zero, the soil surface (see Figure 4.1). This volume is the basis for describing the geometry of deeper macropore volume according to the original concepts in SWAP. Dynamic macropore volume might be added by SWAP when shrinkage, depending on moisture content and inputted shrinkage characteristics, occurs. D_{pol} equals the polygon diameter at the top of the macropore and thus takes the value of DiaPolMin (Table 4.3). See Kroes et al. (2017) for more detailed information on the parameters to describe the macropore system in the soil.

The other parameters that describe macropore geometry have the same meaning as in the original macropore concept. These parameters are the depth of the bottom of the internal catchment domain, Z_{Ica}, the depth of the bottom of the static macropores, ZSta, the fraction of the internal catchment domain at the top of the layer with macropores (Z_{top}), FraIcaTop, and the minimal diameter of soil polygons, DiaPolMin. The adaptations of the interface between the SWAP model and the PEARL model, the 'bfo' output file, are explained in Annex 3.

Another modification to the model is the implementation of boundary pressure head h_e (cm) in all model code where the condition $h \geq 0$ applies In the new version the condition for these processes is changed into $h \geq h_e$. The boundary pressure head resembles the air entry value that marks the boundary capillary height between the soil matrix and the macropores. It has typical values between -1 and -10 cm (Jarvis and Messing, 1995). It was already implemented in SWAP as a modification to the Mualem-VanGenuchten function according to Schaap and Van Genuchten (2006) in order to describe macropore flow in an implicit way. It yields saturated conditions in the matrix for the pressure head range of 0 to h_e. Using it in simulations with the explicit macropore concept in SWAP turned out to give more numerical stability and thus smaller run times. Implementation of the modification described here implies that the explicit and implicit concepts for boundary pressure head-dependent processes are consistent.

Simulations with the new functionality 'covering soil layer without macropores' pointed out that at times with strong breakthrough from the covering soil layer into the macropores the simulated groundwater level tended to oscillate with amplitudes in the order of decimetres (see Annex 2.2). Originally, the groundwater level in SWAP is calculated as the elevation head at which pressure head h amounts to 0 cm. For this purpose, SWAP interpolates linearly between the two adjacent nodes with negative and positive pressure head. In order to damp oscillations in groundwater level calculations in case of macropore flow, a new approach is implemented in SWAP in which groundwater level is determined as the arrhythmic average of the elevation heads at h = -1 cm and h = 1 cm. These two elevation heads are found in a similar way as the original groundwater level elevation head by linear interpolation between two relevant adjacent nodes. This modification yields a smooth course of the simulated groundwater level (see Annex 2, A2.2).

A more detailed evaluation of the input of the original GEM 332 scenario pointed out that some of the included pedotransfer functions (ptf) were not implemented correctly. In the ptf for the calculation of the shrinkage characteristics of the clay layers, mass fractions of clay and organic matter of the soil were used instead of mass-%. In the implementation of the ptf to calculate VolStaTop, the value was rounded off to two decimals, whereas four decimals would give more accurate results. Therefore, an alternative GEM 332 scenario was defined with a corrected implementation of both ptf.

4.2 Comparison of parameterisation of scenarios with original and revised macropore flow

In the following two sections different sets of scenario parameterisations are defined and their results are compared. In Section 4.2.1, the original GEM 332 scenario, with the original macropore concept, is compared with the same scenario but with corrected implementation of pedotransfer functions (ptf). In Section 4.2.2, the GEM 332 New Top Layer (New TL) macropore concept (with corrected ptf) is explained and compared with the GEM 332 scenario with corrected ptf. The parameterisation used in the comparison is based on greenhouse 5 as presented in Wipfler et al. (2014).

4.2.1 Comparison of the GEM 332 surface water scenario with originally and corrected implementation of pedotransfer functions

The descriptions of the original surface water scenario for soil-bound cultivations and that for the same scenario but with corrected implementation of the pedotransfer functions are given in Table 4.1

Table 4.1 *Description of the two GEM 332 scenarios run with the original macropore concept*

Scenario	Description
GEM 332	Simulation with the original PEARL macropore option with macropores fed by precipitation and irrigation at soil surface, using the original implemented pedotransfer functions (ptf)
GEM 332 ptf corrected	As GEM 332 but with corrected pedotransfer functions (ptf) for calculation of VolStaTop and the shrinkage parameters ShrParA and ShrParB per soil layer

4.2.1.1 Model input

Table 4.2 presents the hydraulic functions of the two distinguished soil layers of the GEM 332 scenario in terms of the values of the Mualem-VanGenuchten parameters. These values are the same for both scenarios as the scenarios only differ in the values of the two ptf (Table 4.1).

Table 4.2 *Values of the Mualem-VanGenuchten-parameters of the soil layers in the greenhouse soil for the GEM 332 scenarios*

Scenario	Layer depth (cm)	θ_r (cm^3/cm^3)	θ_{sat} (cm^3/cm^3)	α (1/cm)	n (-)	Ksat,fit (cm/d)	l (-)	α_w (1/cm)	H_{ent} (cm)	Ksat,exm (cm/d)
GEM 332 &	0 -25	0.01	0.53	0.0242	1.28	81.28	-1.476	0.0242	0.0	-
ptf corrected	25-500	0.00	0.57	0.0194	1.089	4.37	-5.955	0.0194	0.0	-

Table 4.3 shows the values of the input parameters to describe the macropore geometry in the original GEM 332 scenario. The table also gives the corrected ptf values.

Table 4.3 *Overview of macropore parameter values for the description of greenhouse soil in the original GEM 332 scenario (incorrect ptf values in bold) and the corrected ptf values in scenario GEM 332 ptf corrected*

Scenario	PEARL input parameter	SWAP input parameter	Value	Unit	Description
GEM 332	ZAHor	Z_AH	30	cm	Depth bottom A-horizon
Original	ZIca	Z_IC	69.59	cm	Depth bottom Internal Catchment (IC) domain
	ZSta	Z_ST	139.19	cm	Depth bottom Static macropores
	VolStaTop	**VLMPSTSS**	**0.07**	**cm3/cm3**	**Volume of Static Macropores at depth Z_{top}**
	FraIcaTop	PPICSS	0.9	-	Proportion of IC domain at depth Z_{top}
	-	NUMSBDM	10	-	Number of Subdomains in IC domain
	PowMac	POWM	1	-	Power M for frequency distribut. curve IC domain
	FraZAHor	RZAH	0	-	Fraction macropores ended at bottom A-horizon
	DiaPolMin	DIPOMI	2	cm	Minimal diameter soil polygons (shallow)
	DiaPolMax	DIPOMA	10	cm	Maximal diameter soil polygons (deep)
	RstDraRapRef	RapDraResRef	10	d-1	Reference rapid drainage resistance
	-	**ShrParA layer 1**	**0.876**	**cm3/cm3**	**Void ratio at moist ratio = 0**
	-	**ShrParB layer 1**	**1.100**	**cm3/cm3**	**Moist ratio at transition from normal to residual shrinkage**
	-	**ShrParA layer 2**	**1.029**	**cm3/cm3**	**Void ratio at moist ratio = 0**
	-	**ShrParB layer 2**	**1.291**	**cm3/cm3**	**Moist ratio at transition from normal to residual shrinkage**
GEM 332	VolStaTop	VLMPSTSS	0.078	cm3/cm3	Volume of Static Macropores at depth Z_{top}
Ptf	-	ShrParA layer 1	0.415	cm3/cm3	Void ratio at moist ratio = 0
Corrected	-	ShrParB layer 1	0.687	cm3/cm3	Moist ratio at transition from normal to residual shrinkage
	-	ShrParA layer 2	0.364	cm3/cm3	Void ratio at moist ratio = 0
	-	ShrParB layer 2	0.522	cm3/cm3	Moist ratio at transition from normal to residual shrinkage

4.2.1.2 Model results

Simulations were carried out with the input of scenarios GEM 332 and GEM 332 ptf corrected for the year 2005. The results of both scenarios are given as annual water balances and as one-year time series of groundwater level depth, drainage fluxes and bottom boundary (seepage) fluxes (Figures 4.3-4.6). The water balances are presented in two ways: as schematic representations (Figure 4.2) and as tables of the total system and the separated macropore system (Table 4.4).

Annual water balances

The top diagram of Figure 4.2 explains the different terms of the water balance of the combined soil matrix and macropore system. Irrigation is distributed over inflow into the matrix at soil surface, and inflow in the two macropore domains Main Bypass (MB) domain and Internal Catchment (IC) domain. ET is evapotranspiration and consists of soil evaporation and crop transpiration. Drainage originates from the soil matrix and from the MB domain (rapid drainage). Some of the terms are net terms, they are underlined in the diagram. In Table 4.4 the gross terms that determine the net terms are given.

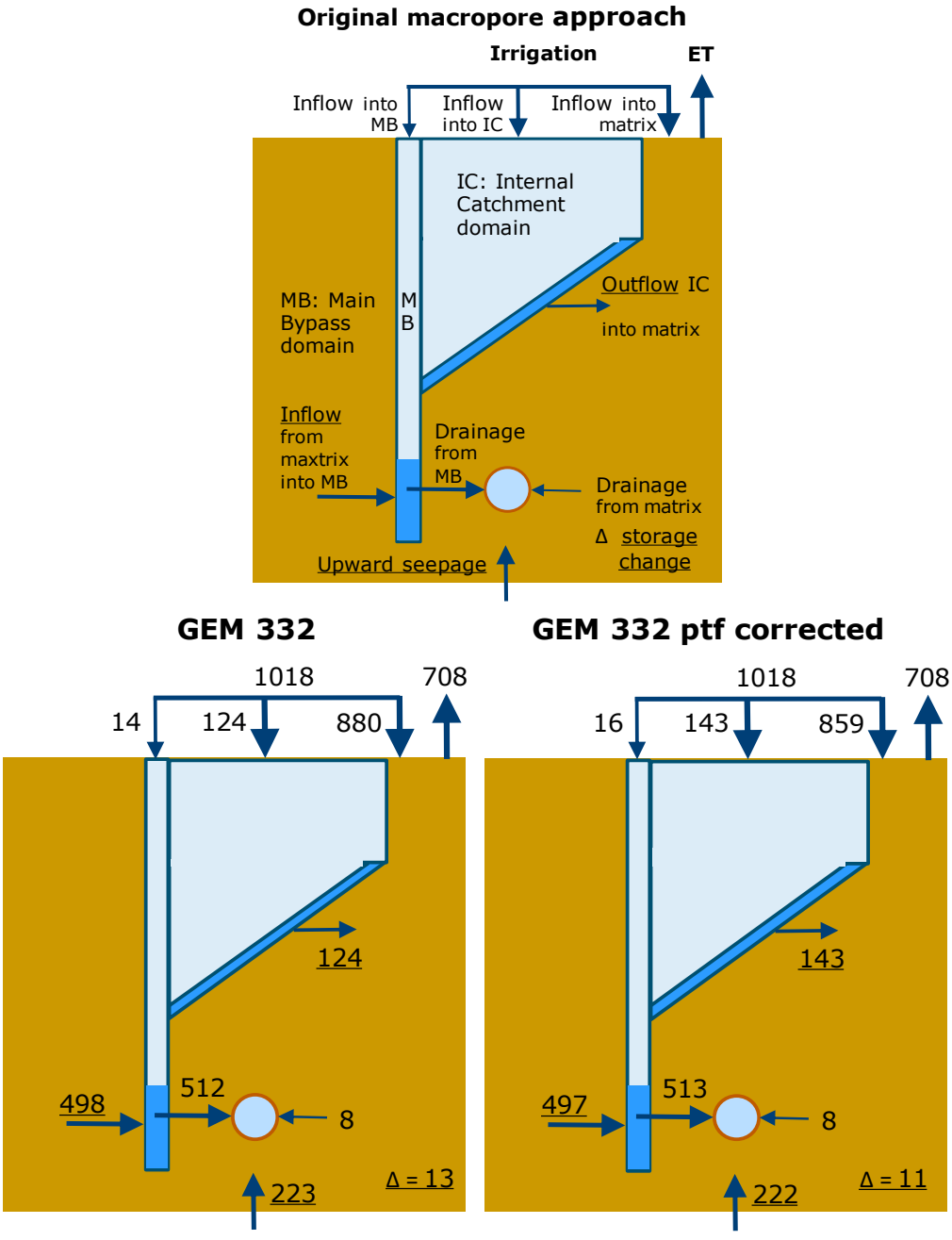

Figure 4.2 *Schematic representation of the water balance of the combined macropore-matrix-system for the original approach in which the macropore domains MB and IC are fed by rain or irrigation water at soil surface. On top an explanation of the terms (ET = soil evaporation and crop transpiration); at the bottom the values (mm per year) of the scenarios GEM 332 and GEM 332 ptf simulated with the corrected pedotransfer functions for parameterisation. Underlined terms are net water balance terms.*

Table 4.4 *Simulated water balances of the scenarios GEM 332 and Gem 332 ptf corrected. Top: total system; bottom: macropore system. All terms are in mm per year*

GEM 332				**GEM 332 ptf corrected**			
IN		**OUT**		**IN**		**OUT**	
Irrigation	1018	Evapotranspiration:		Irrigation	1018	Evapotranspiration:	
		- transpiration	701			- transpiration	701
		- soil evaporation	7			- soil evaporation	7
Infiltration	0	Drainage:		Infiltration	0	Drainage:	
		- matrix	8			- matrix	8
		- macropores (rapid)	512			- macropores (rapid)	513
Upward seepage	225	Downward seepage	2	Upward seepage	223	Downward seepage	1
Δ storage			13	Δ storage			11
Total	1243	Total	1243	Total	1241	Total	1241

GEM 332					**GEM 332 ptf corrected**				
IN			**OUT**		**IN**			**OUT**	
	MB	**IC**		**MB**		**MB**	**IC**		**MB**	**IC**
Inflow at soil surface	14	124			Inflow at soil surface	16	143			
Exfiltration from matrix	568	9	Infiltration into matrix	70	133	Exfiltration from matrix	567	8	Infiltration into matrix	71	151
			Rapid drainage	512					Rapid drainage	513	
Δ storage	0	0				Δ storage	1	0	Total		
Total	582	133	Total	582	133	Total	584	151	Total	584	151

The water balances show minor differences between the GEM 332 scenario and the GEM 332 ptf corrected scenario. The main difference is in the inflow at the top into the soil matrix and the IC domain. In the ptf corrected scenario the volume of static as well as dynamic (shrinkage) macropores is larger at the soil surface than in the original scenario and consequently the inflow into both macropore domains is greater in the ptf corrected scenario. The result of this is a 19 mm greater inflow into the IC domain and a 21 mm smaller inflow into the soil matrix at soil surface. The 19 mm larger outflow out of the IC domain into the soil matrix compensates for this difference. The consequence for solute transport could be the bypass of the upper 30-70 cm (ZAHor-ZIca) of the soil matrix by the 19 mm of extra inflow into the IC domain.

The large net inflow from the matrix into the MB domain is the result of inflow into the matrix at soil surface, outflow from the IC domain into the matrix, upward seepage, drainage from the matrix into the drain and the change in the water storage term (positive value for loss out of soil system). For the ptf corrected GEM scenario the net inflow of 497 mm into MB is equal to the sum of the other terms, i.e. 151 (= 859 – 708), 143, 222, - 8 and - 11 mm, respectively. Hence the MB domain drains the upward seepage. The causes of this are the relatively high saturated conductivity of the matrix of the subsoil layers and the relatively small diameter of the polygons. Both conditions strongly promote exchange between matrix and macropores. In this way the soil matrix conducts the upward seepage water relatively fast to the MB domain due to its low drainage resistance.

Daily levels and fluxes

Figure 4.3 shows the groundwater level depth at the end of the day as a function of time for the two GEM 332 scenarios. Average (87.9 cm) and standard deviation (0.68 cm) values are equal for both scenarios. The difference between scenarios is in the timing of the peaks caused by somewhat different flow paths in the period with the highest irrigation amounts.

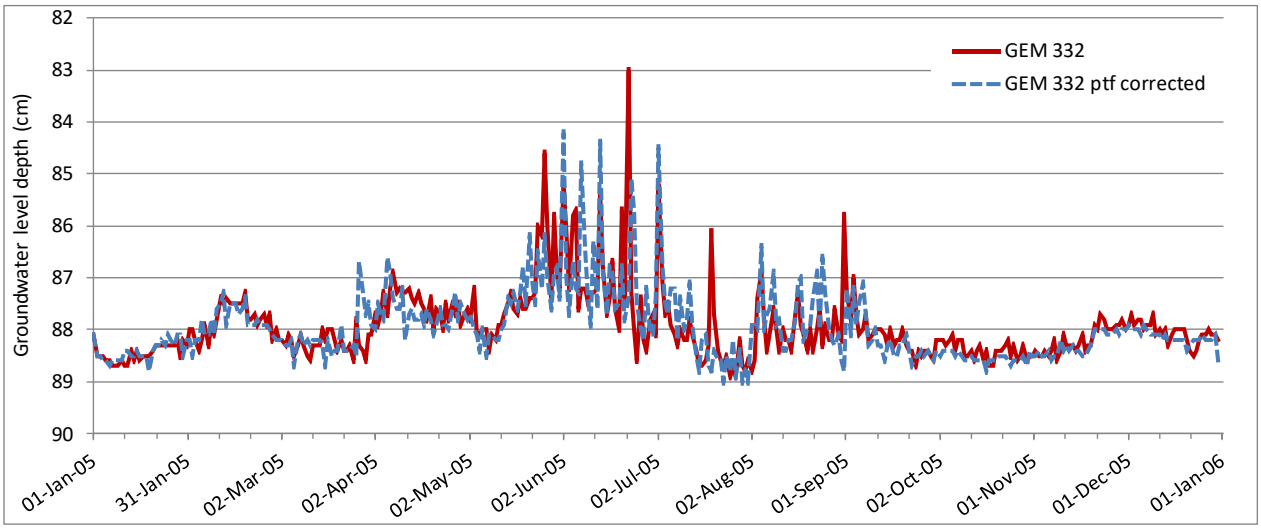

Figure 4.3 *Simulated groundwater levels as state variables at the end of the day in cm below soil surface in 2005 for the scenarios GEM 332 and GEM 332 ptf corrected*

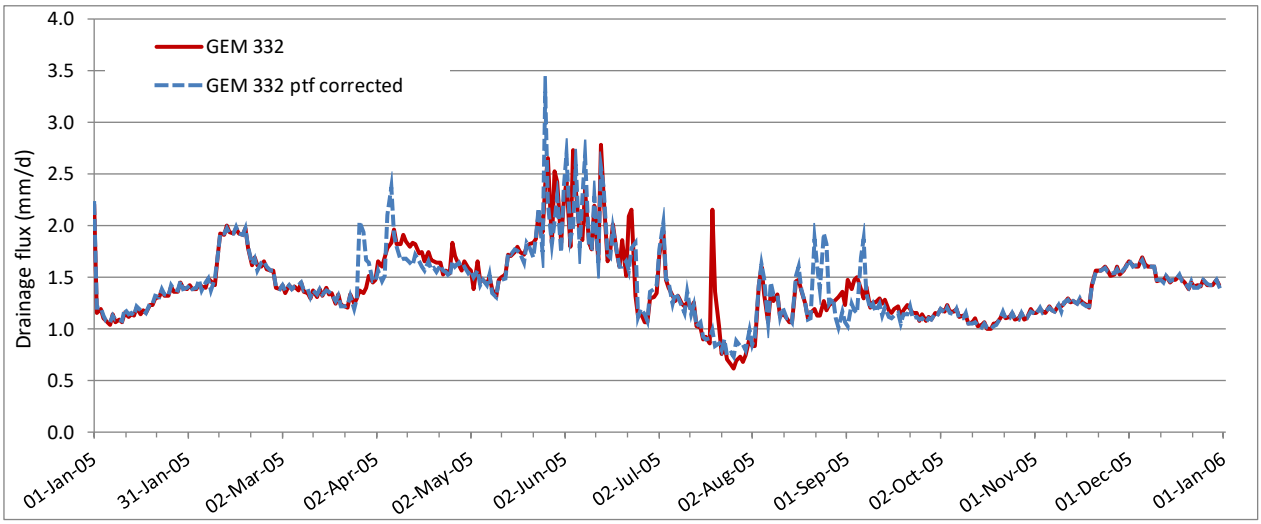

Figure 4.4 *Simulated drainage fluxes (mm/d) in 2005 for the scenarios GEM 332 and GEM 332 ptf corrected*

Figure 4.4 depicts a somewhat similar pattern for the differences in daily drainage fluxes between the GEM 332 scenarios as for the groundwater level: minor differences in the period with smaller irrigation amounts and some deviations in timing of peaks in the period with largest irrigation amounts. The resulting cumulative drainage hardly differs at all between the two scenarios (Figure 4.5). The bottom flux as a function of time is almost equal for both scenarios (Figure 4.6).

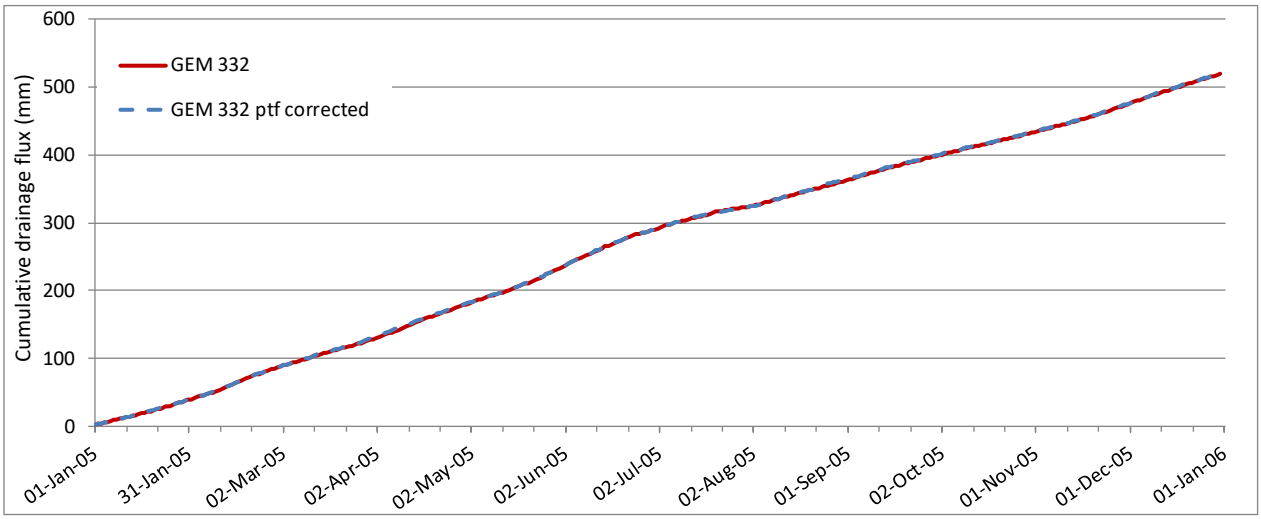

Figure 4.5 *Simulated cumulative drainage fluxes (mm) in 2005 for the scenarios GEM 332 and GEM 332 ptf corrected*

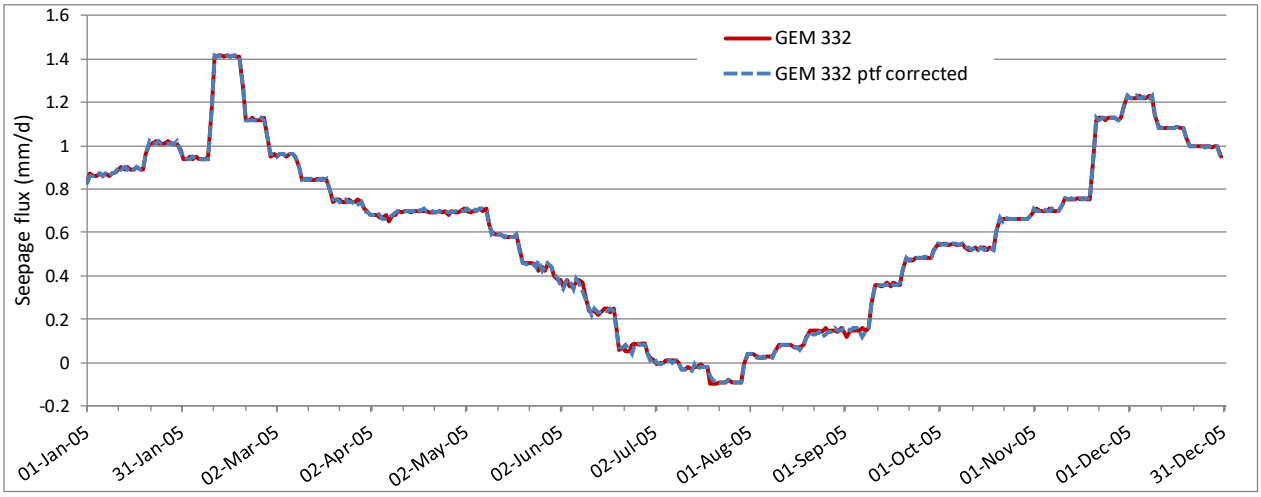

Figure 4.6 *Simulated bottom fluxes (mm/d) in 2005 for the scenarios GEM 332 and GEM 332 ptf corrected. Positive is upward seepage*

4.2.2 Comparison of GEM 332 ptf-corrected scenario with New-Top-Layer ptf-corrected scenario

A similar simulation as for the GEM 332 and GEM 332 ptf corrected scenarios is carried out for the New Top Layer ptf corrected (NewTopLayer) scenario. The results of this simulation are compared with the results of scenario GEM 332 ptf-corrected (see 4.2.1).

The NewTopLayer scenario is derived from the GEM 332 ptf corrected scenario not only by introducing the new parameter Z_{top} but also by adapting the model code for the working of h_e and simulation of the groundwater level (Section 4.1) and by changing the parameterisation (see 4.2.2.1). These changes also affect simulation results and therefore might blur the effects of the covering top layer. Therefore, these changes are investigated in a 'transition scenario'. This 'Transition Top Layer ptf corrected' (TransitionTopLayer) scenario is similar to the NewTopLayer scenario for model code and parameterisation except for the parameter Z_{top} which has the value of zero which implies that a covering top layer is not present in the TransitionTopLayer scenario.

4.2.2.1 Model input

The new macropore concept with covering layer in the NewTopLayer scenario is parameterised on the basis of the GEM 332 ptf corrected parameterisation (Table 4.5). All macropore parameter values of GEM 332 ptf corrected are used and only a new parameter Z_{top} is added. The value of this new parameter is set to -25 cm which is the depth of the tilled top layer.

For the hydraulic functions some changes are made to the Mualem-VanGenuchten parameter values of the original GEM 332 scenario. The value of 4.37 cm d^{-1} for the saturated conductivity K_s of the matrix of the heavy clay subsoil is very high. This value is obtained from unit O13 (heavy clay subsoil) of the Staring Series of hydraulic functions at the regional scale in The Netherlands (Wösten et al., 2001). It represents heavy clay soils with macropore influence. A more appropriate value for the clay matrix is the conductivity at the boundary pressure head h_e that marks the boundary between the soil matrix and the macropores. This pressure head has typical values between -1 and -10 cm (Jarvis and Messing, 1995). Following Tiktak et al. (2012) we take the conductivity value at the pressure head h_e of -5 cm. For unit O13 this yields the value of 0.168 cm d^{-1}.

The use of the concept of a boundary pressure head requires a value for parameter h_e (cm) in the modified Mualem-VanGenuchten functions in SWAP. This parameter h_e takes the value of -5 cm. The volumetric water content θ at this pressure head amounts to 0.5664 cm^3 cm^{-3} for the O13 unit. Using this value for θ_s at saturation combined with the value of 0.168 cm d^{-1} for K_s and h_e = -5 cm implies that for lower pressure heads than -5 cm the θ(h) and K(h) relations are identical to the original functions of the O13 unit and no refitting of the MVG-functions is required (see Annex 4, A41).

In Table 4.5 the parameterisation of the New TopLayer scenario is listed for the Mualem-VanGenuchten parameters to describe the hydraulic functions.

Table 4.5 *Mualem-VanGenuchten-parameters of the soil layers in the greenhouse soil for the New Top Layer ptf corrected scenario*

Scenario	Layer depth (cm)	θ_r (cm^3/cm^3)	θ_{sat} (cm^3/cm^3)	α (1/cm)	N (-)	Ksat,fit (cm/d)	l (-)	α_w (1/cm)	h_e (cm)
New TL	0 -25	0.01	0.53	0.0242	1.28	81.28	-1.476	0.0242	0.0
ptf corrected	25-500	0.08	0.5664	0.0194	1.089	0.168	-5.955	0.0194	-5.0

Furthermore, a sensitivity analysis is carried out to determine the optimal value for input parameter DTMAX, the maximum time step (d) used in SWAP (See Kroes et al., 2017 for more detail). The analysis resulted in an optimal value for DTMAX of 0.01 day. Lower values yielded only very small differences in water balance terms and in time series of groundwater level depth and water fluxes, whereas higher values gave substantial differences (see Annex 4, A4.2). The optimal value was used for all simulations with the new covering top layer.

For better understanding of the differences in results between the NewTopLayer scenario and the GEM 332 ptf-corrected scenario, the TransitionTopLayer scenario is introduced which is similar to the NewTopLayer scenario for model code and input except for the presence of the covering top layer without macropores. Consequently, TransitionTopLayer differs from GEM 332 ptf-corrected as follows:

1. model code: the working of h_e and the alternative simulation of the groundwater level;
2. model input: the lower value of 0.01 day for DTMAX and the value of -5 cm for variable h_e including the for h_e adapted parameters θ_s and K_s for the subsoil (Table 4.5).

4.2.2.2 Model results

The results of the scenarios GEM 332 ptf corrected, TransitionTopLayer and NewTopLayer are presented in a similar way as the results of the GEM 332 scenarios (Section 4.2.1): as annual water balances and as one-year time series of groundwater level depth at the end of the day, drainage fluxes and bottom boundary (seepage) fluxes for the year 2005 (Figures 4.7-4.11). The water balances are presented again in two ways: as schematic representations (Figure 4.7) and as tables of the total system and the separated macropore system (Table 4.6; not for TransitionTopLayer).

Annual water balances

From Figure 4.7 and Table 4.6 it can be seen that the inflow of water into the top of the macropores is much less in the NewTopLayer scenario: more than two times as small as in the GEM 332 ptf corrected scenario. Also the exfiltration from the matrix into the MB domain is much (195 mm or 39%) lower in the new scenario. This is also due to the strong reduction of the upward seepage flux with 185 mm or 83%. The result of this lower inflow into the MB domain is 204 mm or 40% less rapid drainage from the macropores. The draining of the upward seepage via the MB domain in scenario GEM 332 ptf corrected is much less in the NewTopLayer scenario.

The main cause of these phenomena is the much (25 times) lower saturated conductivity of the subsoil matrix in scenario NewTopLayer. These low values decrease vertical flow through the subsoil matrix and lateral exchange between matrix and macropores. In this way the total soil system – matrix and macropore domains – has a lower capacity for draining the subsoil and hence upward seepage. As a consequence, the water table is much higher in the NewTopLayer scenario (Figure 4.8).

Comparing both scenarios with scenario TransitionTopLayer underlines this conclusion. The changes in flows due to the transition from GEM 332 ptf corrected to TransitionTopLayer are much larger than in the transition from TransitionTopLayer to NewTopLayer, despite the differences in top layer between the latter two scenarios. The GEM 332 ptf corrected and TransitionTopLayer scenarios have the same top-layer-option but a different subsoil matrix. In both scenarios the inflow into the macropores at soil surface exists of only direct inflow of irrigation water. Overland flow does not take place because of the high permeability of the topsoil (Table 4.2). The topsoil of GEM 332 ptf corrected is better drained by the subsoil than the topsoil of TransitionTopLayer, due to the higher permeability of the subsoil of the first. The better drained dryer topsoil shrinks more which results in a greater area of macropores at soil surface and a consequently greater inflow of irrigation water into the macropores at soil surface in GEM 332 ptf corrected: 16% of the annual irrigation sum against 8% for TransitionTopLayer. Because there is only direct inflow of irrigation water into the macropores at soil surface and no overland flow, the latter equals the relative area of permanent macropores at soil surface, which implies that the topsoil of TransitionTopLayer remains so wet that it hardly shrinks.

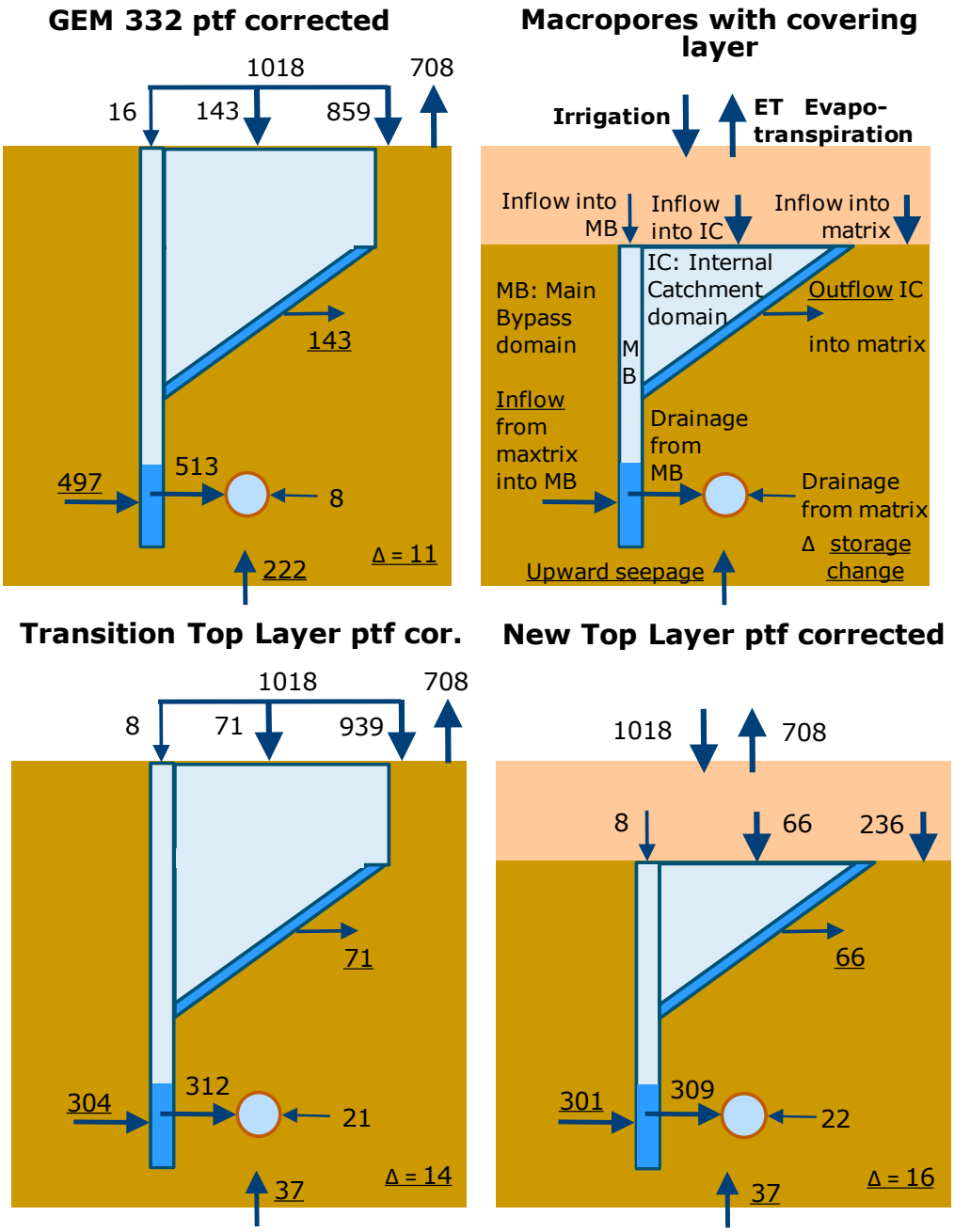

Figure 4.7 *Schematic representation of the water balance of the combined macropore-matrix-system in 2005. Right top: an explanation of the new system with a covering layer without macropores in which macropore domains are fed by water infiltrating from the saturated covering layer. Left top and at the bottom: the values (mm per year) of the scenarios GEM 332 ptf corrected, Transition Top Layer ptf corrected and New Top Layer ptf corrected. Underlined terms are net water balance terms*

The difference in conductivity of the subsoil affects the upward seepage as well. The subsoil beneath the drain until the bottom of the soil column at five meters depth has a resistance to vertical flow that is equal to the thickness of the saturated soil layer divided by the saturated hydraulic conductivity. This amounts to (500 – 90) / 4.37 = 94 days for GEM 332 ptf corrected and to (500 – 90) / 0.168 = 2440 days for Transition/NewTopLayer. This extra internal resistance is added implicitly to the inputted resistance of 320 days as SWAP solves the Richards' equation integrally for unsaturated and saturated zone. This means an almost seven times as high resistance and a consequently six times as small upward seepage for Transition/NewTopLayer compared to GEM 332 ptf corrected.

Furthermore, the higher groundwater tables of scenarios Transition/NewTopLayer imply greater potential differences between groundwater level and drain level. Consequently they increase matrix drainage. Due to

the very high drainage resistance of 971 days of the matrix the increase in matrix drainage is limited to 13-14 mm (almost 200%) only. Higher groundwater levels suppress upward seepage, because in all GEM 322 scenarios seepage is modelled as a Neumann bottom boundary condition in which the seepage flux is described as the difference between groundwater level and hydraulic head in the underlying semi-confined aquifer divided by a resistance to vertical flow. Therefore, the higher groundwater level in Transition/NewTopLayer supresses the upward seepage.

The greatest effect of the lower conductivity of the subsoil is on the rapid drainage via the macropores. In GEM 332 ptf corrected the macropores' MB domain drains the subsoil at a rate of 500 mm per year, while in Transit/NewTopLayer this is 200 mm per year less. Since direct inflow at the soil surface into the MB domain is relatively small and the drainage resistance is equal in both scenarios, this is mainly due to the decreased lateral inflow from the matrix into the MB domain as a result of the lower conductivity of the subsoil that affects water exchange between macropores and saturated matrix.

The differences in the results are related, of course, to the different pathways of the macropore inflow: in scenario GEM 332 ptf corrected irrigation water flows directly into the macropore domains and in scenario NewTopLayer it flows first through the 25 cm thick covering soil layer on top of the macroporous subsoil and then into the macropore domains. The largest inflow into the MB macropore domain is exfiltration from the matrix which is a mix of matrix flow from the top layer, infiltration from the IC domain and upward seepage. These differences in pathways will influence solute concentrations in drainage water. But without running the Pearl model it is impossible to predict the differences in drainage concentrations between the GEM 332 and the NewTopLayer scenario.

Table 4.6 *Simulated water balances of the scenarios GEM 332 ptf corrected and NewTopLayer ptf corrected in 2005. Top: total system; bottom: macropore system. In the GEM 323 ptf corrected scenario all inflow into the macropores at soil surface is by direct irrigation and not by overland flow because of the high permeability of the topsoil. All terms are in mm per year*

GEM 332 ptf corrected				**New Top Layer ptf corrected**			
IN		**OUT**		**IN**		**OUT**	
Irrigation	1018	Evapotranspiration:		Irrigation	1018	Evapotranspiration:	
		- transpiration	701			- transpiration	701
		- evaporation	7			- evaporation	7
Infiltration	0	Drainage:		Infiltration	0	Drainage:	
		- matrix	8			- matrix	22
		- macropores (rapid)	513			- macropores (rapid)	309
Upward seepage	225	Downward seepage	2	Upward seepage	37	Downward seepage	0
Δ storage			13	Δ storage			16
Total	1243	Total	1243	Total	1055	Total	1055

GEM 332 ptf corrected						**New Top Layer ptf corrected**					
IN			**OUT**			**IN**			**OUT**		
	MB	**IC**		**MB**	**IC**		**MB**	**IC**		**MB**	**IC**
Inflow at soil surface	16	143				Inflow from top layer	8	66			
Exfiltration matrix	567	8	Infiltration matrix	71	151	Exfiltration matrix	301	0	Infiltration matrix	0	66
			Rapid drainage	513					Rapid drainage	309	
Δ storage	1	0				Δ storage	0	0			
Total	584	151	Total	584	151	Total	309	66	Total	309	66

Daily levels and fluxes

Figure 4.8 shows the differences in groundwater level for the three scenarios. Average groundwater level depth and standard deviation of the scenarios GEM 332 ptf corrected, TransitionTopLayer and NewTopLayer amount to 88.0 and 0.68, 84.5 and 3.31 and 84.4 and 3.48, respectively (all values in cm). Here again, groundwater levels of TransitionTopLayer are closer to levels of NewTopLayer than to levels of GEM 332 ptf corrected. The lower average and smaller standard deviation of GEM 332 ptf corrected indicate lower groundwater levels and less high peaks compared to the other two scenarios. The higher peaks in the groundwater levels of Transition/NewTopLayer are due to the lower draining by the MB macropore domain as a result of the lower saturated hydraulic conductivity of the matrix in these scenarios compared to GEM 332 ptf corrected.

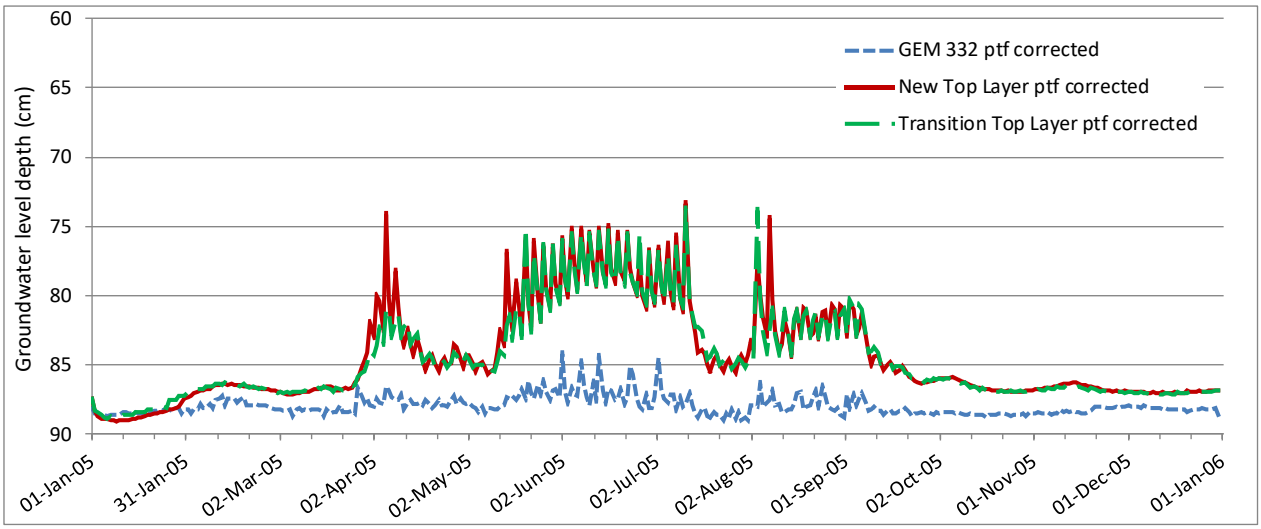

Figure 4.8 *Simulated groundwater levels as state variables at the end of the day in cm below soil surface in 2005 for the GEM 332 ptf corrected, Transition Top layer ptf corrected and New Top Layer ptf corrected scenarios. Depth of drainpipe 0.90 m*

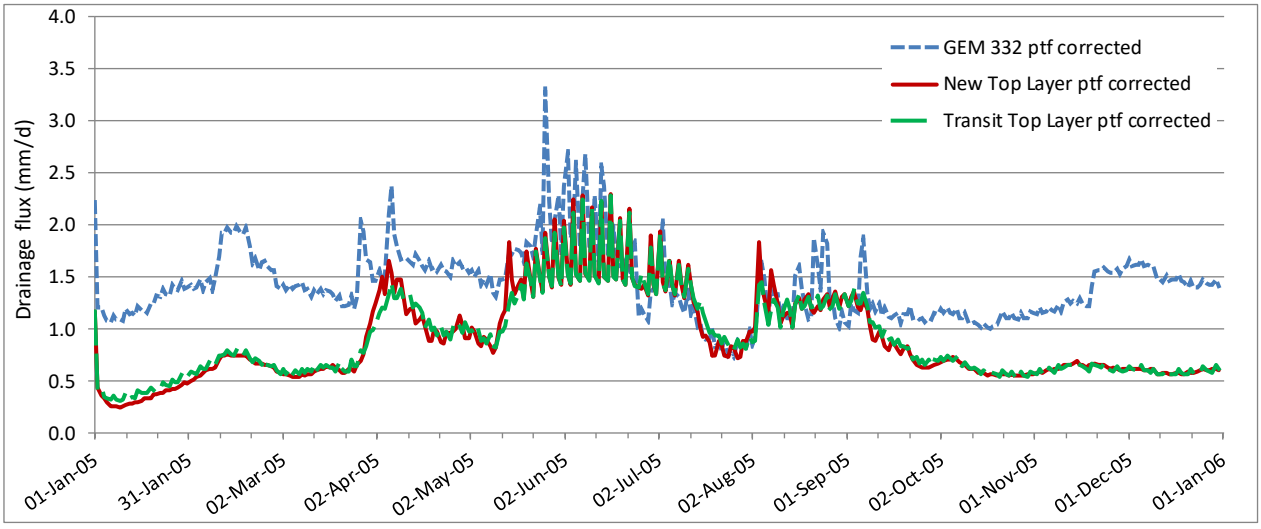

Figure 4.9 *Simulated drainage fluxes (mm/d) in 2005 for the GEM 332 ptf, Transition Top Layer ptf corrected and New Top Layer ptf corrected scenarios*

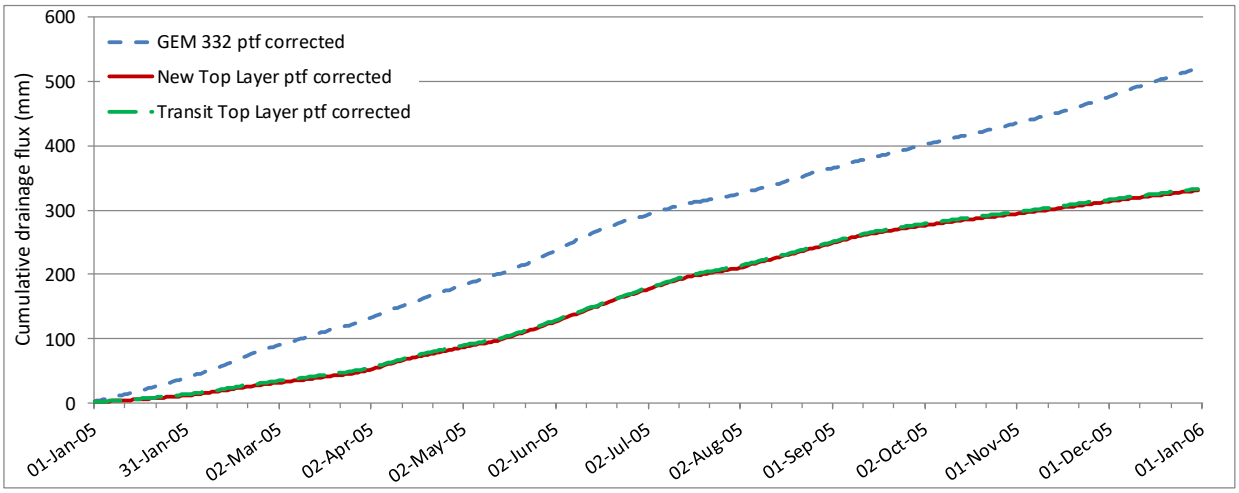

Figure 4.10 *Simulated cumulative drainage fluxes (mm) in 2005 for the GEM 332 ptf corrected, Transition Top Layer ptf corrected and New Top Layer ptf corrected scenarios*

Figure 4.9 shows lower peaks of drainage fluxes for scenarios TransitionTopLayer and NewTopLayer compared to scenario GEM 332 ptf corrected. As differences in drain fluxes between the first two scenarios are relatively small the difference in inflow at the top of the macropores apparently plays only a minor role. For both these scenarios the peaks in fluxes coincide exactly with the peaks in the groundwater level (Figure 4.8). For GEM 332 ptf corrected this is less clear.

Peaks in drain fluxes originate mainly from rapid drainage via the MB domain which is strongly related to peaks in groundwater level. Most water that drains from the MB domain enters this domain as exfiltration from the soil matrix. Higher groundwater levels in the matrix imply higher differences in water potential between matrix and MB domain and consequently greater rapid drainage fluxes. Drainage from the MB domain is so rapid that it keeps water levels in this domain low. This principle counts for all three scenarios, but the higher conductivity of the matrix of GEM 322 ptf corrected causes faster reactions to groundwater level rise and consequently higher peaks in drain fluxes which rapidly lower groundwater levels again. This mechanism blurs the relation between the groundwater level as state variable at the end of the day and the daily cumulative drain flux. For the other two scenarios this fast mechanism does not count because of the lower conductivity of the soil matrix.

The 'base flow' component in the drainage, that originates from the upward seepage, of Transition/NewTopLayer is less than half that of GEM 332 ptf corrected: the difference is at least 0.5 mm d^{-1}. This amounts to 0.5 x 365 = 183 mm per year, which is about the entire difference in drainage between the GEM 332 ptf corrected and Transition/NewTopLayer scenarios. The cumulative annual flux is 40% lower for the Transition/NewTopLayer scenario (Figure 4.10).

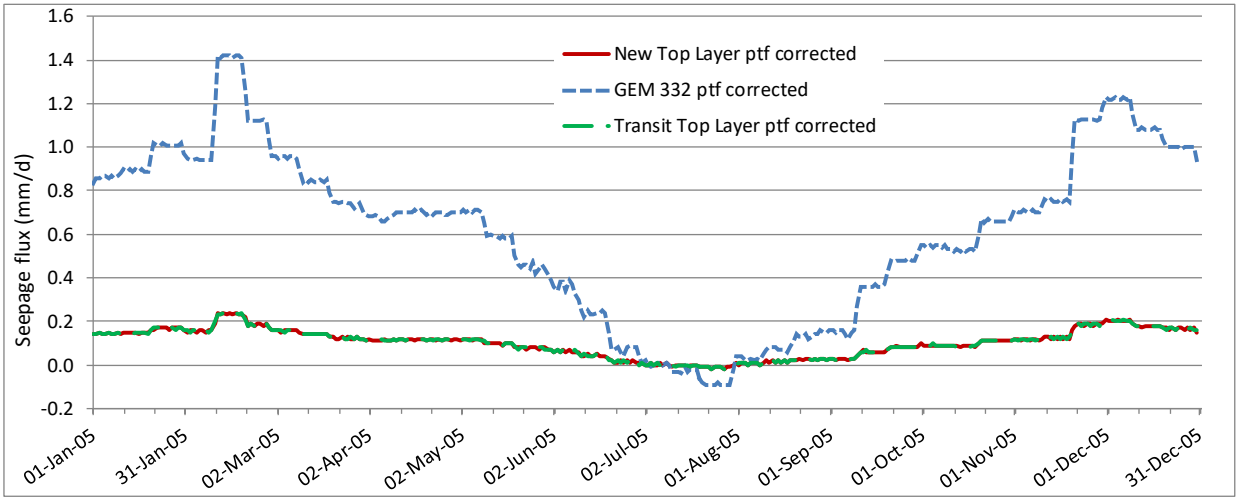

Figure 4.11 *Simulated bottom fluxes (mm/d) in 2005 for the scenarios GEM 332 ptf corrected, Transition Top Layer ptf corrected and New Top Layer ptf corrected. Positive is upward seepage*

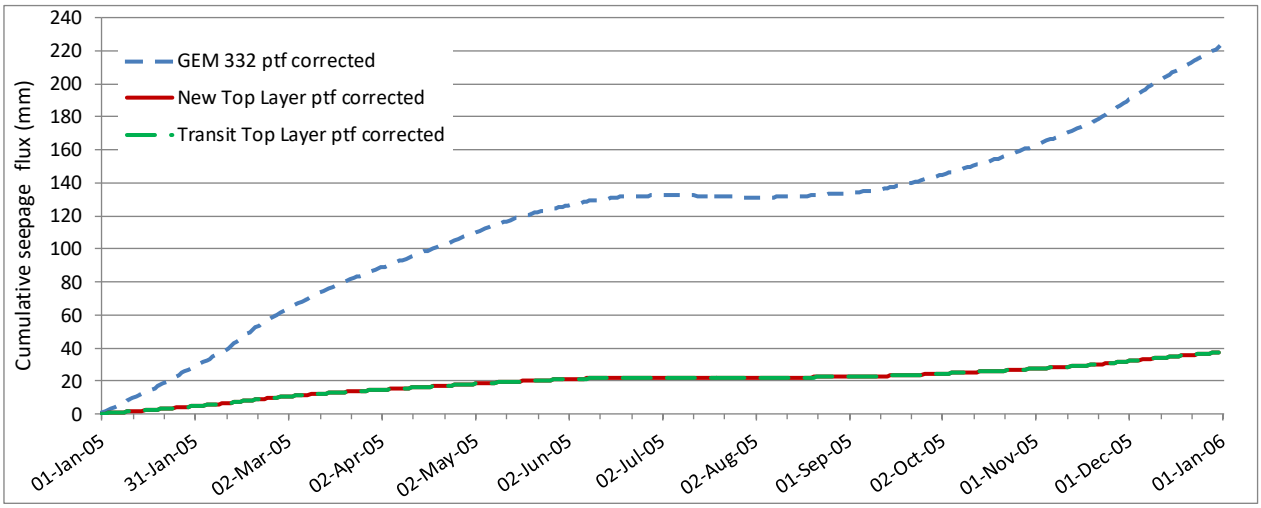

Figure 4.12 *Simulated cumulative bottom fluxes (mm) in 2005 for the GEM 332 ptf corrected, Transition Top Layer ptf corrected and New Top Layer ptf corrected scenarios. Positive is upward seepage*

Daily and annual upward seepage fluxes are much higher for GEM 332 ptf corrected than for Transition/NewTopLayer (Figures 4.11 and 4.12). This is mainly due to the higher resistance to vertical flow of the soil profile below drain level in the latter scenarios, that is caused by the lower conductivity of the subsoil matrix. But also the higher groundwater level of the latter scenarios and the resulting smaller difference in potential as driving force for the upward seepage plays a role.

4.3 Comparison of three cultivation sections of chrysanthemum crop with the New Top Layer

Similar simulations as for the NewTopLayer scenario are carried out for three different cultivation sections of chrysanthemum crop: To evaluate the effect of the time shift in the crop cycles between the 24 crop cultivation sections, simulations have been carried out for cultivation sections 1, 7 and 11, with a time shift of about 20 days between them. The results of the simulations of the three cultivation sections are compared in this paragraph.

4.3.1 Model input

The NewTopLayer parameterisation with covering layer is used as the basis of the new scenarios for the three chrysanthemum cultivation sections (Tables 4.3 and 4.5). Only the irrigation schemes and the related chrysanthemum crop transpiration are adapted. Each section has its own input file with meteorological data. Each cultivation section has a different irrigation regime, but the global radiation, temperature, humidity and evaporation are the same for all cultivation sections. Simulations are conducted for the years 1994-2000 and analysed for the year 2000.

Annual irrigation amounts and amounts of crop transpiration and soil evaporation of the three cultivation sections are listed in Table 4.7 and 4.8 and in Figure 4.13. Daily values are depicted in Figures 4.16 and 4.17 as gross irrigation and actual transpiration, respectively.

Irrigation application starts at the beginning of the day at 0:00:00 hour and is distributed over one to four events of around 5 mm each intermitted by a dry spell of one hour. The number of irrigation gifts per event depends on the irrigation amount. Accordingly, the following irrigation schemes are applied:

1. amount of 0 to 7.5 mm: one single event;
2. amount of 7.5 to 12.5 mm: two equal events intermitted by an one hour dry spell;
3. amount of 12.5 to 17.5 mm: three equal events each intermitted by an one hour dry spell;
4. amount of 17.5 to 22.5 mm: four equal events each intermitted by an one hour dry spell.

The irrigation intensity of all events is 1 mm per minute. This implies that the duration in minutes of each event equals its amount in mm.

4.3.2 Model results

The results for the three cultivation sections are presented in a similar way as the results of the NewTopLayer scenario (Section 4.2.2): as water balances and as one year time series of groundwater level, drainage fluxes and seepage fluxes for the year 2000.

4.3.2.1 Annual water balances

The annual water balances are presented as schematic representations (Figure 4.13) and as tables of the total system and the separated macropore system (Tables 4.7 and 4.8). For the tables, this is done in pairs of which cultivation Section 1 is the reference that is compared to either cultivation Section 7 or cultivation Section 11. In the schematic representations all three schemes are compared in the same graph.

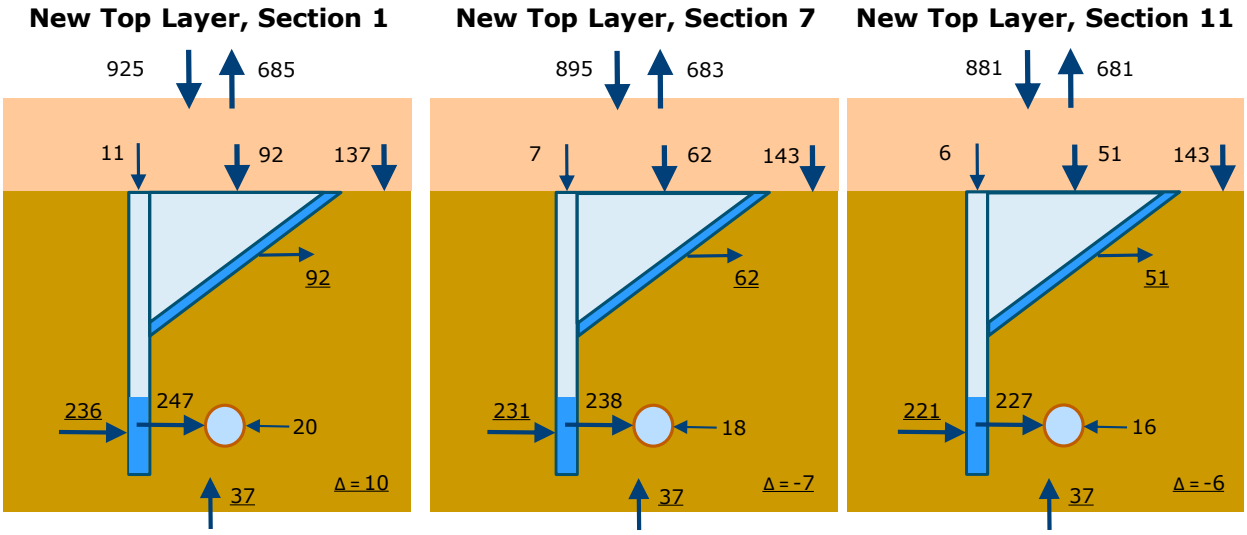

Figure 4.13 *Schematic representation of the water balance of the combined macropore-matrix-system for the year 2000 as the values (mm per year) of the three cultivation sections 1, 7 and 11 with New Top Layer. Underlined terms are net water balance terms*

The water balances of the three cultivation sections are in general quite similar, except for the irrigation and the inflow into the top of the macropores with the consequent outflow out of the IC domain into the matrix. Section 1 shows a 30 mm (3.5%) higher irrigation than Section 7 and a 44 mm (5%) higher irrigation than Section 11. The absolute differences in inflow into the macropore top and the outflow out of the IC domain resemble these differences quite well: 34 and 46 mm for the inflow and 30 and 41 mm for the outflow. Differences in total drainage are much less: 11 mm (5%; Section 1 vs. 7), 24 mm (9%; Section 1 vs. 11) and 13 mm (4%; Section 7 vs. 11) (see also Figure 4.14).

Table 4.7 *Simulated water balances of the cultivation sections 1 and 7 with New Top Layer for the year 2000. Top: total system; bottom: macropore system. All terms are in mm per year*

Cultivation Section 1 New Top Layer				**Cultivation Section 7 New Top Layer**			
IN		**OUT**		**IN**		**OUT**	
Irrigation	925	Evapotranspiration:		Irrigation	895	Evapotranspiration:	
		- transpiration	436			- transpiration	438
		- evaporation	249			- evaporation	245
Infiltration	0	Drainage:		Infiltration	0	Drain:	
		- matrix	20			- matrix	18
		- macropores (rapid)	247			- macropores (rapid)	238
Upward seepage	37	Downward seepage	0	Upward seepage	37	Downward seepage	0
Δ storage	0		10	Δ storage	7		0
Total	962	Total	962	Total	939	Total	939

Cultivation Section 1 New Top Layer						**Cultivation Section 7 New Top Layer**					
IN			**OUT**			**IN**			**OUT**		
	MB	**IC**		**MB**	**IC**		**MB**	**IC**		**MB**	**IC**
Inflow from top layer	11	92				Inflow from top layer	7	62			
Exfiltration matrix	237	1	Infiltration matrix	1	93	Exfiltration matrix	232	0	Infiltration matrix	1	62
			Rapid drainage	247					Rapid drainage	238	
Δ storage	0	0		0	0	Δ storage	0	0		0	0
Total	248	93	Total	248	93	Total	239	62	Total	239	62

Table 4.8 *Simulated water balances of the cultivation sections 1 and 11 with New Top Layer for the year 2000. Top: total system; bottom: macropore system. All terms are in mm per year.*

Cultivation Section 1 New Top Layer				**Cultivation Section 11 New Top Layer**			
IN		**OUT**		**IN**		**OUT**	
Irrigation	925	Evapotranspiration:		Irrigation	881	Evapotranspiration:	
		- transpiration	436			- transpiration	444
		- evaporation	249			- evaporation	237
Infiltration	0	Drainage:		Infiltration	0	Drainage:	
		- matrix	20			- matrix	16
		- macropores (rapid)	247			- macropores (rapid)	227
Upward seepage	37	Downward seepage	0	Upward seepage	37	Downward seepage	0
Δ storage	0		10	Δ storage	6		0
Total	962	Total	962	Total	924	Total	924

Cultivation Section 1 New Top Layer						**Cultivation Section 11 New Top Layer**					
IN			**OUT**			**IN**			**OUT**		
	MB	**IC**		**MB**	**IC**		**MB**	**IC**		**MB**	**IC**
Inflow from top layer	11	92				Inflow from top layer	6	51			
Exfiltration matrix	237	1	Infiltration matrix	1	93	Exfiltration matrix	221	0	Infiltration matrix	0	51
			Rapid drainage	247					Rapid drainage	227	
Δ storage	0	0		0	0	Δ storage	0	0		0	0
Total	248	93	Total	248	93	Total	227	51	Total	227	51

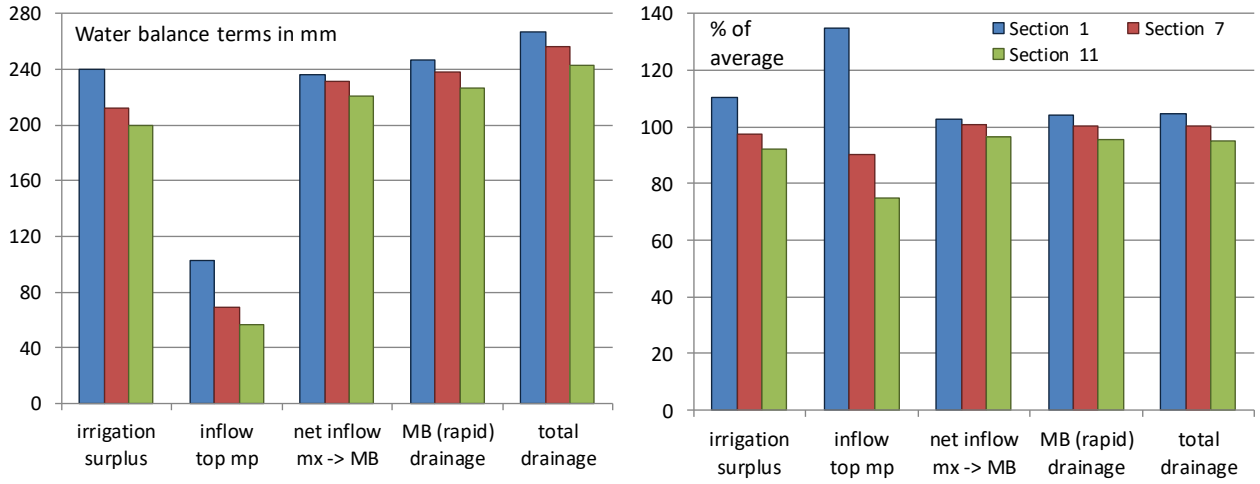

Figure 4.14 *Most important water balance terms of the cultivation sections 1,7 and 11, for the year 2000. Left: absolute values in mm; right: relative to the average of the three sections in %. 'Net inflow mx -> MB' = net inflow from the subsoil matrix into the MB macropore domain*

Figure 4.14 depicts the absolute and relative values of the comparison between the three sections of the five most important water balance terms. Section 1 has consequently the highest values, Section 11 consequently the lowest and Section 7 is in between. Differences between successive sections are around 10 mm or 5%. Exceptions are the differences of around 30 mm between Section 1 and 7 for irrigation surplus and inflow into the top of the macropores. The irrigation surplus is the main driver of the inflow into the top of the macropores and of the drainage. Despite the much larger irrigation surplus of Section 1 – 30 mm more than Section 7 and 40 mm more than Section 11 – the differences in drainage with sections 7 and 11 are only 10 and 20 mm, respectively. The 20 mm shortage of irrigation surplus of sections 7 and 11 compared to Section 1 are compensated by the change in water storage of the matrix (Tables 4.7 and 4.8). Sections 7 and 11 show a 7 mm draw out of the matrix storage instead of the 10 mm increase in matrix storage of Section 1. It should be noted that as irrigation regimes differ over the years, the differences in annual irrigation amounts between the cultivation sections in other years will change too.

The rapid drainage from the MB domain does resemble the net inflow from the subsoil matrix into the MB domain very well, but not the inflow into the top of the macropores, which is 2.5-4 times as small. The flow path of the draining water is predominantly (93%) through the MB macropore domain, but this rapid draining water originates from four different sources: direct inflow into the MB domain from the covering top layer (ctl) (for Section 1 to Section 11: 4% to 2%), indirect inflow from the ctl via the IC macropore domain (37% to 23%), indirect inflow from the ctl via the subsoil matrix (50% to 70%) and indirect inflow as upward seepage through the subsoil matrix (9% to 5%). The upward seepage is a relatively small source – 37 mm or 10-15% of the total drainage – and it is the same for all sections. The consequence is that most (85-90%) of the draining water flows through the covering topsoil and most (96-98%) of that also through the subsoil.

The portion of the draining water that originates from the IC domain infiltrates into the subsoil matrix at depths between 25 and 70 cm (depth of bottom IC domain) and thus partly bypasses this part of the subsoil. Figure 4.15 depicts the cumulative inflow from the IC domain into the subsoil matrix as a function of depth for the three sections. The figure shows for each depth between 25 and 70 cm the amount of IC-domain-water that infiltrates into the matrix below that depth and above 70 cm. Consequently, this amount bypasses the part of the subsoil matrix above this depth. It is clear that for each cultivation section the total amount of water that flows into the top of the IC domain (Tables 4.7 and 4.8) bypasses the depth of 27.5 cm which is the top 2,5 cm of the subsoil. The thin vertical lines in Figure 4.15 show per section the amount of IC-water that bypasses the upper 25 cm of the subsoil between 25 and 50 cm. For Section 1 this amount equals 36.2 mm (39% of the total), for Section 7 23.3 mm (38%) and for Section 11 20 mm (39%).

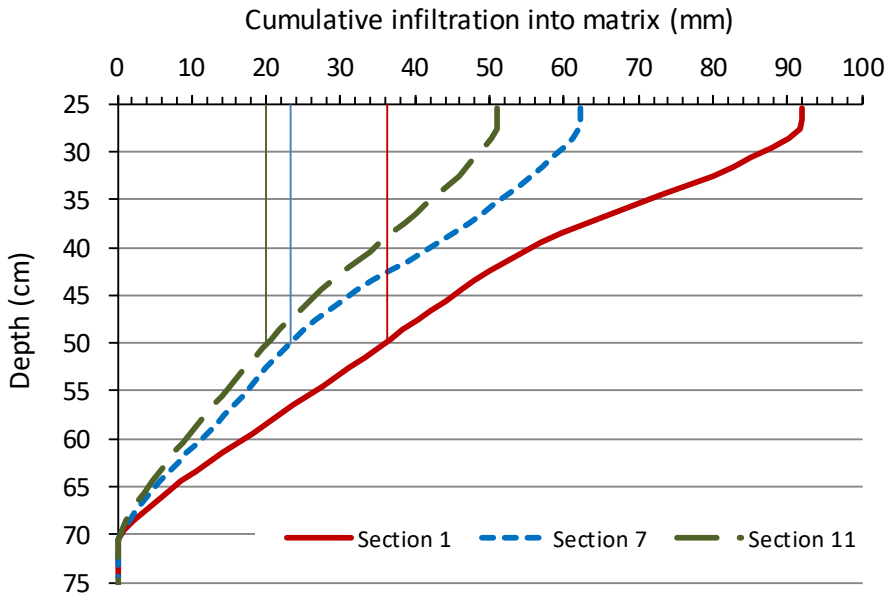

Figure 4.15 *Simulated cumulative infiltration (mm) from the IC macropore domain into the subsoil matrix as a function of depth (cm) below soil surface in 2000 for the cultivation sections 1, 7 and 11 with the New Top Layer. At 25 cm depth the covering soil layer ends and the macropores in the subsoil begin. At 70 cm depth the IC domain ends. The thin vertical lines indicate the amount of infiltration water that bypasses the part of the subsoil between 25 and 50 cm per section*

4.3.2.2 Daily levels and fluxes

Differences in irrigation surplus originate from the typical irrigation schemes in relation to the soil evaporation and crop transpiration as determined by seasonal fluctuations in solar radiation, heating and ventilation, air and soil temperature and crop management, as has been described in Section 3.1.1. Irrigation patterns are depicted in Figure 4.16 that also shows water breakthrough events from the covering top layer into the top of the two macropore domains MB and IC. Simulated actual transpiration for the three sections is depicted in Figure 4.17.

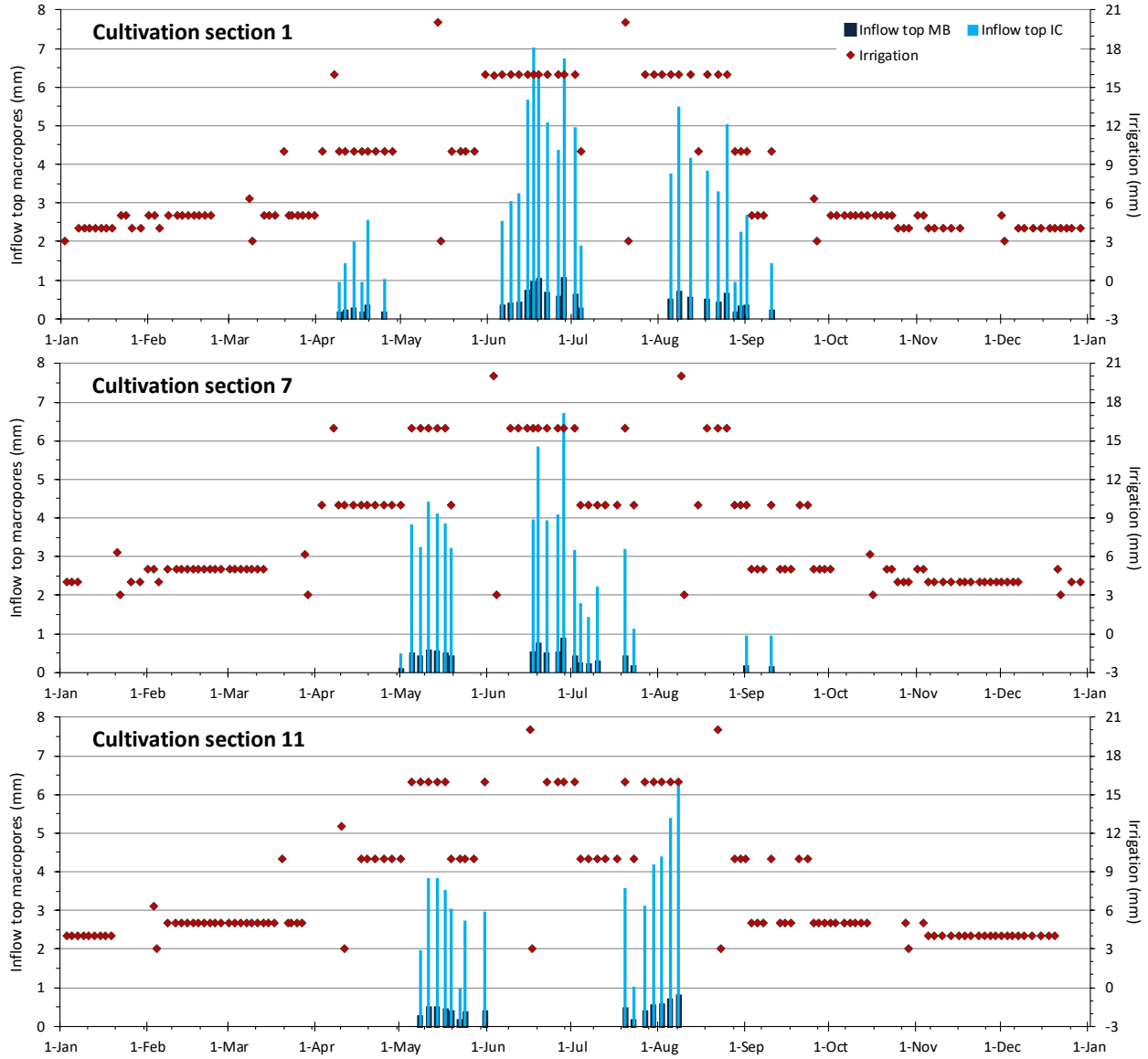

Figure 4.16 *Irrigation amount (mm) and simulated inflow (mm) from the covering layer into the top of the macropores i0 for the cultivation sections 1, 7 and 11 with the New Top Layer. See text at Section 4.3.1 for explanation of irrigation schemes.*

Figure 4.16 shows eight different classes of irrigation amounts that are applied in all three sections, which follow logically from the irrigation scenario (Section 3.1.1). In Figure 4.18-right these classes are indicated. This figure also depicts the distribution of the number of irrigation events over the eight classes. The total number of irrigation events is 118 for sections 1 and 11, and 114 for Section 7. The class of 12.5 mm is only applied once in Section 11; not in the other two sections. The numbers of events of the classes of 5, 10 and 16 mm differ the most between the sections. The last two classes are the most important for water breakthrough from the top layer into the macropores. Section 1 has 3-4 events of class 10 mm less than sections 7 and 11, but 3 and 6 events of class 16 mm more than Section 7 and Section 11, respectively.

The irrigation patterns of all sections roughly resemble each other, but differ in detail, especially in the summer half-year (April-September), when irrigation is highest due to the environmental conditions that determine the crop water demand. Figure 4.18-left shows several relative steep periods with high irrigation amounts in the curves of the cumulative irrigation, that all occur in the summer half-year. For Section 1 there are three of these periods: April 3-28, May 14-July 3 and July 20-September 10. These periods contain all 10 mm irrigation events but one, and all > 10 mm irrigation events (see Figure 4.16). Within these periods the number of days between irrigation events is mostly two or less. Section 7 has only two of these steep periods – April 3-May 19 and June 3-July 23 – and one less steep period from Augustus 9 to September 23.

All irrigation events of 10 mm and higher take place in these periods. The crop cycle sequence in Section 11 has a time-shift of about 14 days compared to Section 7, which result in only the second and third crop cycles and part of the first and fourth crop cycles in the period of high irrigations. Consequently, only two clear steep periods occur in cultivation Section 11 and two less steep periods.

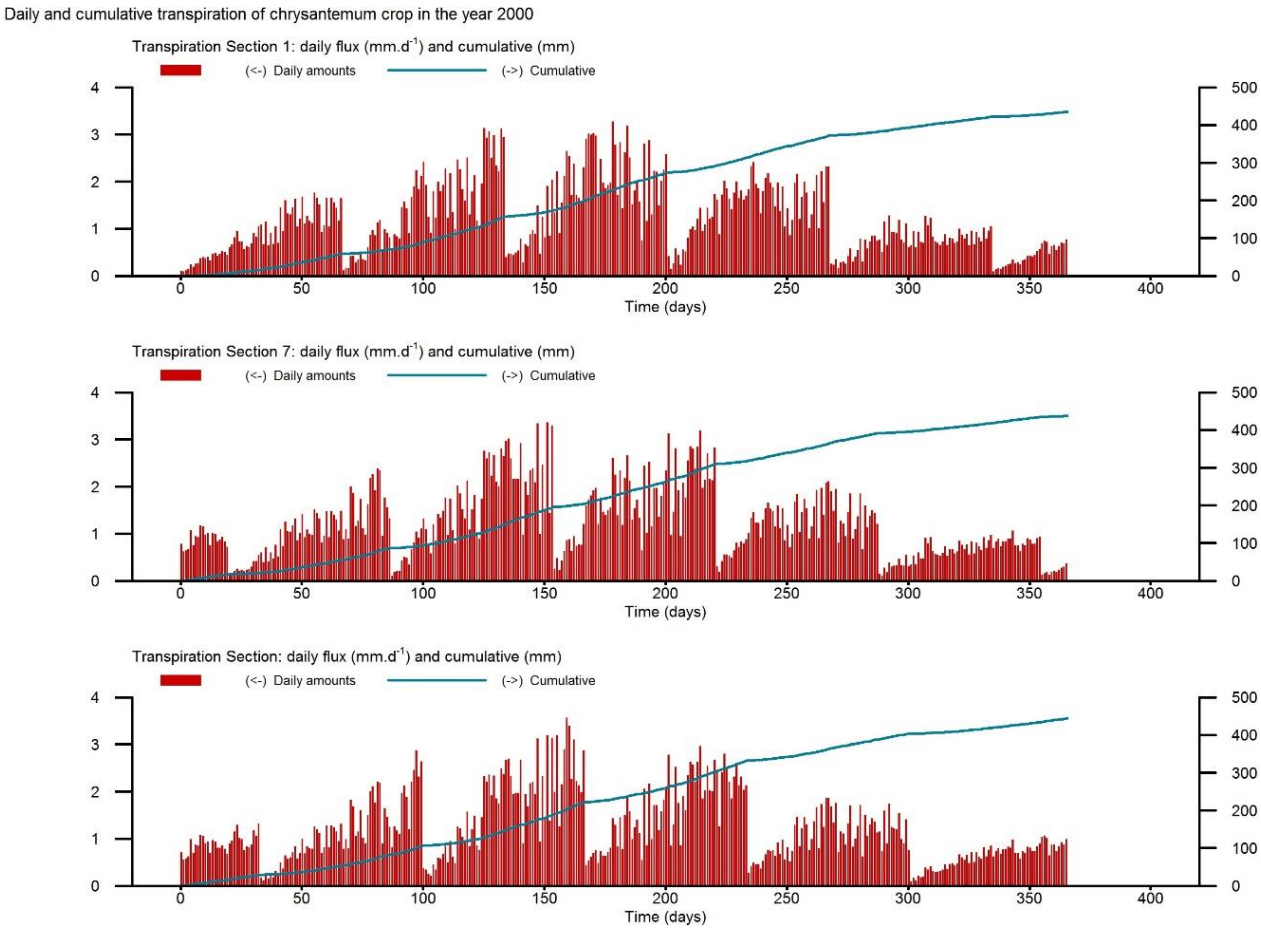

Figure 4.17 *Simulated daily (mm per day) and cumulative (mm) actual transpiration amounts for the three sections in 2000*

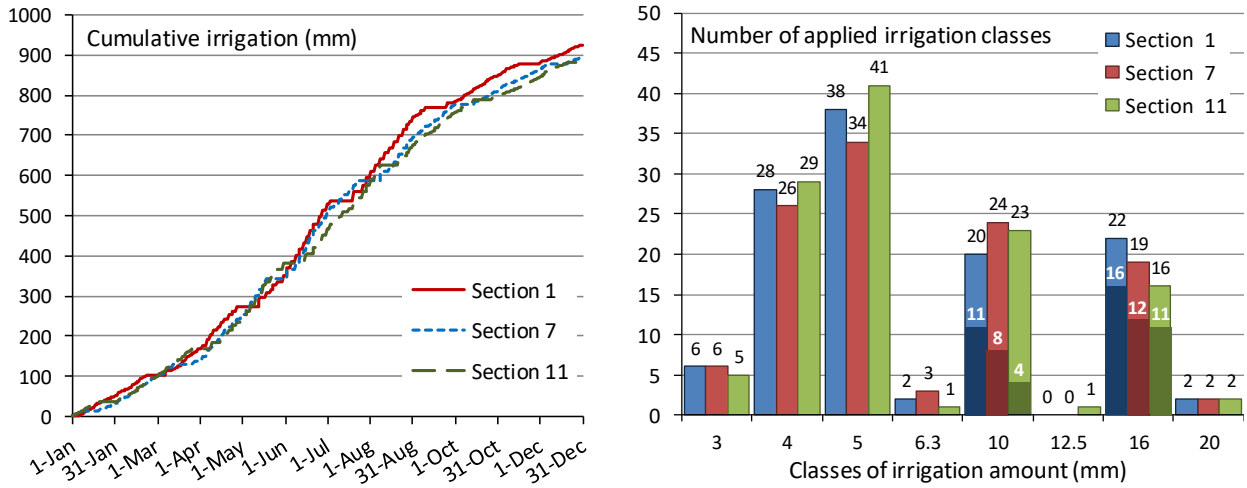

Figure 4.18 *Left: cumulative irrigation amounts (mm) for the three sections in 2000. Right: distribution of the number of applied irrigation events over the eight classes of irrigation amounts for the three sections in 2000. The dark lower parts of the bars of the classes of 10 and 16 mm and the white figures represent the number of breakthrough events from the top layer into the top of the macropores for these classes*

Figures 4.16 and 4.18-right show that the irrigation schemes of the three sections yield 27 breakthrough events grouped in three distinct periods for Section 1, 20 breakthrough events grouped in three distinct periods for Section 7 and 15 breakthrough events grouped in two distinct periods for Section 11. These distinct periods coincide more or less with the above mentioned steep periods in the cumulative irrigation curve of Figure 4.18-left. Figure 4.16 shows a time-shift of around 10 days to 1 month of breakthrough events between the sections: Section 1 comes first, followed by Section 7 and Section 11 comes last. This shift is more distinct for the breakthrough events than for the irrigation periods, stressing the complex relationship between irrigation events and breakthrough events.

There seems to be a clear general relationship between the irrigation amount and the breakthrough events: only the irrigation events of 10 mm and 16 mm induce a breakthrough. The two events of 20 mm of each section and the one event of 12.5 mm of Section 11 do not result in inflow into the top of the macropores. Furthermore, not all events of 10 mm and 16 mm lead to a breakthrough. Figure 4.18-right shows which numbers of both classes per section do (of the total number of events: 34% of class 10 mm and 68% of class 16 mm). This number is higher for Section 1 than for the other sections and higher for class '16 mm' than for class '10 mm'. Therefore, taking the irrigation amount (Iact) alone as predictor for water inflow into the top of the macropores (Itop,mp) by conducting simple linear regression yields no statistically sound relation and consequently gives very low values of R2 (coefficient of determination, the proportion of the variance in Itop,mp that is predictable from Iact): values of 0.18 (all classes of irrigation ≥ 10 mm) and 0.34 (only the classes of 10 and 16 mm). This effect is likely to be caused by the preceding period of individual events. Some of the events are preceded by a drying out period (last phase of each crop) or following a period of rather high radiation but not high enough to trigger an irrigation surplus large enough to initiate inflow into the macropores. This is evident from Figure 4.16 which shows that in order to produce inflow into the top of the macropores events of 10 and 16 mm of irrigation should be preceded by periods of several irrigation events of at least 5 mm and intermitted by only a few days. This also explains the lack of breakthrough in the 20 mm events: these are strongly isolated events, as these are the events deliberately done in the first week after planting, meant to rewet the soil after the drying-out period in the last phase of the preceding crop; preceding irrigation events take place about 15 days before. In this two-weeks period, evapotranspiration continues and depletes moisture content θ of the top layer down to an average as low as 0.343 cm3 cm-3 (θ at saturation = 0.53 cm3 cm-3). Apparently the top layer is too dry to meet the criterion for breakthrough of zero pressure head at the bottom (eq. 4.1) with this highest irrigation amount, given the high irrigation intensity.

From these findings, it is concluded that the irrigation event is the trigger for water breakthrough from the top layer into the macropores and that the initial moisture content determines whether this breakthrough actually takes place. Each irrigation event has a minimum required initial moisture content for reaching saturation (zero pressure head) at the bottom of the top layer. The actual initial moisture content is obtained by irrigation events preceding a breakthrough-inducing irrigation event. To investigate the reliability of this mechanism of a trigger irrigation event depending on a minimum initial moisture content as precondition for breakthrough, a twofold linear regression analyses is conducted with irrigation amount and initial moisture content as predicting variables for breakthrough, only for the irrigation events that yield a breakthrough. All data of the three sections are lumped and used. This yields the following twofold linear regression model:

$$I_{\mathrm{top,mp}} = a_1 \cdot I_{\mathrm{act}} + a_2 \cdot D_{\mathrm{top}} \cdot \theta_0 - b \qquad \text{Eq. 4.4}$$

where:

$I_{\mathrm{top,mp}}$ = inflow from the covering layer into the top of the macropores (mm);
I_{act} = actual irrigation amount applied (mm);
D_{top} = thickness of the top layer (250 mm);
θ_0 = initial average volumetric moisture content of the top layer ($cm^3\ cm^{-3}$);
a1, a2 = regression coefficients (-);
b = regression constant (mm).

The regression coefficients and constant are depending on the thickness and properties of the topsoil and subsoil layers, and the properties of the macropores. For the soil system of the cultivation sections of the chrysanthemum crop the regression yields the following values of the regression parameters: a_1 = 0.927, a_2 = 1.05, b = 133.25 (mm) and R^2 (adjusted) = 0.946.

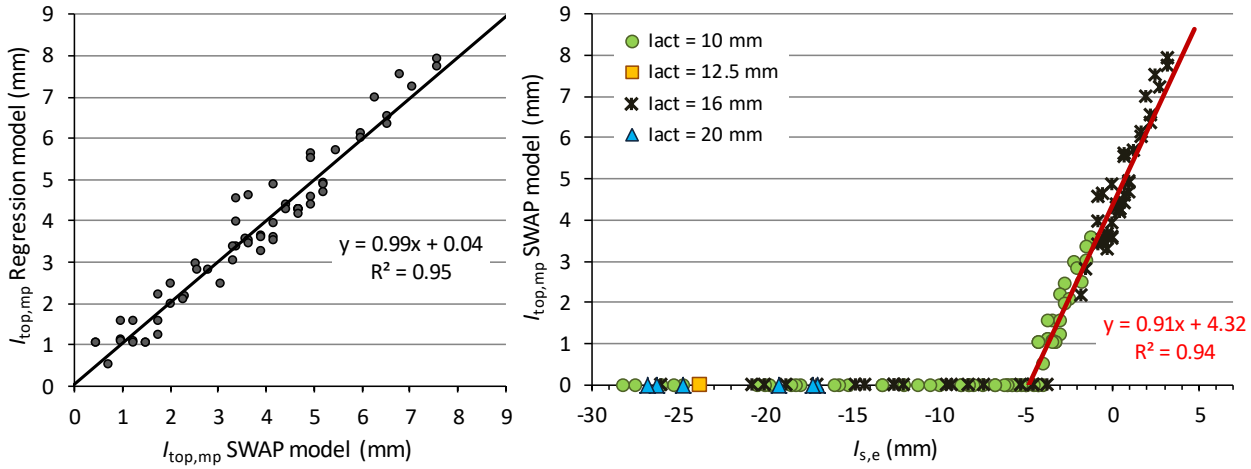

Figure 4.19 *Left: scatterplot of the regression model results plotted against the SWAP results for inflow into the top of the macropores $I_{top,mp}$ (mm). Included is a simple linear regression line according to Eq. 4.4. All data with $I_{top,mp} > 0$ of the three cultivation sections are lumped and used.*
Right: SWAP results for $I_{top,mp}$ (mm) plotted against effective irrigation surplus $I_{s,e}$ (mm, Eq. 4.5) for the data from the four irrigation classes $I_{act} \geq 10$ mm of the three sections. The red line is a simple linear regression model for all data with $I_{top,mp} > 0$, according to Eq. 4.6

Figure 4.19-left depicts a visual representation of the results of this statistical model as a scatterplot of the model results plotted against the SWAP results. The R^2 of the model is high and the slope of the regression line in the plot is close to 1 and the intercept close to 0, indicating a strong resemblance between the results of the statistical model and the SWAP results. It is concluded that the model for predicting inflow into the top of the macropores from irrigation amount and initial moisture content of the top layer is reliable. The initial moisture content is predominantly determined by the irrigation surplus as irrigation amount minus evapotranspiration.

The constraint of the model is that it is not very useful for visualising the status of all combinations of I_{act} and θ_0. Therefore, these two predicting variables are combined in one new predicting variable: an 'effective irrigation surplus' $I_{s,e}$ (mm). 'Effective' for water breakthrough from the top layer and an 'irrigation surplus' in the sense of deducting from the irrigation amount the moisture deficit of the top layer. It is mathematically defined as:

$$I_{s,e} = I_{act} - D_{top} \cdot (\theta_s - \theta_0) \qquad \text{Eq. 4.5}$$

where moisture content at saturation θ_s equals 0.53 $cm^3\ cm^{-3}$. Here again, all data of the three sections are lumped and used.

Figure 4.19-right depicts the results of plotting the $I_{top,mp}$ of SWAP against $I_{s,e}$. But only the data of the irrigation classes of 10 mm and higher are depicted. All irrigation classes smaller than 10 mm yield values of $I_{s,e}$ of -6.0 mm or lower which is well below the threshold value for inducing breakthrough (Eq. 4.6). Simple linear regression on the data for $I_{top,mp} > 0$ with $I_{s,e}$ as predicting variable yields the statistical model below:

$$I_{s,e} \geq -4.75 \rightarrow I_{top,mp} = a \cdot I_{s,e} + b \qquad \text{Eq. 4.6}$$

$$I_{s,e} < -4.75 \rightarrow I_{top,mp} = 0$$

Regression coefficient a = 0.91 and regression constant b = 4.32 (mm); R^2 = 0.936. The value of -4.75 for $I_{s,e}$ is the threshold value of the model below which $I_{top,mp}$ equals zero:

The fact that the threshold value of $I_{s,e}$ for inducing breakthrough is smaller than zero indicates that a completely saturated top layer is not a precondition for breakthrough. This is due to the high irrigation intensity in combination with the high saturated hydraulic conductivity of the topsoil of 81.28 cm d^{-1}. A downward moving water front in an adequately moist but not saturated top layer can reach the bottom of the top layer to create a saturated sub layer where pressure head $h_z > 0$ cm, which is the precondition for breakthrough (Eq. 4.1).

The linear regression model of Eq. 4.6 yields a similar high R^2 as the model of Eq. 4.4 and thus is a similarly reliable model. Figure 4.19 shows clearly that the irrigation classes of 12.5 and 20 mm yield very low values for $I_{s,e}$ that are far below the threshold value due to very low initial moisture contents of the top layer. This is the reason for no breakthrough from the top layer into the top of the macropores for these two classes. It is also clear that in general the class of 16 mm of irrigation yields higher inflow into the top of the macropores than the class of 10 mm of irrigation. Consequently, the class of 16 mm also achieves a higher relative breakthrough-yield than the class of 10 mm:
100% x 188 mm / (57 x 16 mm) = 21% of the total irrigation of the class, versus
100% x 42 mm / (67 x 10 mm) = 6% (see also Figure 4.18-right for total number of events of both classes).

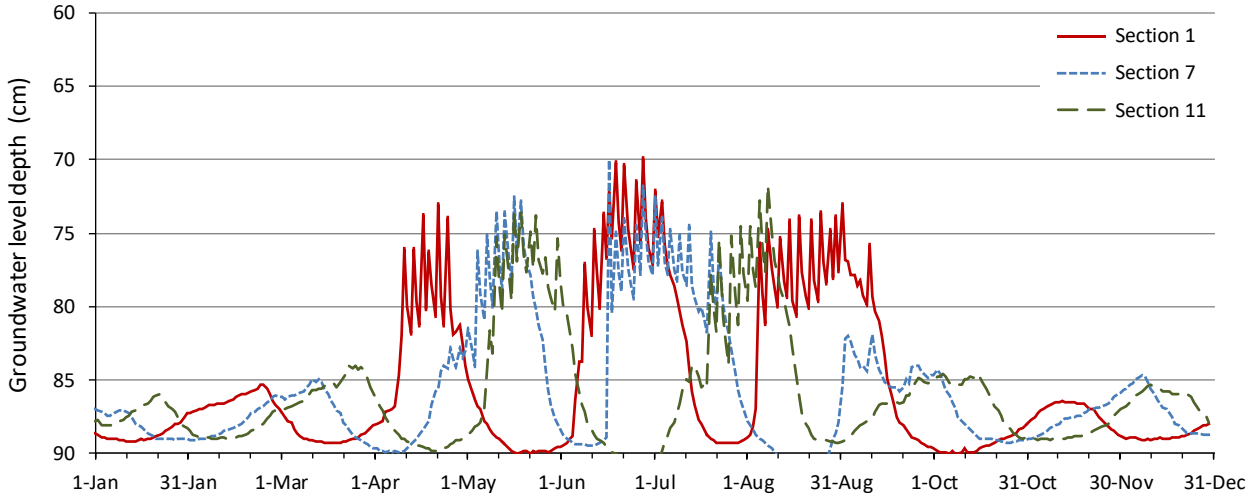

Figure 4.20 *Simulated groundwater levels as state variables at the end of the day in cm below soil surface in 2000 for cultivation sections 1, 7 and 11 with the New Top Layer*

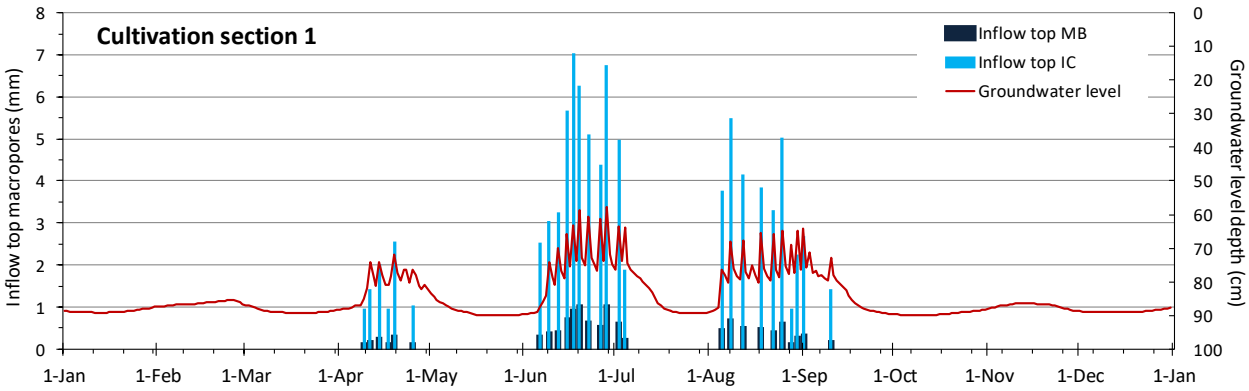

Figure 4.21 *Time series of simulated inflow (mm) from the covering layer into the top of the macropores and groundwater level (cm below soil surface) as state variable at the end of the day in 2000 for cultivation Section 1 with the New Top Layer*

Figure 4.20 depicts groundwater level patterns that strongly resemble the patterns of the irrigation and the patterns of the inflow into the top of the macropores. Figure 4.21 illustrates the latter for cultivation Section 1. Groundwater level movement occurs in two basic patterns: a slow fluctuation on a timescale of a month with a peak amplitude of a few cm and a fast peaking on a timescale of a day with peak heights of 5-10 cm. The latter is typically related to the inflow into the top of the macropores. Upward seepage is low due to the low hydraulic conductivity of the subsoil. To better understand the irrigation pattern in general, which includes the inflow into the top of the macropores, it should be noted that the highest 'wave tops' in this fluctuation start with an inflow into the macropores. Section 1 shows five of these larger timescale wave tops of which three high ones are related to inflow into the top of the macropores; sections 7 and 11 show

both six wave tops with three and two high ones, respectively. These high wave tops are shifted in time among the three sections as discussed above concerning Figures 4.16 and 4.18.

Rapid groundwater level rise is triggered by inflow into the top of the macropores. This is mainly due to the inflow into the IC domain that captures most (ca. 90%) of the inflow into the top of the macropores and rapidly transports this to depths of 25-70 cm. Because in the clay subsoil above drain level (90 cm) the matrix is close to saturation (*h* between 0 and -65 cm) only a small amount of water is needed to rapidly raise the groundwater level (see pF-curve Annex 4, A4.1). On the other hand, only little water loss by drainage is needed to cause the groundwater level to drop. Consequently, groundwater level rise occurs in the form of short-lasting (hours) peaks.

Figures 4.20 and 4.21 show the groundwater level as state variable at the end of the day, the values that are used in the PEARL model. Because irrigation starts at the beginning of the day the peaks occur after 2-3 hours with an initial height of about 50 cm below soil surface. Afterwards, they fade out to the level depicted in Figure 4.20. Annex 2, A2.2 shows examples of the initial peak heights.

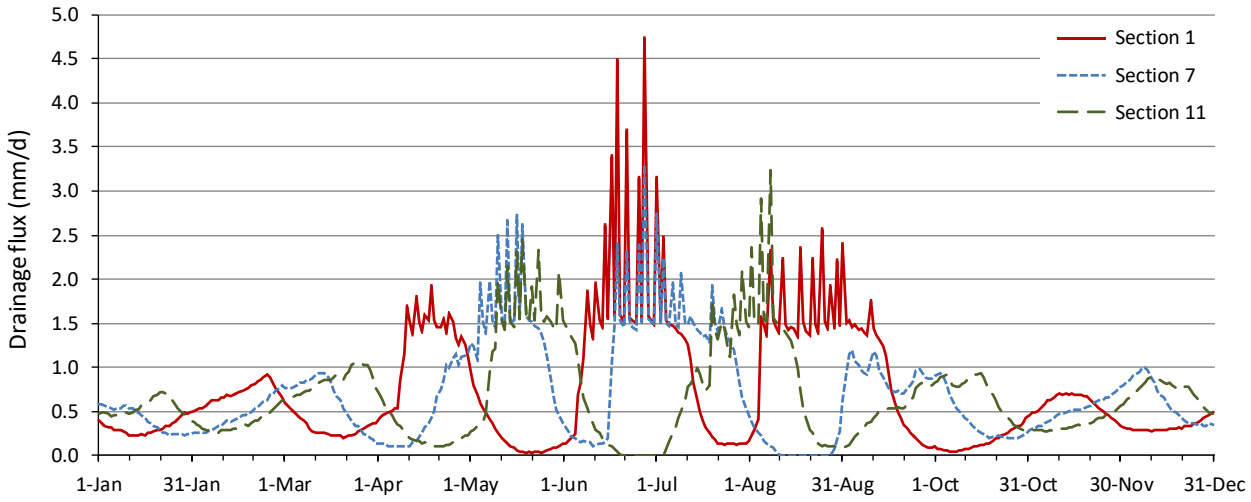

Figure 4.22 *Simulated daily drainage fluxes (MB domain + matrix, in mm/d) in 2000 for the cultivation sections 1, 7 and 11 with the New Top Layer*

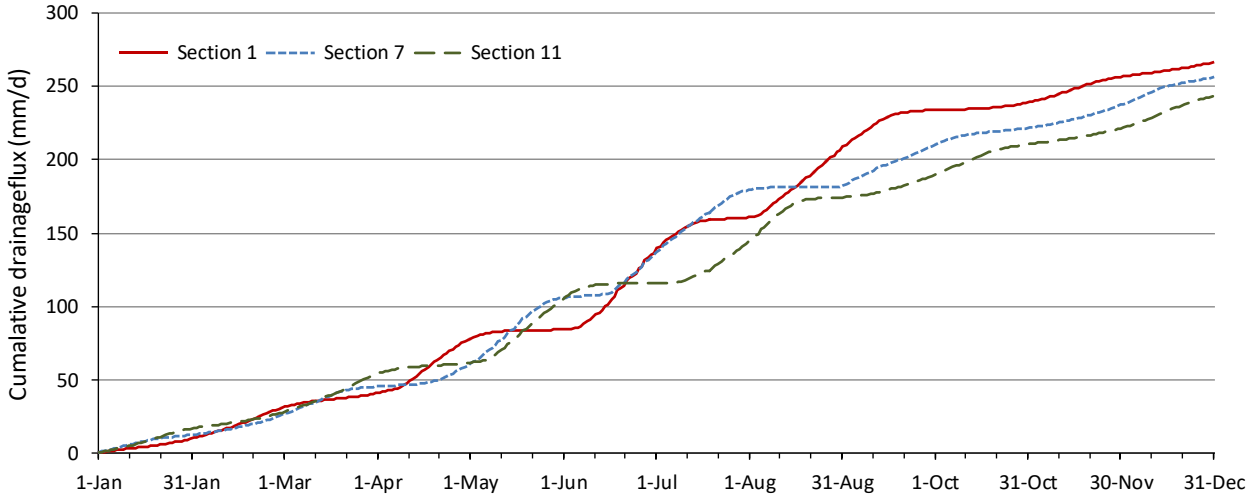

Figure 4.23 *Simulated cumulative drainage fluxes (MB domain + matrix, in mm) in 2000 for the cultivation sections 1, 7 and 11 with the New Top Layer*

The drain fluxes of Figure 4.22 and Figure 4.23 also resemble the patterns of irrigation and inflow into the top of the macropores and thus the pattern of the groundwater level. The same patterns with the same shifts among the three sections occur for the drainage as for the groundwater levels, with a slow fluctuation on a timescale of a month and a fast peaking on a timescale of a day related to irrigation and inflow into the top of the macropores (see Figure 4.20). Drainage is strongly correlated with groundwater level as the difference in hydraulic head between drain level and groundwater level is the driving force of the drainage. For the matrix drainage the matrix groundwater level counts and for the rapid drainage from the MB domain the water level in this domain counts. Since the top-inflow into the MB domain is small compared to the inflow from the matrix into the MB domain (Figures 4.13 and 4.7 top-right) the difference between these two groundwater levels will be small and in times of drainage - when groundwater level is above the drain depth of 90 cm - lower in the MB domain (because the matrix is draining into the MB domain).

The relationship between groundwater level and drainage flux is non-linear (Figure 4.24). When the rising groundwater level reaches the bottom of the IC domain the water exchange between IC domain and MB domain via the soil matrix is enhanced by the soil matrix becoming saturated at a depth where both IC and MB macropores exists. Consequently, rapid drainage from the MB domain increases. The static macropores of the IC domain end at a depth of 70 cm below the soil surface. But the drain fluxes show an increase for groundwater levels starting from about a depth of 75 cm below the soil surface and shallower. This is due to the boundary pressure head h_e of -5 cm that implies a saturated matrix at a depth of 5 centimetres above groundwater level.

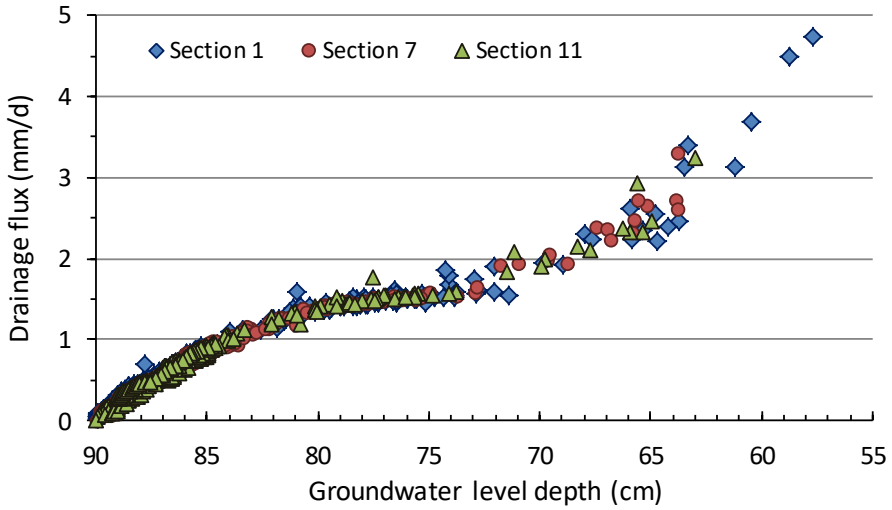

Figure 4.24 *Simulated daily drainage fluxes (MB domain + matrix, in mm/d) plotted against simulated daily average groundwater levels (cm below soil surface) for the cultivations sections 1, 7 and 11 with the New Top Layer. Depth of drainpipe 0.9 m.*

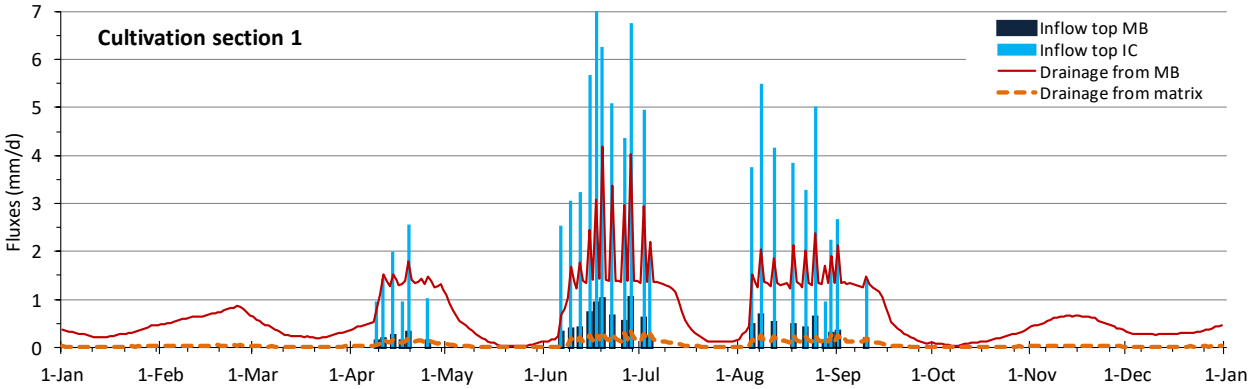

Figure 4.25 *Simulated inflow (mm) from the covering top layer into the top of the macropores and daily drainage fluxes (mm/d) from the MB domain and from the soil matrix in 2000 for the cultivation Section 1 with the New Top Layer*

Figure 4.25 is an example of the resemblance between the patterns of daily drainage fluxes and inflow into the top of the macropores for Section 1. Only for the rapid drainage from the MB domain the resemblance with the top-inflow pattern is good. The base flow drainage from the matrix only resembles the slow fluctuation-pattern of the groundwater level with its five 'wave tops' (see Figure 4.21).

As is expressed by Eq. 4.1, inflow into the top of the macropores can occur when the pressure head h_z at the bottom of the top layer at 25 cm depth is equal to or greater than zero (in the model this is implemented as in Eq. 4.3). When this condition is met, the bottom compartment of this layer is saturated. Figure 4.26 visualises this condition for Section 1 as the time-series of daily maximum pressure head h_z (maximum of the one-hundred output values per day, thus with a time-resolution of about 15 min.). The figure shows that peaks in the drainage from the MB domain coincide with values of zero (or slightly higher) for pressure head h_z. The drainage peaks are slightly behind because they count for the end of the day while the maximum pressure heads count for the exact moment within the day which is between 0.05 and 0.13 day (1:20 h and 3:12 h).

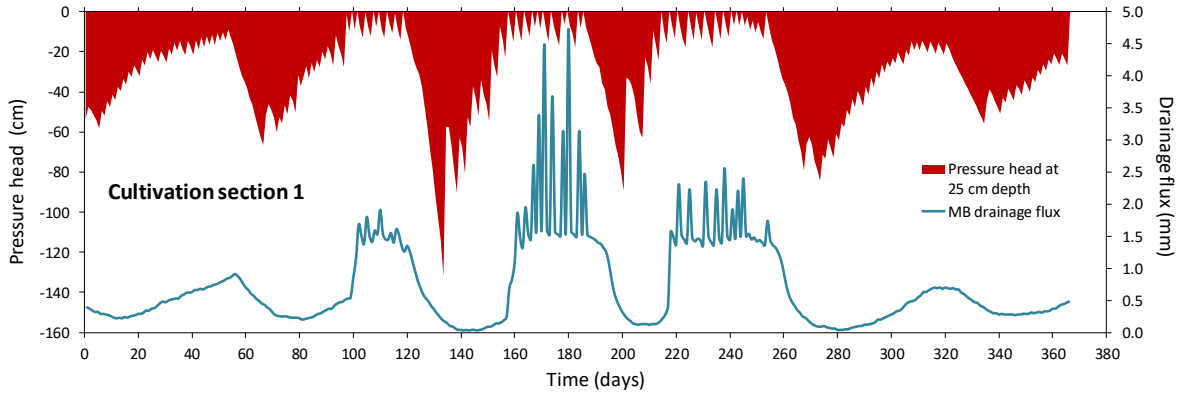

Figure 4.26 *Simulated daily maximum pressure heads (cm) at the bottom of the top layer at 25 cm depth and daily drainage fluxes (mm/d) from the bypass (MB) domain in 2000 for the cultivation Section 1 with the New Top Layer. Zero time = 1 January 2000.*

In Figure 4.27, this comparison is made for all sections, but with the pressure head output at the end of the day, the data that is used by PEARL. The values of the pressure head at the end of the day are lower than those shortly after the irrigation application at the beginning of the day. Thus in the figure they do not reach up to values of zero or higher. But still the patterns are similarly illustrative as the pattern shown in Figure 4.26. They show that all high pressure heads and thus moments with saturated bottom compartment of the top layer occur in the summer half-year (day 92 to 275) when irrigation is highest with irrigation amounts mostly equal or higher than 10 mm.

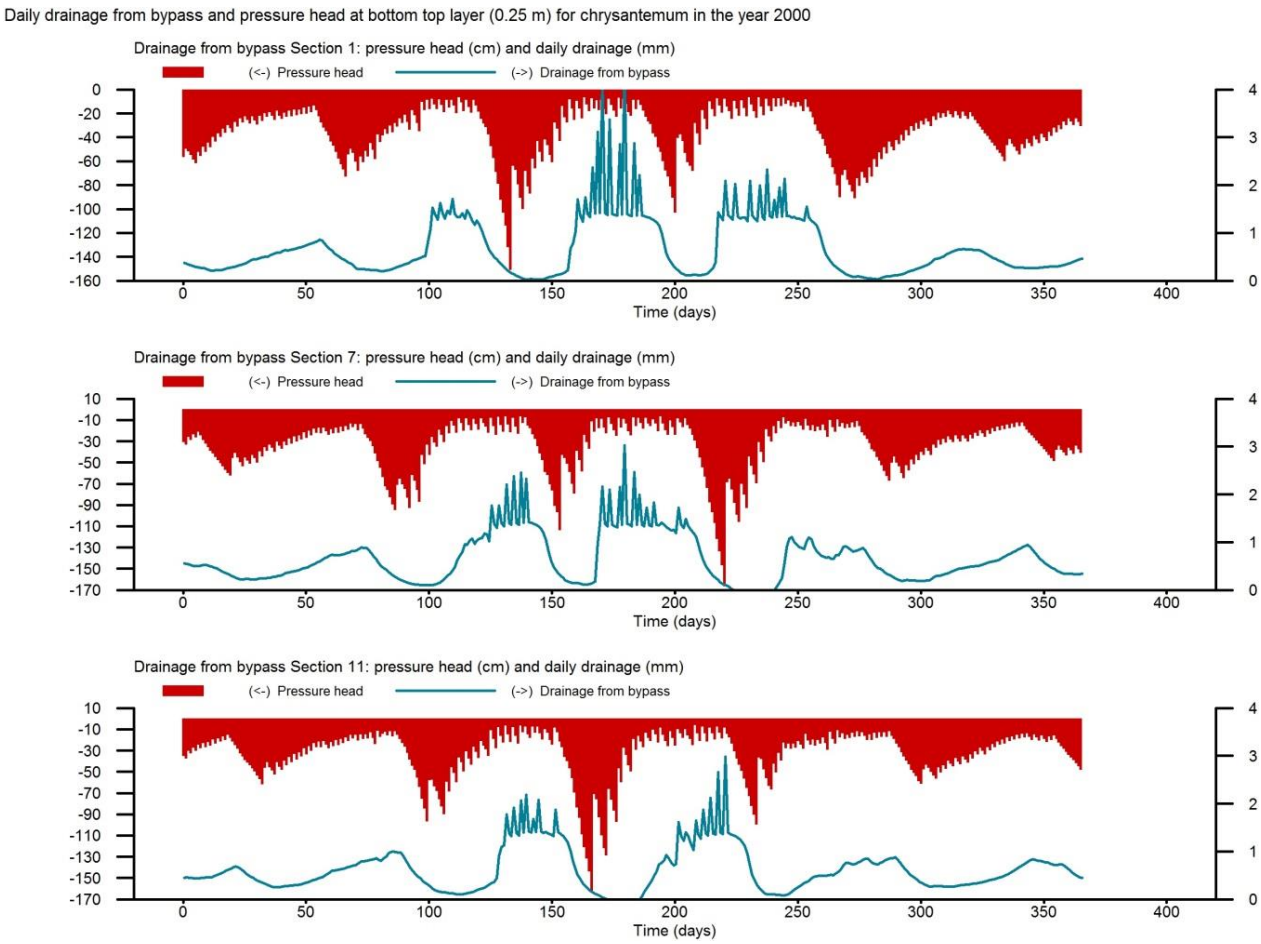

Figure 4.27 *Simulated pressure heads (cm) at the bottom of the top layer as state variables at the end of the day and daily drainage fluxes (mm/d) from the bypass (MB) domain in 2000 for the cultivation sections 1, 7 and 11 with the New Top Layer. Zero time = 1 January 2000.*

They also show that in dry periods with little or no irrigation and high transpiration, low pressure heads h_z coincide with low or no drainage fluxes. No-drainage only occurs in the model if the groundwater level is below drain depth (90 cm below soil surface). When in dry periods pressure head at 25 cm depth rises again due to substantial irrigation, the increase of the drainage flux is 20-25 days behind because of the time it takes for the irrigation water to flow from 25 cm depth to drain depth.

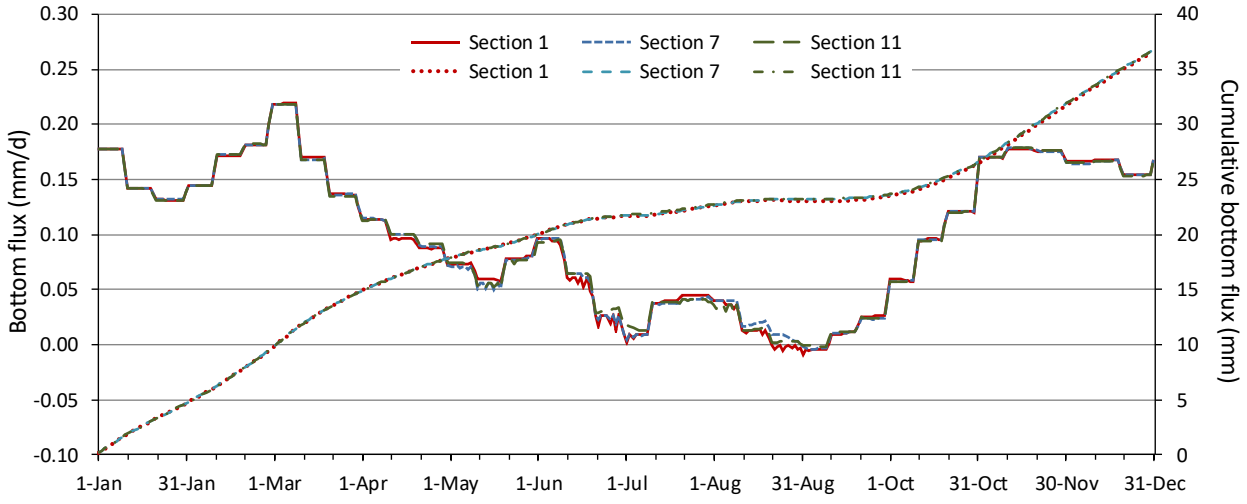

Figure 4.28 *Simulated daily and cumulative bottom fluxes (mm/d and mm) in 2000 for the cultivation sections 1, 7 and 11 with the New Top Layer. Positive is upward seepage.*

Daily and cumulative bottom fluxes hardly differ between the three cultivation sections (Figure 4.28). The small differences in the summer half-year are due to differences in groundwater levels between the sections.

4.4 Recommendations for the revised description of the soil system

The description of the soil profile of the greenhouse soil was improved by introducing a top layer of 0.25 m thick without macropores. The absence of macropores is justified by the practice of rototillage of the topsoil after each chrysanthemum cultivation period. Another improvement of the parameterisation of the soil system was made by lowering the value for the saturated hydraulic conductivity of the subsoil, i.e. 0.168 cm d^{-1} instead of the original value of 4.37 cm d^{-1}. The lower value of K_{sat} for the subsoil resulted in a strong decrease of the upward seepage across the bottom boundary of the soil profile.

The occurrence of peaks in the drainage from the bypass domain depends on the moisture condition in the bottom compartment of the top layer. As soon as the pressure head reaches a value of – 5 cm, water infiltrates the bypass domain of the subsoil. These high moisture contents occur mostly during the summer period, since in this period regular irrigation occurs with amounts ranging between 10 and 16 mm a day. Because of the absence of macropores in the topsoil there is a delay in the occurrence of peaks in the drainage from the bypass domain compared to the timing of the irrigation events. The bottom layer of the topsoil has to become nearly water-saturated first before drainage from the bypass domain starts.

Because the greenhouse represented in the GEM 3.3.2 surface water scenario was selected from a set of twelve representative greenhouses, the change in the description of the soil profile of this greenhouse may result in a different vulnerability compared to that obtained for the GEM 3.3.2 scenario. Therefore, the selection procedure needs to be repeated to check whether greenhouse 5 remains the greenhouse to be used for the surface water scenario. As other representative greenhouses also have a macro-porous soil system, the parameterisation of the soils need to be adjusted to include a similar top layer without macropores as has been done for the soil of greenhouse 5. The set-up and results of the greenhouse selection procedure is presented in Chapter 6.

5 Transport of substance into a macroporous subsoil

In the current (GEM 3.3.2) concepts for the entry of pesticides in a macroporous soil, it is assumed that the macropores start at the soil surface. In that case the mass of pesticide entering the macropores via run off is described by:

$$R_{r,byp} = (f_{mix} \cdot I_{r,byp} \cdot c_{L,mix}) / z_{mix} \qquad \text{Eq. 4.7}$$

$$R_{r,ica} = (f_{mix} \cdot I_{r,ica} \cdot c_{L,mix}) / z_{mix} \qquad \text{Eq. 4.8}$$

with:

$R_{r,byp}$	=	volumic mass rate of pesticide run-off into bypass domain	(kg m^{-3} d^{-1})
$R_{r,ica}$	=	volumic mass rate of pesticide run-off into internal catchment domain	(kg m^{-3} d^{-1})
$I_{r,byp}$	=	areic volume rate of run-off into bypass domain	(m^3 m^{-2} d^{-1})
$I_{r,ica}$	=	areic volume rate of run-off into internal catchment domain	(m^3 m^{-2} d^{-1})
z_{mix}	=	depth of mixing layer	(m)
f_{mix}	=	coefficient for interaction between run-off and soil in mixing layer	(-)
$C_{L,mix}$	=	concentration of pesticide in liquid phase of mixing layer	(kg m^{-3})

In these equations the factor f_{mix} is included to take account for the interaction between the water entering the macropores and the soil in a top layer with thickness z_{mix}.

For a soil profile with a top layer without macropores this interaction does not occur. In that case the mass flux entering the macropore domain at depth *z* is related to the concentration in the liquid phase at the bottom boundary of the top layer. Hence, the factor f_{mix} is not relevant. Therefore, the equations for the transport of substance into the macropores are changed into:

$$J_{r,byp} = (I_{r,byp} \cdot c_{L,btl}) \qquad \text{Eq. 4-9}$$

$$J_{r,ica} = (I_{r,ica} \cdot c_{L,btl}) \qquad \text{Eq. 4-10}$$

with:

$J_{r,byp}$	=	areic mass rate of pesticide run-off into bypass domain	(kg m^{-2} d^{-1})
$J_{r,ica}$	=	areic mass rate of pesticide run-off into internal catchment domain	(kg m^{-2} d^{-1})
$c_{L,btl}$	=	concentration in liquid phase at bottom of soil layer without macropores	(kg m^{-3})

The terms $I_{r,byp}$ and $I_{r,ica}$ represent the water flux entering either the main bypass domain or the internal catchment domain at the depth in soil below which a macropore system exists.

6 Greenhouse selection

For the scenarios as developed by Wipfler et al. (2014), twelve greenhouse class-soil combinations were identified with a coverage larger than 3% of the total area with soil-bound crops. They selected representative growers for each greenhouse class – soil combination. The groundwater tables classes for the locations of these growers were obtained using the map on groundwater table classes as prepared by Massop et al. (2006). The locations on the soil map and the groundwater table map are shown in Figure 6.1 (see also Wipfler et al., 2014). The characteristics of the selected representative greenhouses are given in Table 6.1.

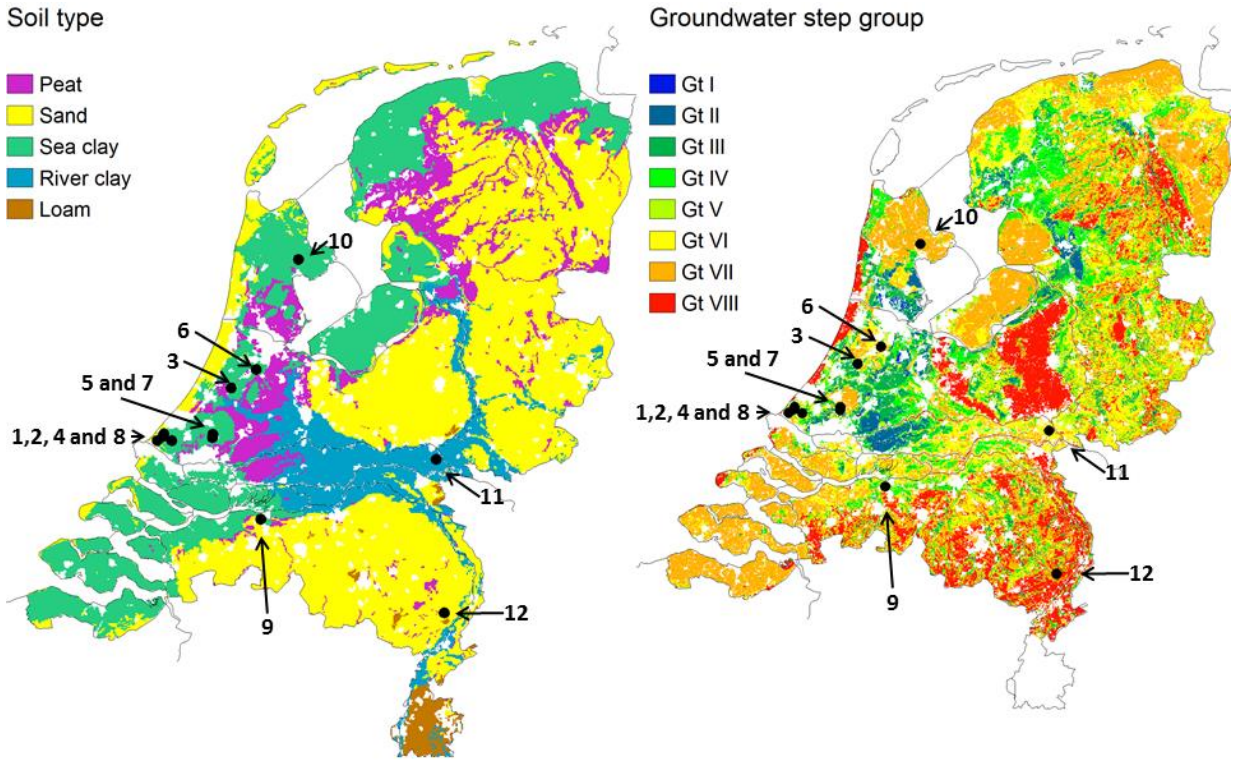

Figure 6.1 *Selected representative greenhouses nr 1 to 12 projected on the soil type map and the groundwater map with table classes (definitions are provided in Annex 2 of Wipfler et al. (2014))*

Table 6.1 *Characteristics of the selected representative greenhouses. The geographical location of the greenhouses is given in Figure 6.1. More details on hydrotypes in Massop et al., 2006*

Greenh. nr	size (ha)¶	Soil type	Groundw. Table class[1]	Crop type	Hydrotype
1	1.716	Heavy sandy clay	IIIb	Chrysanthemum	Westland DHC
2	2.1	Light sandy clay	IIIb	Chrysanthemum	Duinstrook
3	1.8119	Peat	IIIb	Alstroemeria and other flowers	Westland HC
4	10.7	Sand	IIIb	Vegetables	Westland D
5	5	Heavy clay	IV	Chrysanthemum	Westland C
6	2	Heavy sandy clay	IV	Vegetables	Westland C
7	4	Light clay	IV	Flowers	Westland C
8	1.98	Light sandy clay	IV	Chrysanthemum	Westland D
9	6.24	Sand	IV	Chrysanthemum	Westland DH
10	3.8	Heavy sandy clay	V	Freesia	Westland DC
11	5.24	Light sandy clay	V	Freesia and other flowers	Betuwe komgronden
12	3.85	Sand	V	Chrysanthemum	Dekzand profiel

¶ Size represents the average area of the greenhouse type.

[1] Definitions of the groundwater table classes are given in Annex 2 of Wipfler et al. (2014).

6.1 Surface water

6.1.1 Procedure

The target of the exposure assessment is the 90th percentile of the peak concentration in surface waters adjacent to greenhouses growing soil-bound crops. So we need a procedure to simulate the frequency distribution of all peak concentration in surface waters adjacent to these greenhouses. We used the procedure in Wipfler et al. (2014) with the following modifications in the parameterisation of the chrysanthemum crop and the greenhouse soil:

- All cultivation and cultivation sections were parameterized separately;
- The irrigation scheme is different for each cultivation section and differs from year to year for each section;
- If a macropore system was present, the top layer was assumed to have no macropores due to ploughing between cultivations.

The frequency distribution was constructed as follows:

- Simulations were done with PEARL and the TOXSWA metamodel for all 24 cultivation sections within the 12 representative greenhouses described in Wipfler et al. (2014). So this gave 12x24=288 model runs;
- Each simulation gives 7 annual maximum concentrations. We selected only the year with the highest annual maximum concentration for the construction of the frequency distribution, which corresponds to the 93rd-temporal percentile.
- These data points were sorted to obtain a cumulative frequency distribution. Each greenhouse represents an area (cf. Section 5.2 in Wipfler et al. (2014)), which was used as a weighting factor.

Tiktak et al. (2012) showed that the ranking of locations (in this case greenhouses) is substance dependent. This implies that a greenhouse that is sufficiently conservative for one substance may not be conservative for another substance. For this reason, we performed simulations for six substances (see Table 6.2 in Wipfler et al. 2014) and selected the greenhouse that was sufficiently conservative for all substances.

Because the irrigation regime was now different between the years, timing might have an effect on the maximum annual concentration. For this reason, we performed simulations with an application date of February 15, May 15, August 15, and November 15. Application was done to the crop canopy with a dosage of 1 kg/ha (see Section 6.9.2 in Wipfler et al. (2014) for details).

6.1.2 Results

The next step is to find the greenhouses for which the 93rd temporal percentile is most often above the 90th overall percentile. Table 6.2 shows that this is the case for greenhouse 5. So this greenhouse was selected as the scenario greenhouse. This greenhouse is situated on a heavy clay soil, where preferential flow may occur. Greenhouse 5 was already selected by Wipfler et al. (2014), so the new procedure did not change the selected greenhouse.

Table 6.2 *Number of times that the 93rd temporal percentile is above the 90th overall percentile*

Greenhouse	**Substance**					
	P01	**P02**	**P03**	**P04**	**P05**	**P06**
1	13	20	10	20	15	20
2	4	0	10	0	0	0
3	0	0	0	0	0	0
4	0	0	0	0	0	0
5	73	92	92	92	92	92
6	2	0	0	0	0	0
7	3	0	0	0	0	0
8	0	0	0	0	0	0
9	0	0	0	0	0	0
10	0	0	0	0	0	0
11	3	0	0	0	0	0
12	15	0	0	0	5	0

6.2 Groundwater

6.2.1 Procedure

Following the decision tree for groundwater risk assessment for field crops in the Netherlands, the annual leaching concentration at 10 m depth should not exceed the drinking water criterion of 0.1 µg/L under realistic worst case conditions. For this protection goal the working group for the revision of the scenarios used the same criterion as was used by the previous working group to derive the exposure scenarios (Wipfler et al. (2014). This criterion is defined as the average annual concentration in groundwater for at least 90th of the population (in time and space). As a conservative approach the target concentration should be less than 0.1 µg/L at 1 m depth.

Compared to the scenarios developed by Wipfler et al. (2014), the following changes were made in the parameterisation of the 12 greenhouse class – soil combinations:

- All cultivation sections were parameterized separately
- All cropping cycles within a single cultivation section were parameterized separately
- The irrigation schedules for each cultivation section follow the same parameters, but due to the shift in planting sequence, they differ from each other and consequently are different from year to year
- If a macropore system was present, the top layer was assumed to have no macropores due to soil tillage between cultivations

The scenario selection procedure for groundwater was similar to the procedure adopted by Wipfler et al. (2014). For each greenhouse class - soil type combination, the 90th-percentile of the leaching concentration at 1 m depth was calculated for the FOCUS groundwater substances A to D (FOCUS, 2000). The annual application rate was set at 1 kg/ha and the application dates were 15 February, 15 May, 15 August or 15 November. The calculations were done for all cultivation sections with uneven numbers.

6.2.2 Results

For each substance – application date combination the cumulative frequency distribution was determined for each greenhouse type. The analysis was limited to substance B and the metabolite of substance C, being compounds with a comparatively high leaching potential.

Based on the cumulative frequency distribution, the number of times were counted for the median PEC (PEC50) computed to be in the target percentile range, i.e. 87 to 93. The results are given in Table 6.3.

Table 6.3 *Occurrence of PEC leaching in required percentile range 87-93*

Substance	**Application date**	**Number of times median PEC in leaching water in spatial percentile range 87-93**		
		Representative greenhouse (GH) number		
		GH 8	**GH 10**	**GH 11**
B	15 February	6	6	5
	15 May	4	9	0
	15 August	2	7	4
	15 November	4	3	6
Metabolite C	15 February	8	6	3
	15 May	7	4	2
	15 August	6	5	5
	15 November	4	9	2
Total number of times selected		41	49	27

The results show that both greenhouse 8 and 10 are comparable in view of the number of times the PEC was calculated to be in the required percentile range. Greenhouse 8 belongs to greenhouse class 3b that is linked to ground water table class III and IV (see Wipfler et al. 2014). This greenhouse class covers 34% of the

area of soil-bound cultivations. Greenhouse 8 has a type IV groundwater class (see Table 6.1). This means that the groundwater level fluctuates. Seepage, infiltration as well as percolation of excess water to groundwater may occur. The mean highest groundwater level is between a depth of 40 and 80 cm and the mean lowest groundwater level is between a depth of 80 and 120 cm (see Annex 2 for more details). Furthermore, greenhouse 8 is located in the Westland area with a large proportion of soil bound greenhouse cultivations. Therefore, this greenhouse was selected for the groundwater scenario.

In a next step an assessment was done to select the appropriate cultivation section. Upon reviewing the percentiles of the PEC50 for each cultivation section for all substance – application date combinations the cultivation Section 21 was selected. In 7 out of 8 substance-application date combinations the percentile was calculated to be in the percentile range of 87-93. In one case a percentile value of 85.5 was calculated, but this value is close to the lower boundary of the required range. More details on the results of these calculations are presented in Annex 5.

6.3 Specification of surface water scenario

The results of the renewed scenario selection procedure showed that greenhouse 5 was selected again. As the greenhouse comprises 24 cultivation sections that have been parameterized separately, with different starting times of the crop cycle, the number of sections that have to be considered to result in a representative scenario for this greenhouse has to be assessed. In principle all cultivation sections could be considered to calculate the water flux discharged via the drains and the concentration of the substance in the drain water. This could be done by averaging the water fluxes and calculate the flux-weighted average of the concentration in the drain water. There are about five crop cycles per year for each of the cultivation sections. Therefore differences in starting time of a crop between the different cultivation sections are small: for the odd cultivation sections the differences between two subsequent cultivation sections was only 3-8 days. A reduction of the number of cultivation sections may result in representation of the greenhouse system with acceptable accuracy. Therefore, a series of runs were executed for three substances in combination with an absolute application for a set of 3, 6 or 12 cultivation sections out of the total of the 12 odd cultivation section numbers.

In the parameterisation of the TOXSWA model, the discharge of drain water from greenhouse is considered to be a point source at the upper boundary of the ditch. The mass of substance in the drain water is taken to be an incoming mass flux this upper boundary. The concentration in the water layer calculated may then be driven by the daily concentration in the drainage water or by the daily flux of substance in the drainage water (i.e. the product of concentration and water flux) or by a combination of these two. If the daily water volume of the drainage flux is negligibly small compared to that of the ditch, then the concentration in the water layer as calculated by TOXSWA is driven by the drainage substance flux and if this volume of the drainage flux is much larger than that of the ditch then the concentration in the water layer is driven by the drainage concentration. The scenario assumes that 1 ha of greenhouse is linked to 100 m ditch. The drainage fluxes are in summer typically 2 mm/d (see Figure 4.22). This gives 20 $m^3.ha^{-1}$ which flows into a ditch with a volume of typically 50 m^3. So we are in the intermediate range where the concentration in the water layer as calculated by TOXSWA is driven both by the drainage concentration and the drainage substance flux.

The simulation period consists of six warming up years (1994-1999) followed by seven years (2000-2006) used for the evaluation. Results are shown for these seven years. The endpoint of the evaluation is based on the yearly maxima of the concentrations in TOXSWA so the analysis in Section 6.3.1 focusses on the yearly maxima of the drainage fluxes and that in Section 6.3.2 on the yearly maximum substance mass fluxes and substance concentrations.

6.3.1 Drainage water fluxes

The temporal pattern of the drainage fluxes is shown in Figure 6.2 for the 12 odd sections separately and averaged. This figure shows that the seven yearly maxima of the average drainage flux of water are about 2-3 times lower than the seven yearly maxima of all simulated cultivation sections. It can be derived from the figure that maxima occur mostly somewhere between 1 May and 1 October. Figure 6.3 zooms in on two

of the seven years and shows that differences between the cultivation sections were highest in June-July: the yearly maximum of a certain cultivation section may coincide with a zero flux of another cultivation section. Between about 1 October and 1 May the differences are smaller and none of the cultivation sections generates a zero flux. The differences are driven by the water demand of the crop and the irrigation regime: between 1 May and 1 October both the demands and irrigation gifts are higher (See Section 4.3.2.2, Figure 4.16).

Further inspection of the data showed that the seven yearly maxima of all 12 cultivation sections were generated by different cultivation sections. This could be expected because the starting dates of the growth cycles of a single cultivation section differ from year to year.

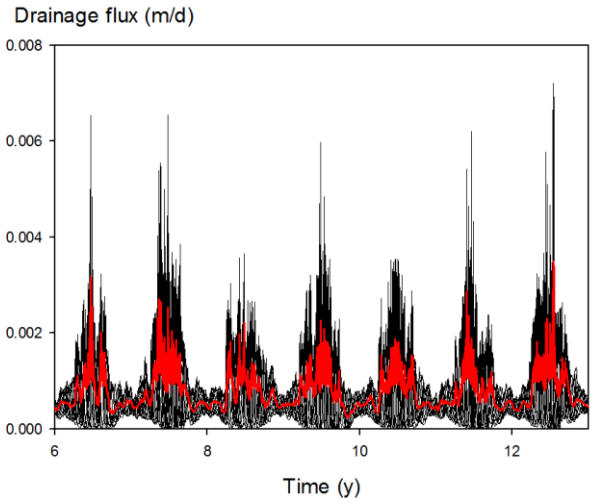

Figure 6.2 *Daily average drainage fluxes of water from 12 sections (black lines) as a function of time compared with the average flux (red line) for the evaluation period of seven years*

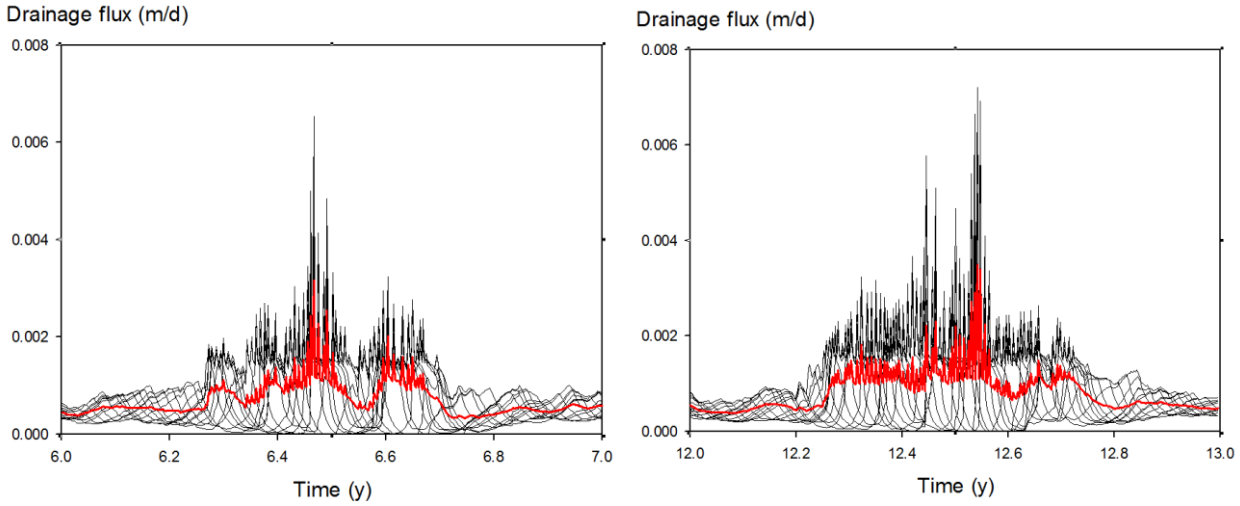

Figure 6.3 *Daily average drainage fluxes of water from 12 cultivation sections (black lines) as a function of time compared with the average flux (red line) for two selected years of the 7-y evaluation period*

6.3.2 Concentrations and mass fluxes in drainage water

Calculations were made for a tracer substance (no plant uptake, no sorption, no degradation and no volatilisation) with applications to the soil surface of 1 kg/ha at either 15 May or 15 August.

The average concentration in the drainage water was calculated by multiplying each concentration with its water flux and dividing by the sum of all water fluxes. Figure 6.4 shows that the difference between the yearly maxima of the individual cultivation sections and those of the average was no more than 20-30%, so smaller than the difference for the water fluxes. Detailed inspection of the data showed that the seven yearly maxima were generated by seven different cultivation sections. Application on 15 May generated higher maximum concentrations than on 15 August, probably because the highest drainage fluxes occurred before 15 August (Figure 6.3).

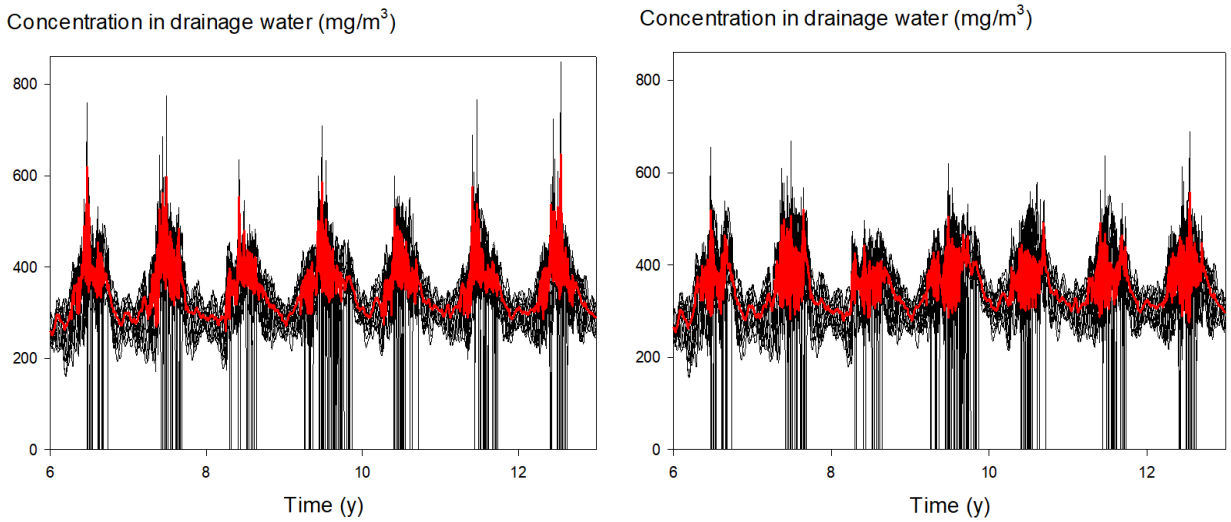

Figure 6.4 *Daily average concentrations of tracer in drainage water from 12 cultivation sections (black lines) as a function of time compared with the average concentration (red line) for the evaluation period of seven years after yearly application of 1 kg/ha on 15 May (left) and 15 August (right)*

Figure 6.5 shows that the difference between the maxima of the average and the individual mass fluxes is typically a factor of 2 so much larger than found for the concentrations and close to the differences found for the water fluxes. The patterns of the average fluxes after application on 15 May and 15 August are very similar and they are also very similar to that of the average water fluxes shown in Figure 6.2.

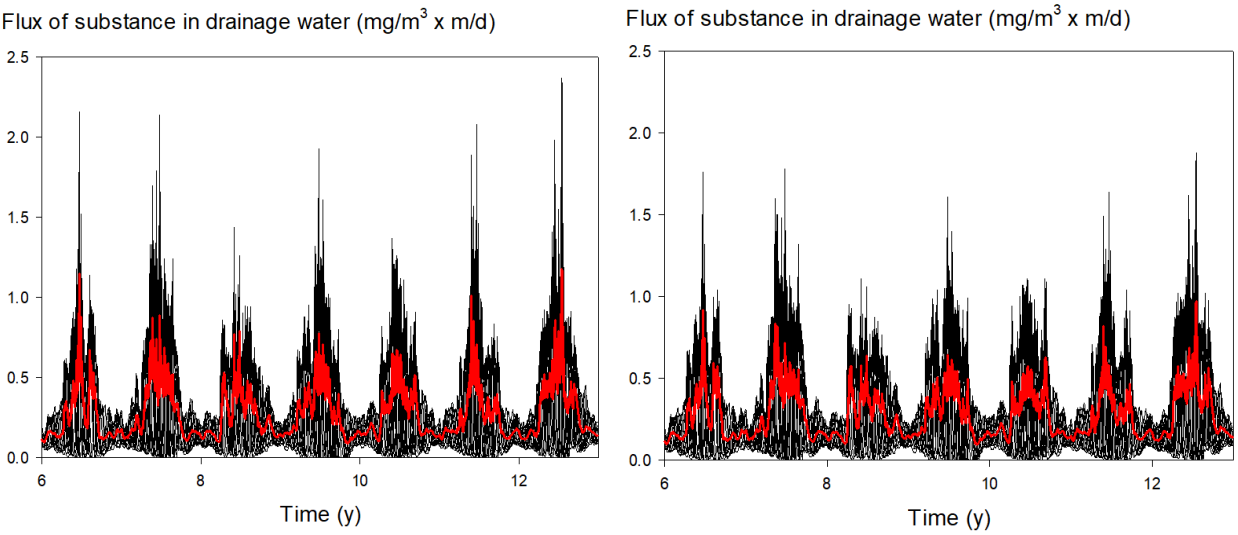

Figure 6.5 *Daily mass fluxes of tracer in drainage water from 12 cultivation sections (black lines) as a function of time compared with the average mass flux (red line) for the evaluation period of seven years after yearly application of 1 kg/ha on 15 May (left) and 15 August (right)*

To assess whether the surface water scenario can be based on a subset of cultivation sections, a series of runs were done for a selection of 3, 6 or 12 cultivation sections. By lowering the number of cultivation sections the computation time could be reduced substantially. On the other hand it would lead to greater uncertainty in the mass flux of substance or the concentration of the substance in drain water.

For a subset of 12 cultivation sections the cultivation numbers selected were 1, 3, 5, …, 23. For a subset of 6 cultivation sections, the section numbers were 1, 5, 9, 13, 17 and 21 and for the subset of 3 cultivations sections, the section numbers were 1, 9 and 17. For these 3 sections there are four options (1-9-17, 3-11-19, 5-13-21 and 7-15-23) of which only the first is considered. It should be noted that the numbers were selected based on the criterion that the differences between the numbers should be equal to obtain as much spread between the crop cycles as possible.

The calculations were done for tolclofos-methyl, being a frequently-used compound in the cultivation of chrysanthemum. The value for the K_{om} of this substance was set at 2099 L/kg and the DegT50 was taken to be 108 d. The application rate was set at 16 kg ha^{-1} just before the start of four of the five growing cycles of each year. As the start of the growing cycles differ between the cultivation sections, the actual application dates, as they are relative to the start of the growing cycle, are also different.

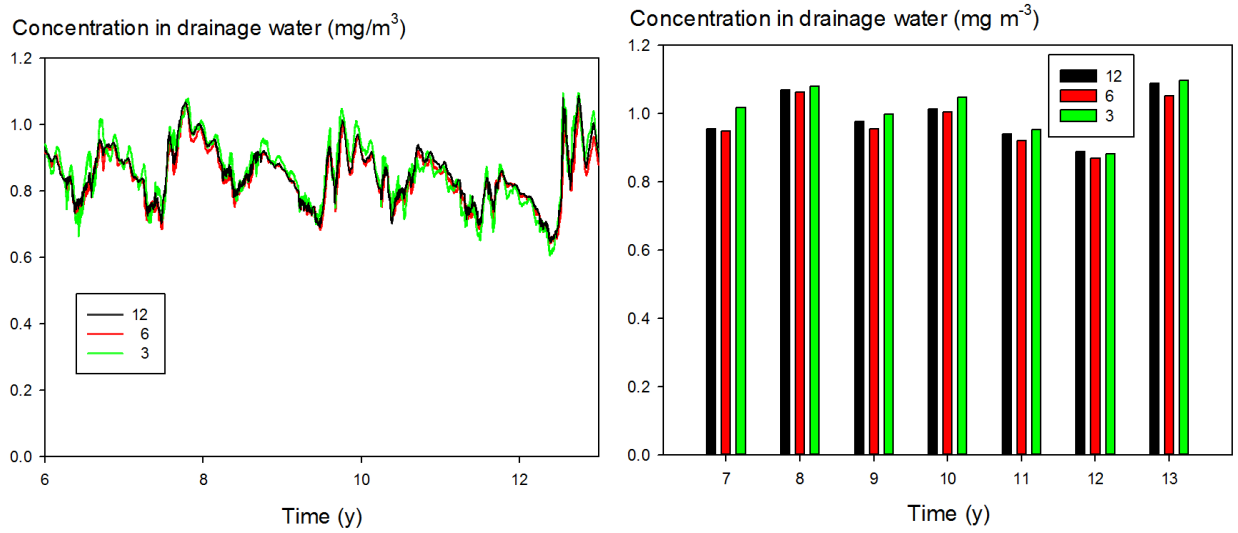

Figure 6.6 *Average concentrations in drain water of tolclofos-methyl as a function of time for the 7-y evaluation period (left) and their annual maxima (right). Averages are based on 12, 6 or 3 cultivation sections as indicated*

Figure 6.6 and Figure 6.7 show that the annual maxima of the concentrations and the mass fluxes in the drainage water differed no more than about 10% from each other. The fluxes show much more variation than the concentrations, so the fluxes are more critical. The average flux of the 6 cultivation sections is systematically lower than the average of 12 cultivation sections for 6 of the 7 years. So taking the average of the 6 other sections (3, 7, 11, 15, 19 and 23) would give a systematically higher result. The average flux of the 3 sections is most of the years higher than the average of 12. However, this may be the reverse for another set of 3 cultivation sections.

The fluxes show much more variation than the concentrations, so the fluxes are more critical. The average flux of the 6 cultivation sections selected is systematically lower than the average of 12 sections for 6 of the 7 years. So taking the average of the 6 other sections, i.e. 3, 7, 11, 15, 19 and 23, would give a systematically higher result. The average flux of the set of 3 sections selected is most of the years higher than the average of 12.

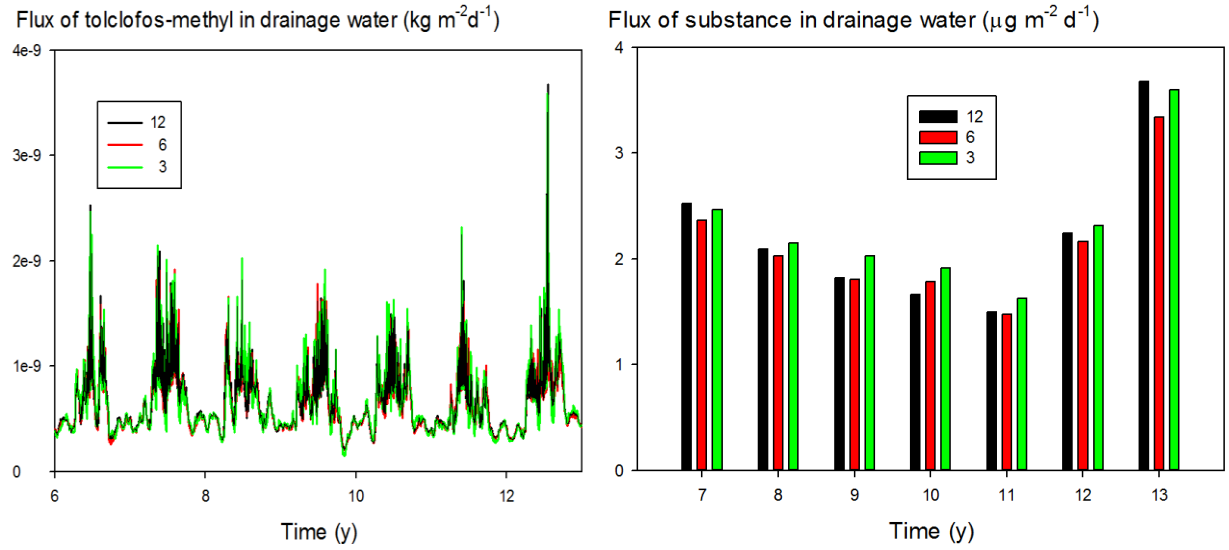

Figure 6.7 *Average fluxes of tolclofos-methyl in drainage water as a function of time for the 7-y evaluation method (left) and their annual maxima (right). Averages are based on 12, 6 or 3 cultivation sections as indicated*

Further checks were done for example substances E and F. The value for the K_{om} of substance E was set at 50 L kg^{-1} and the DegT50 was set at 100 d. The value for the K_{om} of substance F was set at 20 L kg^{-1} and the DegT50 was set at 20 d. For both substances the application method was spraying of the soil surface at a rate of 1 kg ha^{-1} each year on 15 May.

The results on the concentration of substance E in drainage water and the substance flux are shown in Figures 6.8 and 6.9, respectively. The differences between the averages for 3, 6 and 12 cultivation sections were larger than for tolclofos-methyl. For the concentrations annual maxima of 3 or 6 sections differed no more than about 10% from those of 12 sections and for the mass fluxes no more than about 20%.

The averaging had a moderate effect on the concentrations of substance E: the highest concentration maximum of an individual cultivation section was 13 mg m^{-3} (generated by Section 23, values of individual sections not shown in the graphs) compared with about 10 mg m^{-3} in Figure 6.8 for the averaging over 3,6 and 12 cultivations; for the flux the effect was larger: the highest maximum was 70 µg m^{-2} d^{-1} (also Section 23) compared with about 30 µg m^{-2} d^{-1} in Figure 6.9.

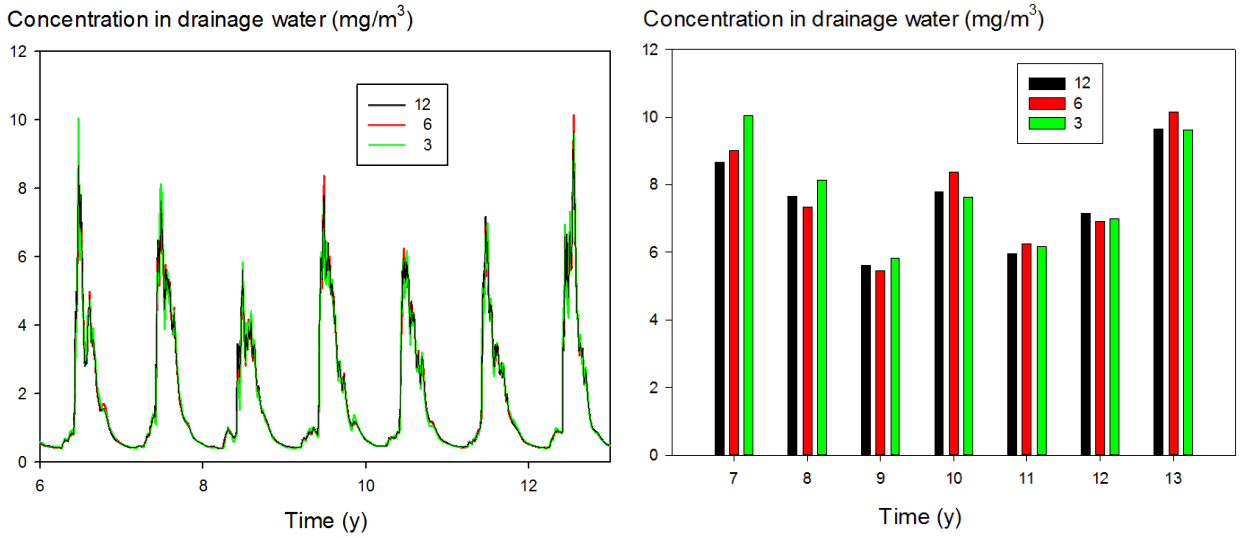

Figure 6.8 *Average concentrations in drain water of substance E as a function of time for the 7-y evaluation period (left) and their annual maxima (right). Averages are based on 12, 6 or 3 cultivation sections as indicated*

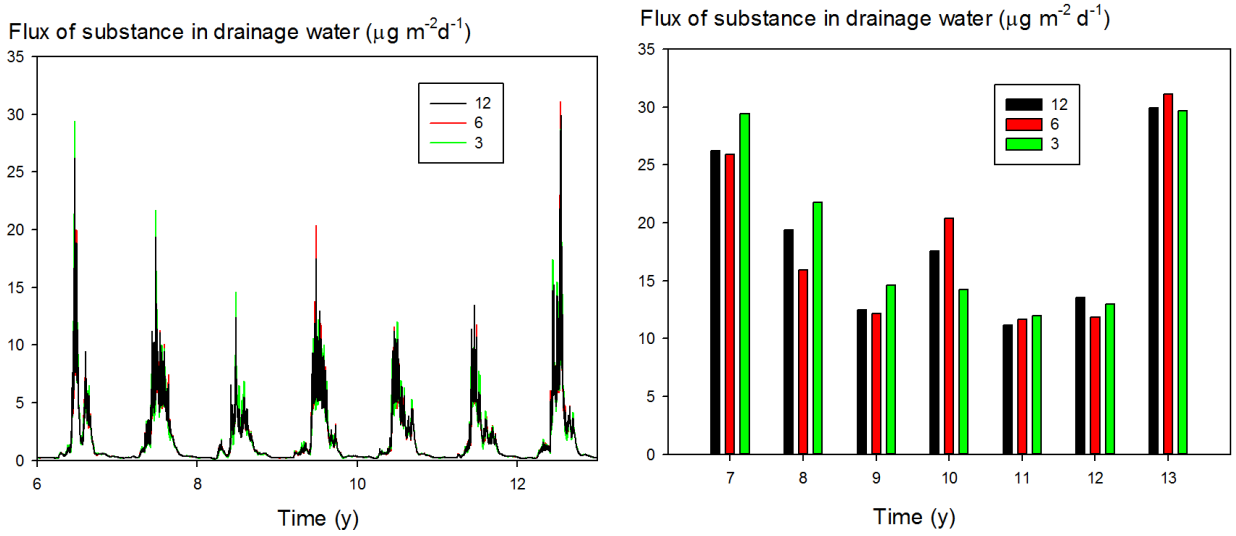

Figure 6.9 *Average fluxes of substance E in drainage water as a function of time for the 7-y evaluation method (left) and their annual maxima (right). Averages are based on 12, 6 or 3 cultivation sections as indicated*

The effect of averaging the concentrations and fluxes for pesticide F were comparable to those for pesticide E. For the concentrations annual maxima differed no more than about 15% and for the fluxes no more than about 20%.

Considering the results of these three pesticides, averaging of drainage fluxes of different sections is likely to result in considerably lower annual maximum concentrations in the surface water compared to using the compartment with the highest annual maximum concentration (about a factor 1.3 for the concentrations in these drainage fluxes and a factor 2-3 for the substance fluxes).

We calculated averages of absolute differences of yearly maxima of concentrations and fluxes between 6 and 12 cultivation sections: the concentrations gave 2, 5 and 7% and the fluxes 5, 9 and 8% for tolclofos-methyl, E and F, respectively. The same values for the difference between 3 and 12 cultivation sections were 2, 9 and 5% (concentrations) and 7, 11 and 10% (fluxes) for tolclofos-methyl, E and F, respectively. So taking 6 instead of 3 cultivation sections reduces the uncertainty in the fluxes only with about 2%. As described before, there are in reality 24 cultivation sections in a Dutch chrysanthemum greenhouse. The shift between two consecutive sections in a subset of 12 sections selected in total as described above is about 6 days. When selecting all 24 sections, the shift between two consecutive sections is about 3 days. As a shift of 6 days is relatively small, a further refinement to a shift of only 3 days is expected to result in a comparatively small decrease in the range the absolute differences. In view of the results on the averaged based on 3, 6 or 12 sections, this decrease is likely to be of the order of a few percent.

As discussed above, the absolute difference in the yearly maximum concentrations between calculations based on 3 or 12 cultivation sections were calculated to range from 2 to 9% for the concentrations and from 7 to 11% for the mass fluxes. Increasing the number of cultivation sections would only decrease the uncertainty in the mass fluxes by 2%. Therefore we have set the number of cultivation sections to be considered to 4. The overall uncertainty in the mass fluxes and concentrations and fluxes by reducing the number of cultivation sections from 24 to 4 would be roughly 20%. To obtain as much spread between the crop cycles as possible, cultivation sections 1, 7, 13 and 19 were selected for the surface water scenario.

The differences in the irrigation regimes and inflow in macropore domain between the 4 cultivation sections as selected in the surface water scenario are illustrated in Figures 6.10 to 6.13. For cultivation Section 1 the periods with substantial inflow are April, June and August (see also Figure 4.16), whereas for cultivation Section 7 the periods are roughly the first half of May and the second half of June. For cultivation Section 13 the periods of inflow into the macropore domain are mid May until the first week of June and the last week of July to mid August and for cultivation Section 19 the periods are the first half of April, mid May to Mid June and August.

It should be noted that the input for the TOXSWA model on the drain water flux and the concentration of the substance in this water is obtained by calculating the flux-weighed average of the output on drain water and drain water concentrations for these four cultivation sections. The resulting output is then considered to be representative for the greenhouse as a whole.

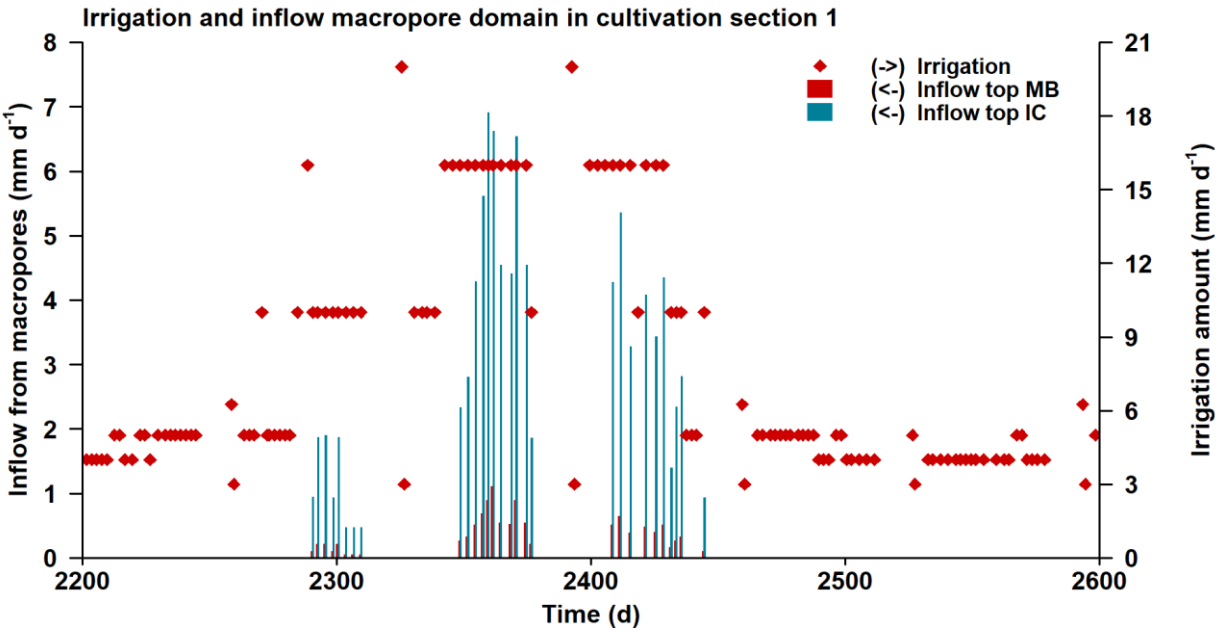

Figure 6.10 *Irrigation amount (mm) and simulated inflow (mm) from the covering layer into the top of the macropores for cultivation Section 1. Time 2200.0 corresponds to 10-Jan-2000 0h00*

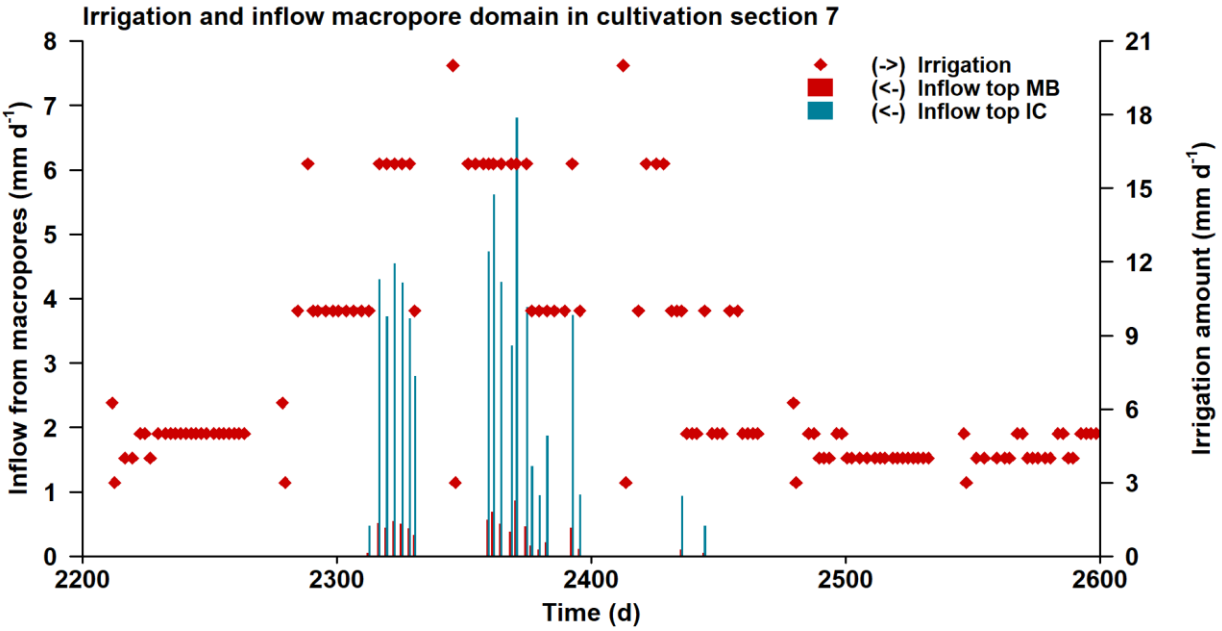

Figure 6.11 *Irrigation amount (mm) and simulated inflow (mm) from the covering layer into the top of the macropores for cultivation Section 7. Time 2200.0 corresponds to 10-Jan-2000 0h00*

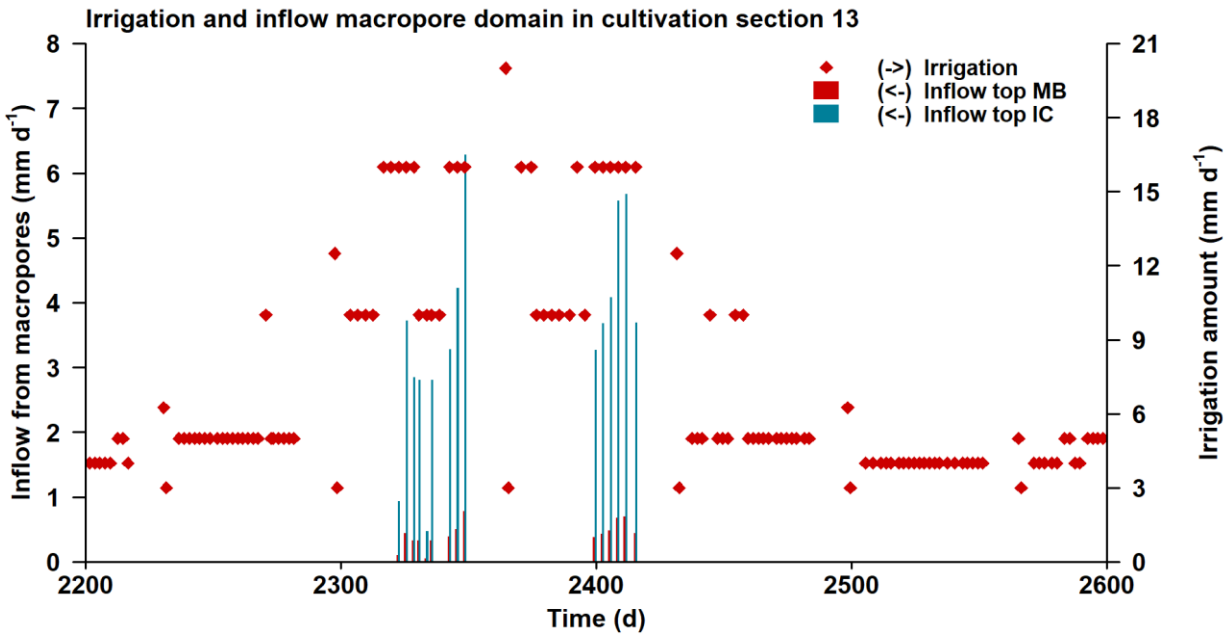

Figure 6.12 *Irrigation amount (mm) and simulated inflow (mm) from the covering layer into the top of the macropores for cultivation Section 13. Time 2200.0 corresponds to 10-Jan-2000 0h00*

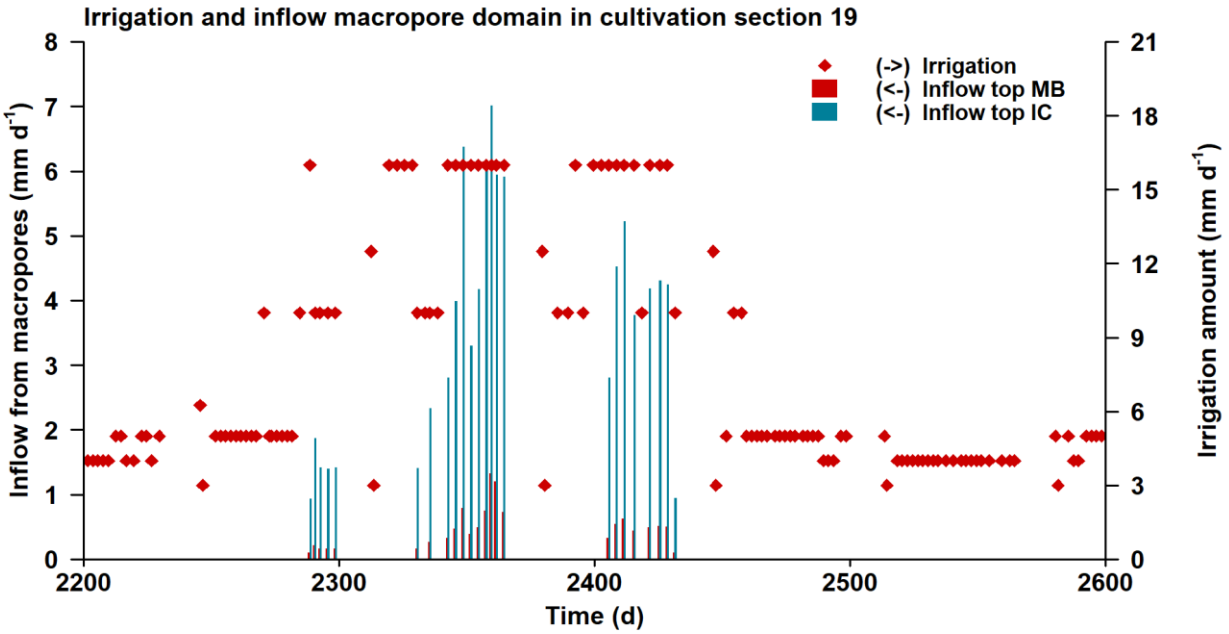

Figure 6.13 *Irrigation amount (mm) and simulated inflow (mm) from the covering layer into the top of the macropores for cultivation Section 19. Time 2200.0 corresponds to 10-Jan-2000 0h00*

7 Testing the revised surface scenario using example compounds

7.1 Procedure

Three example compounds were selected with different physico-chemical properties, i.e. example substances E and F and a tracer. The DegT50 values for substances E and F were taken to be 100 and 20 d, respectively. The sorption coefficient to soil organic matter, K_{om}, was set to 50 and 20 L kg^{-1}, respectively. The sorption coefficient for the tracer was set to 0 L kg^{-1} and the half-life to 1 000 000 days, so transformation is negligible.

The application type selected was soil surface application and the application rate was 1 kg ha^{-1}. Runs using the revised surface water scenario were done for cultivation sections 1, 7, 13 and 19, because these sections have been included in the revised surface water scenario. Four application dates were defined: 15 February, 15 May, 15 August and 15 November.

7.2 Results for the revised surface water scenario

For each run the drain water flux and the concentration of the substance in the drain water over time following the warming-up period were plotted for cultivation sections 1, 7 and 13. The output for cultivation Section 19 is not shown, because this is expected to have little added value.

The flux of the drain water from sections 1, 7 and 13 as well as the concentration of substance E in the drain water in the year 2000 for application dates of 15 February, 15 May, 15 August is and 15 November are shown in Figures 7.1 to 7.4, respectively.

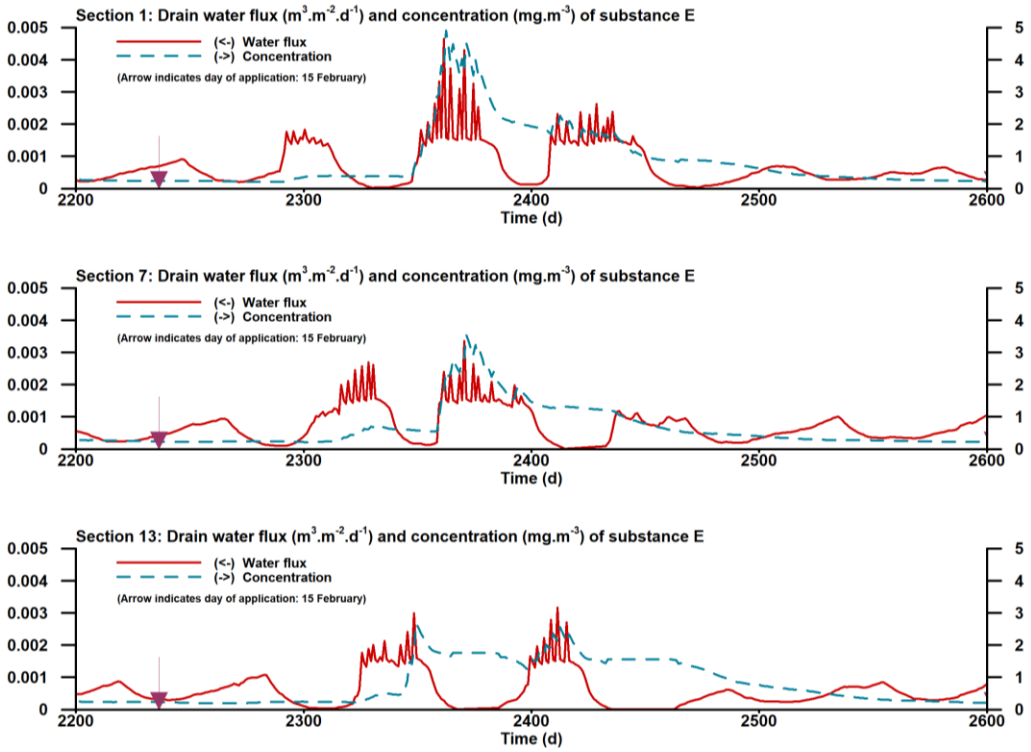

Figure 7.1 *Drain water flux and concentration of substance E in drain water. Application date 15 February. Time 2200.0 corresponds to 10-Jan-2000 0h00*

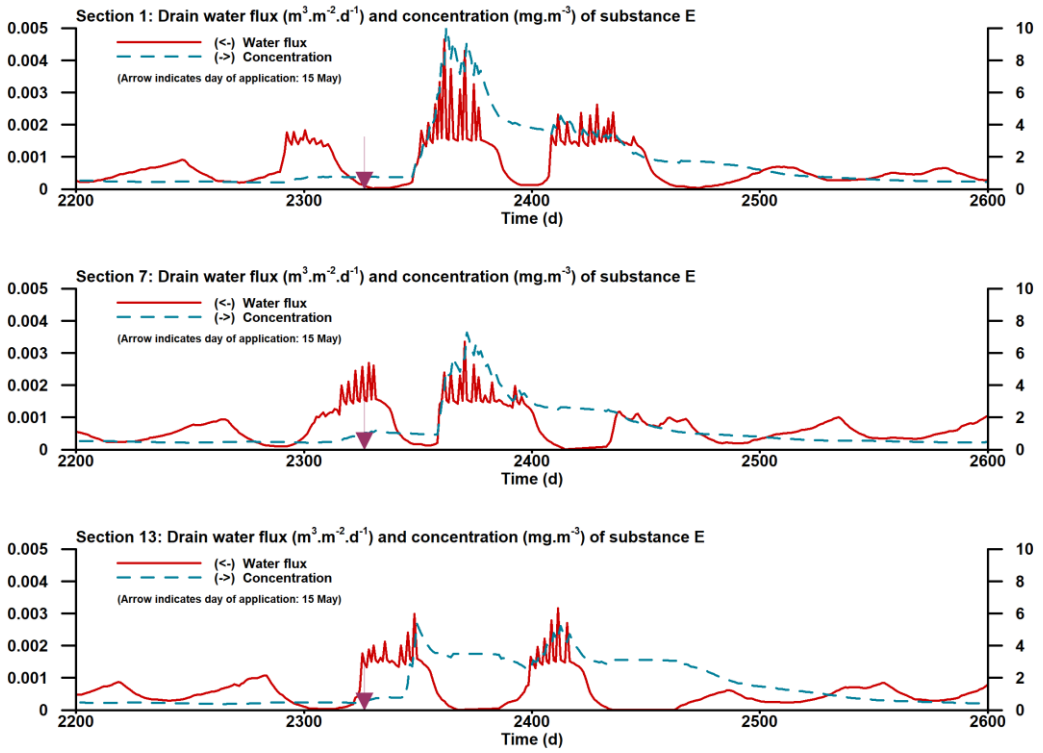

Figure 7.2 *Drain water flux and concentration of substance E in drain water. Application date 15 May. Time 2200.0 corresponds to 10-Jan-2000 0h00*

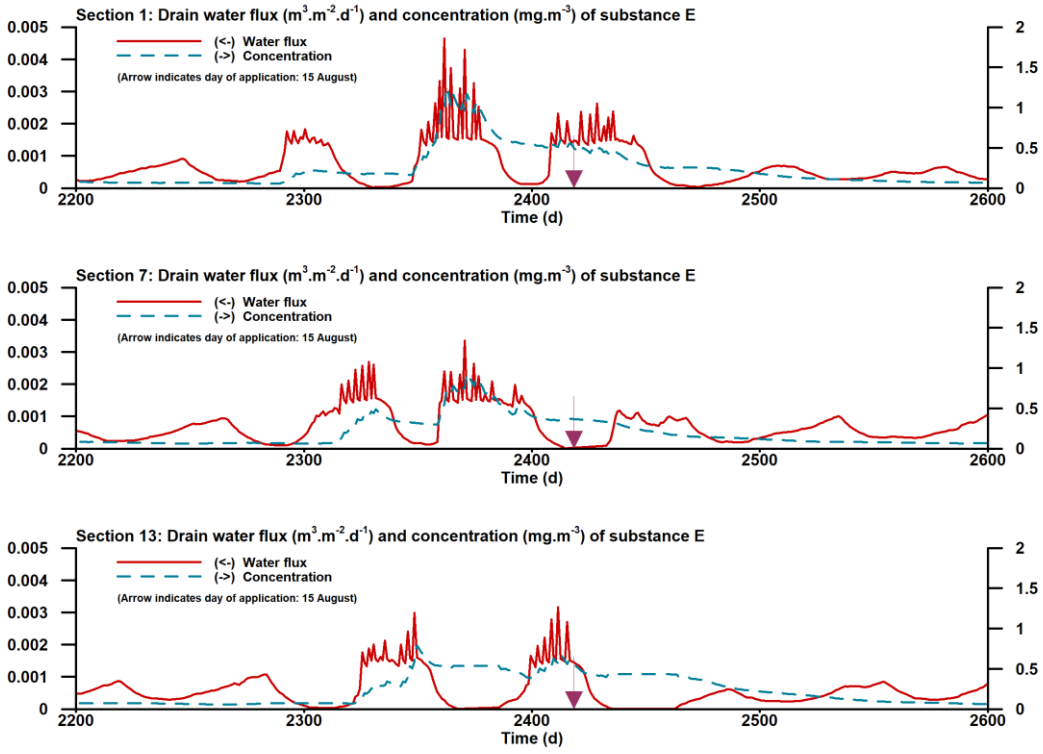

Figure 7.3 *Drain water flux and concentration of substance E in drain water. Application date 15 August. Time 2200.0 corresponds to 10-Jan-2000 0h00*

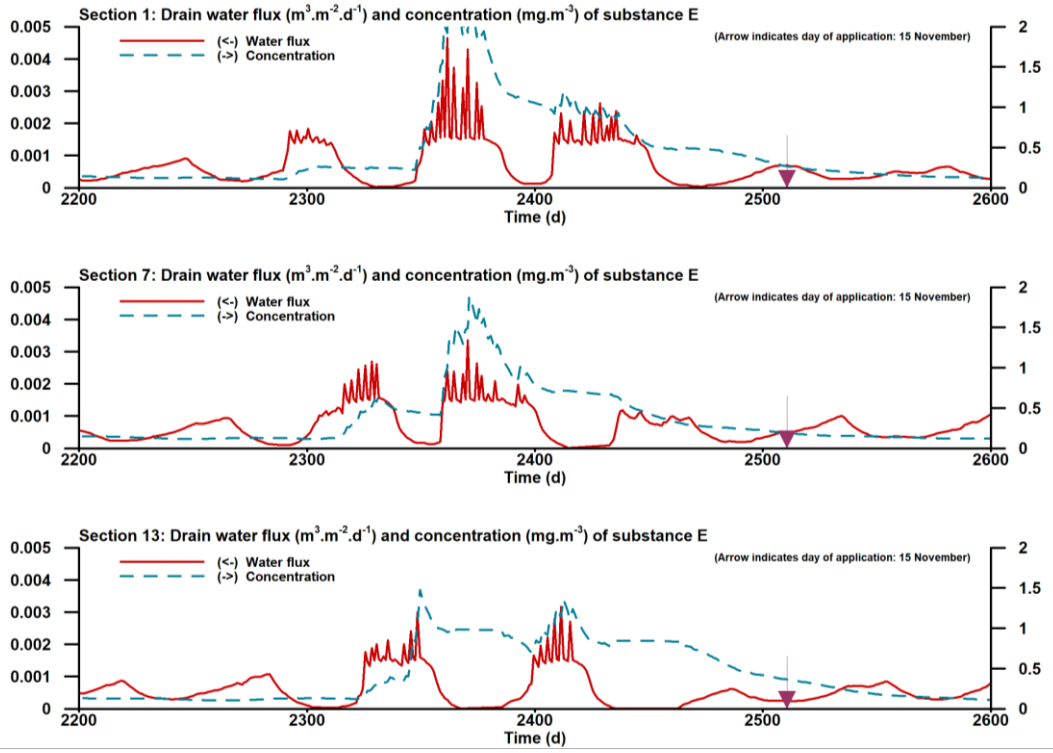

Figure 7.4 *Drain water flux and concentration of substance E in drain water. Application date 15 November. Time 2200.0 corresponds to 10-Jan-2000 0h00*

The results as presented in Figures 7.1 to 7.4 demonstrate that comparatively high concentrations in drain water are calculated for periods with high drain water fluxes, in particular during the summer period. It should be noted that the concentration range as shown in these Figures is different. The highest concentrations are calculated for the application date of 15 May, up to about 10 µg L^{-1}. Concentrations in drain water following an application in November are lower, because of lower amounts in the soil remaining in the next summer period. This decrease is less pronounced for an application on 15 February. As the half-life in soil for substance E is 100 d, substantial amounts are still present in the soil during the summer period. In the first few months after the November application drain water fluxes in the main bypass domain are low, so less substance enters the drainage system during that period.

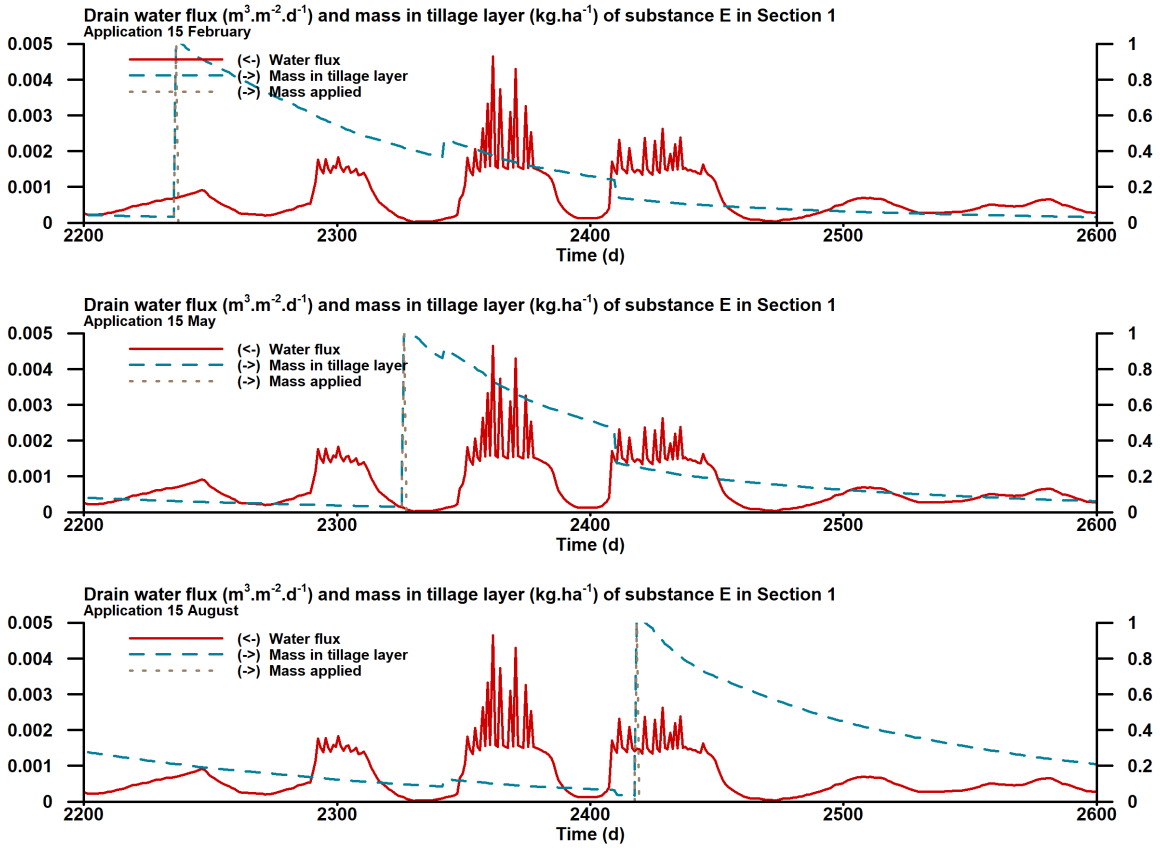

Figure 7.5 *Drain water flux and mass of substance E in tillage layer of Cultivation Section 1. Time 2200.0 corresponds to 10-Jan-2000 0h00*

In Figure 7.5 the mass of substance E in the tillage layer is plotted versus time in the year 2000. This figure shows that during the summer period with high drainage events, substance mass levels in the top layer are highest following an application on 15 May.

The flux of the drain water from cultivation sections 1, 7 and 13, as well as the concentration of substance F in the drain water in the year 2000 for application dates of 15 February, 15 May, 15 August is and 15 November are shown in Figures 7.6 to 7.9, respectively.

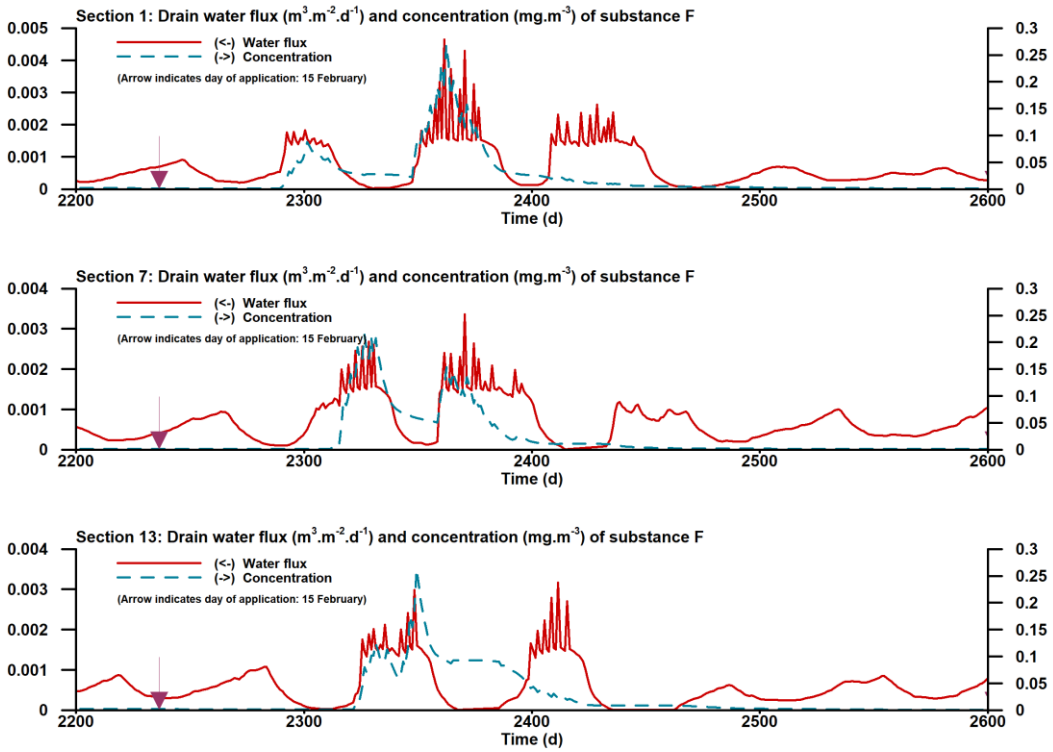

Figure 7.6 *Drain water flux and concentration of substance F in drain water. Application date 15 February. Time 2200.0 corresponds to 10-Jan-2000 0h00*

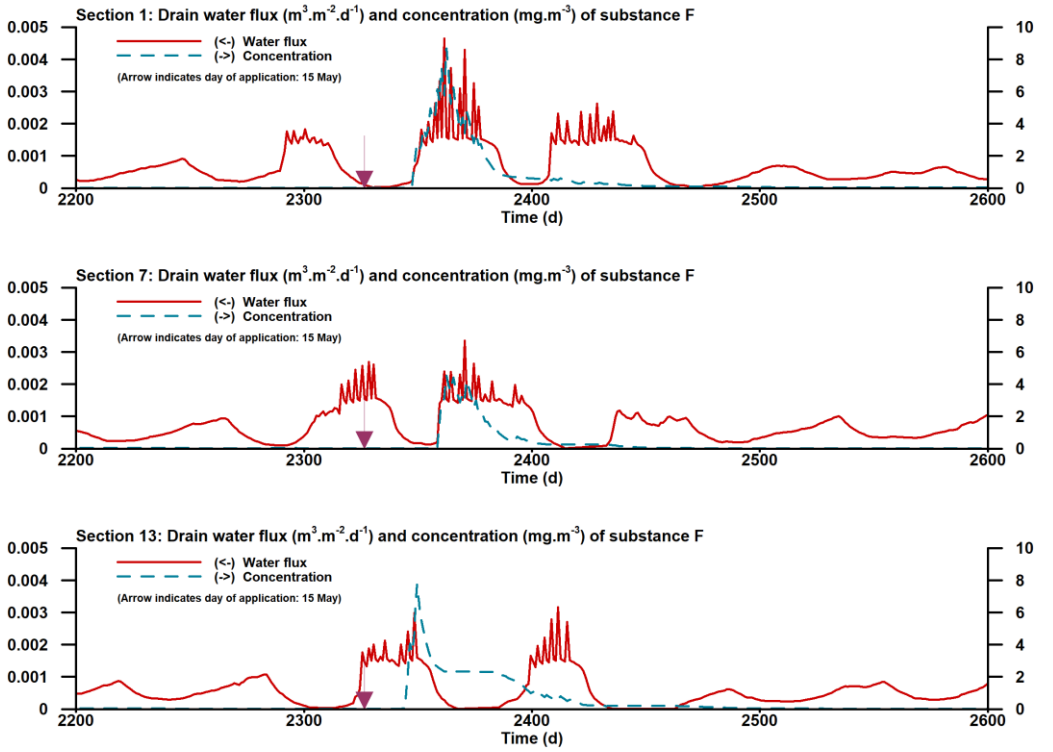

Figure 7.7 *Drain water flux and concentration of substance F in drain water. Application date 15 May. Time 2200.0 corresponds to 10-Jan-2000 0h00*

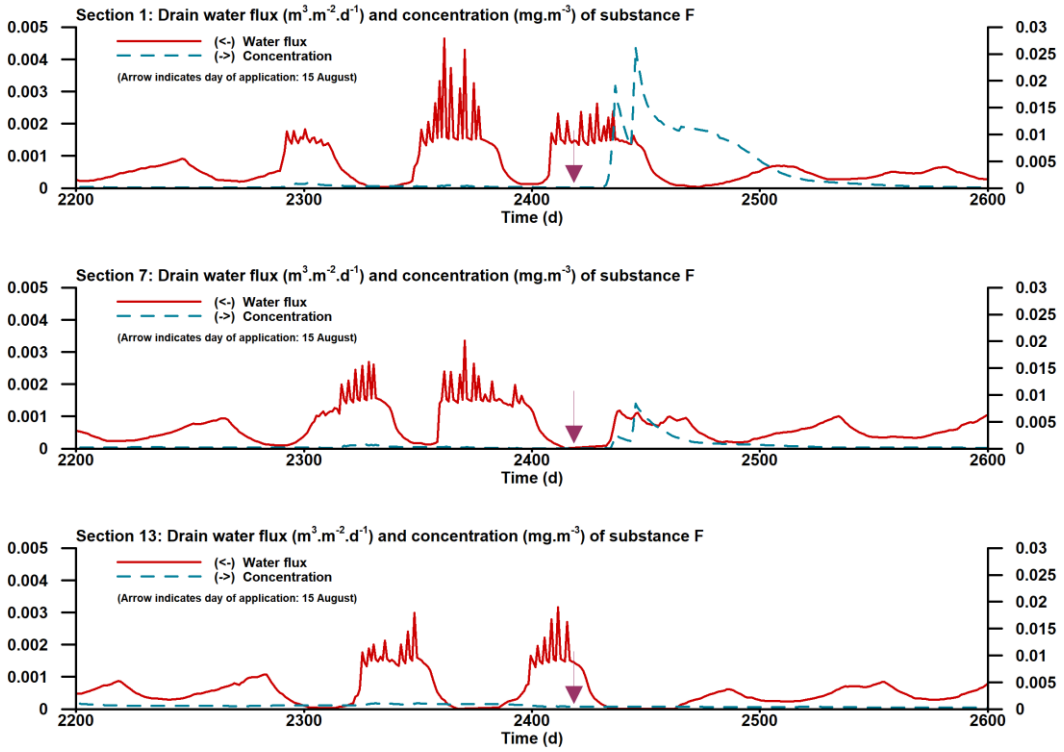

Figure 7.8 *Drain water flux and concentration of substance F in drain water. Application date 15 August. Time 2200.0 corresponds to 10-Jan-2000 0h00*

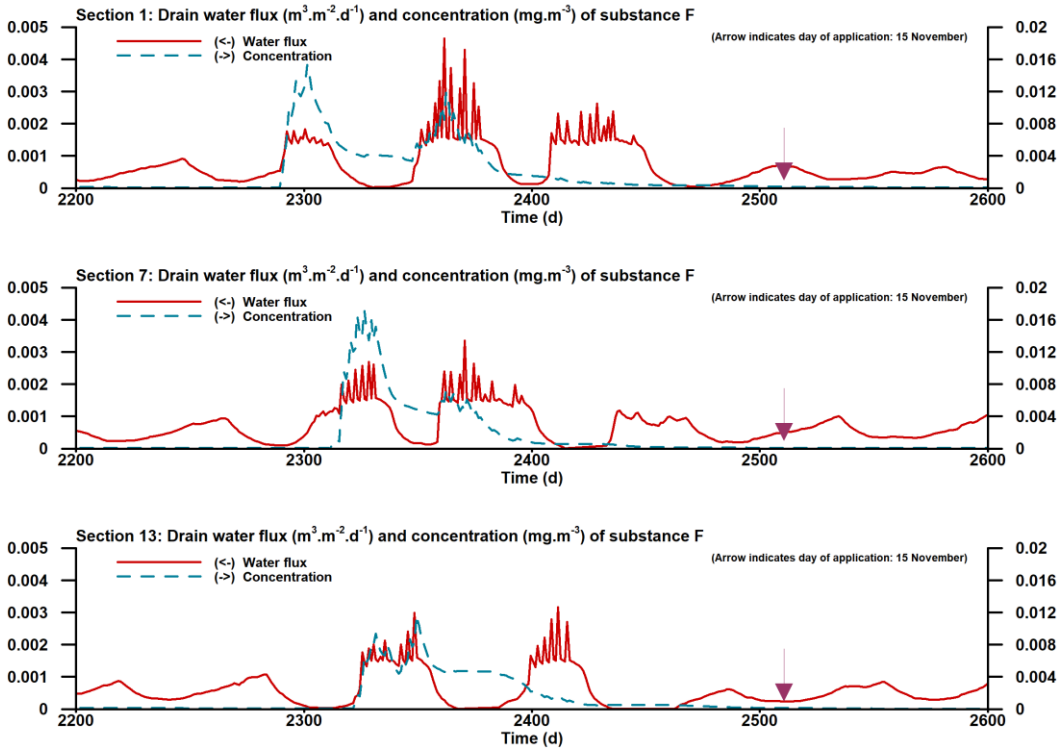

Figure 7.9 *Drain water flux and concentration of substance F in drain water. Application date 15 November. Time 2200.0 corresponds to 10-Jan-2000 0h00*

Similar to the results for substance E, concentration levels of substance F in drain water are highest during the summer period with comparatively high drainage events. For the February application, the maximum concentrations of substance F were about a factor 10 lower than the maximum concentrations computed for substance E (see Figures 7.1 and 7.6). Maximum concentrations in drain water were lowest for the November application.

In Figure 7.10 the mass of substance F in the tillage layer is plotted versus time in the year 2000. This figure shows that during the summer period with high drainage events, substance levels in the top layer are highest following an application on 15 May. The half-life in soil for this substance was set at 20 d, so the mass remaining in the soil decreases fairly rapidly. In addition, substance F is comparatively mobile with a K_{om} of 20 L kg^{-1}, which can be expected to result in more leaching to deeper soil layers and less discharge via drainage as compared to substance E.

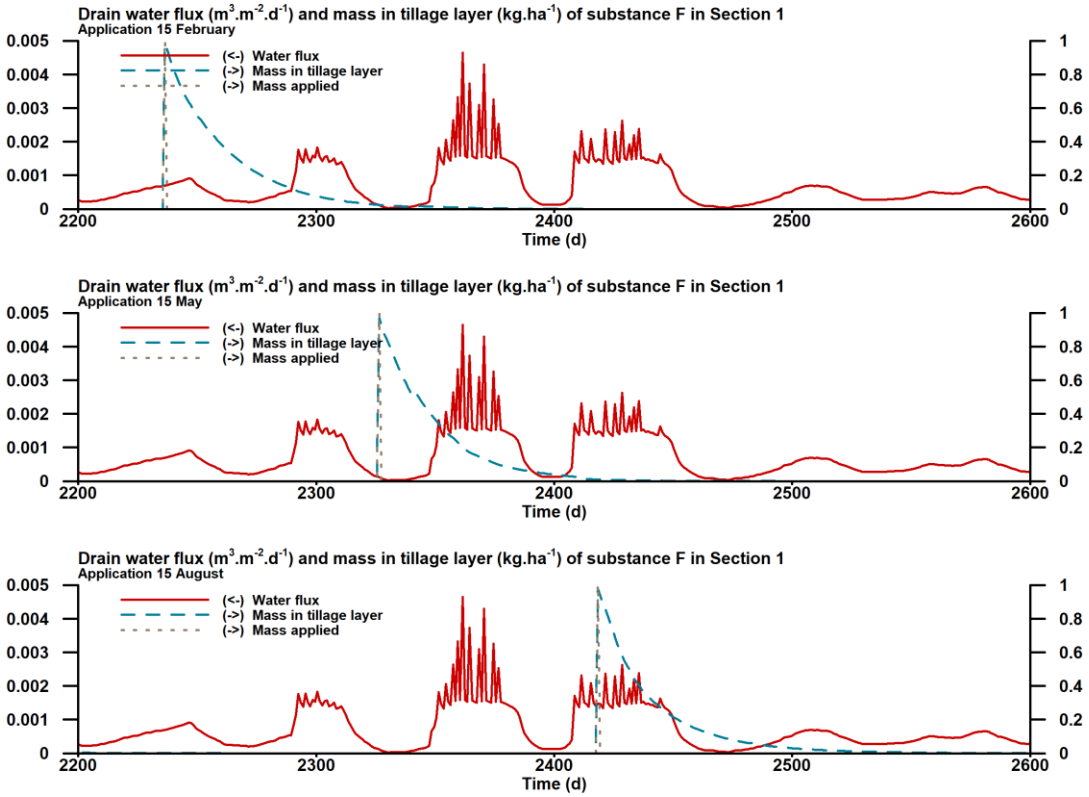

Figure 7.10 *Drain water flux and mass of substance F in tillage layer of Cultivation Section 1. Time 2200.0 corresponds to 10-Jan-2000 0h00*

The flux of the drain water from cultivation sections 1, 7 and 13, as well as the concentration of the tracer in the drain water in the year 2000 for application dates of 15 February, 15 May, 15 August is and 15 November are shown in Figures 7.11 to 7.14, respectively.

As expected, the highest concentrations were computed to occur during the summer period. In this period the daily irrigation amounts are highest and as the tracer has zero sorption to soil particles the substance is transported to the drains along with the water flow. The highest concentrations in drain water were computed for the February and May applications. This can be explained by the higher amounts in the top soil during the summer months as compared to those for the August and November applications. This difference in the amount in the topsoil is illustrated in Figure 7.15.

During the winter period concentrations of the tracer were generally on a lower level than during the summer period for all application dates.

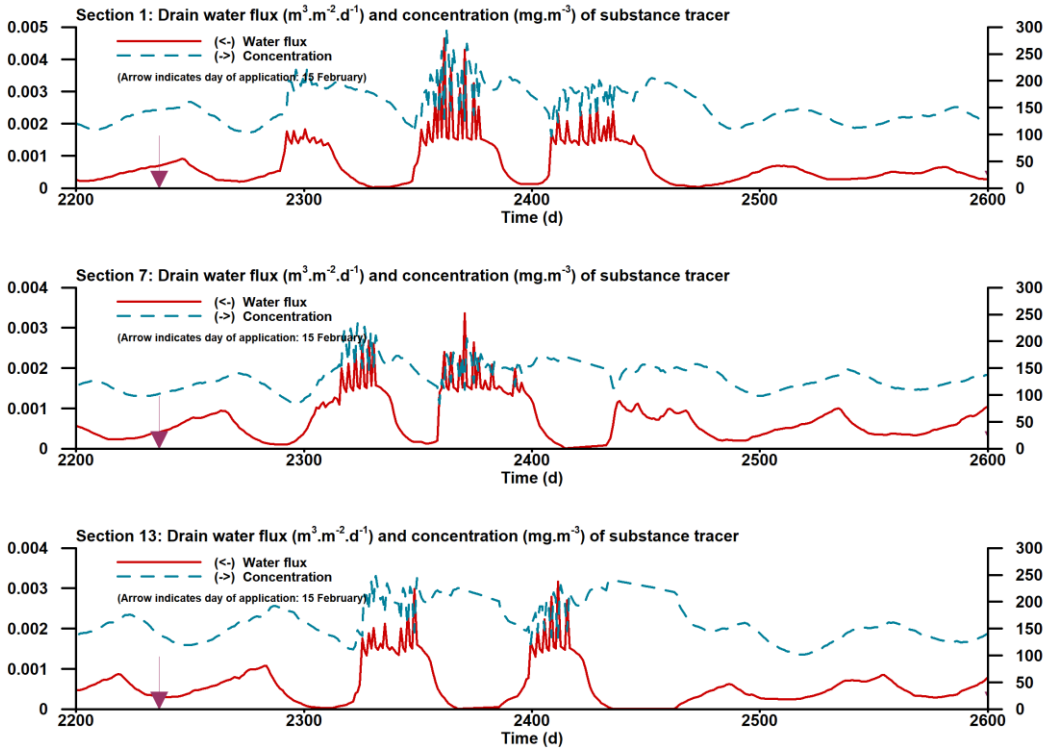

Figure 7.11 *Drain water flux and concentration of the tracer in drain water. Application date 15 February. Time 2200.0 corresponds to 10-Jan-2000 0h00*

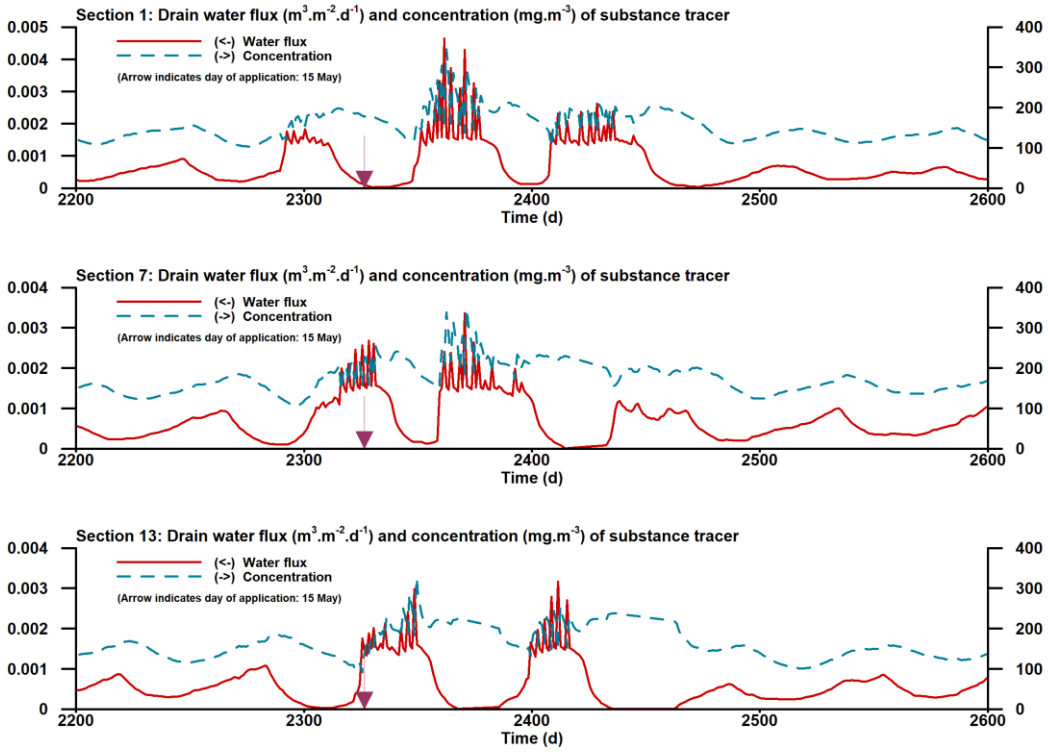

Figure 7.12 *Drain water flux and concentration of tracer in drain water. Application date 15 May. Time 2200.0 corresponds to 10-Jan-2000 0h00*

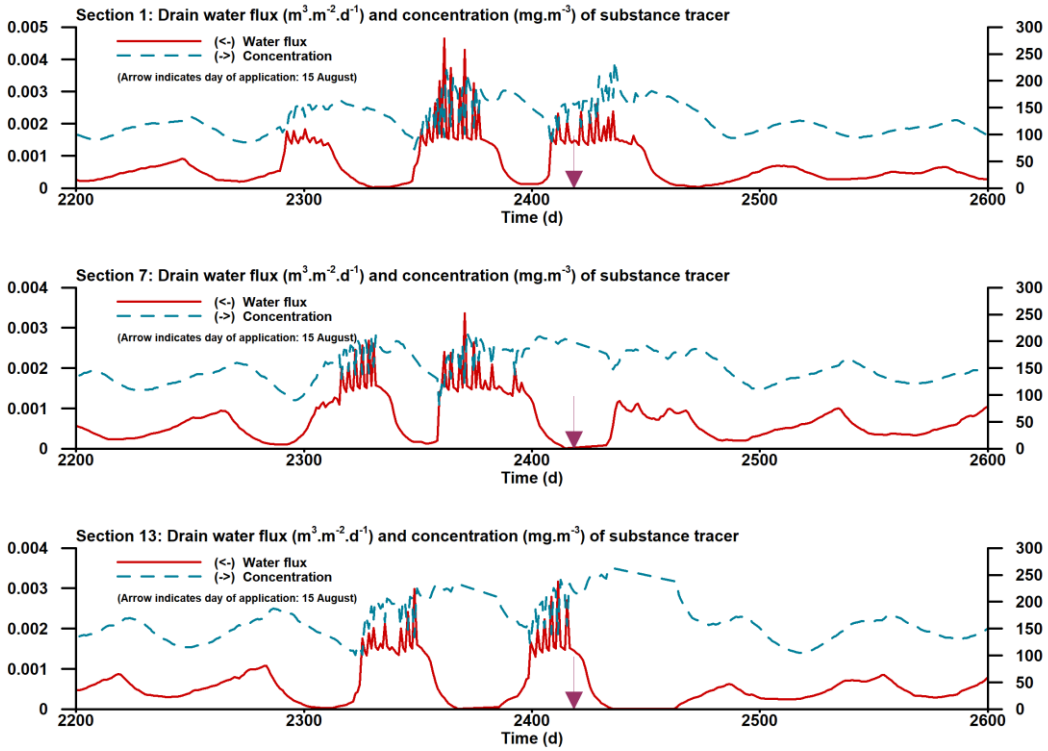

Figure 7.13 *Drain water flux and concentration of tracer in drain water. Application date 15 August. Time 2200.0 corresponds to 10-Jan-2000 0h00*

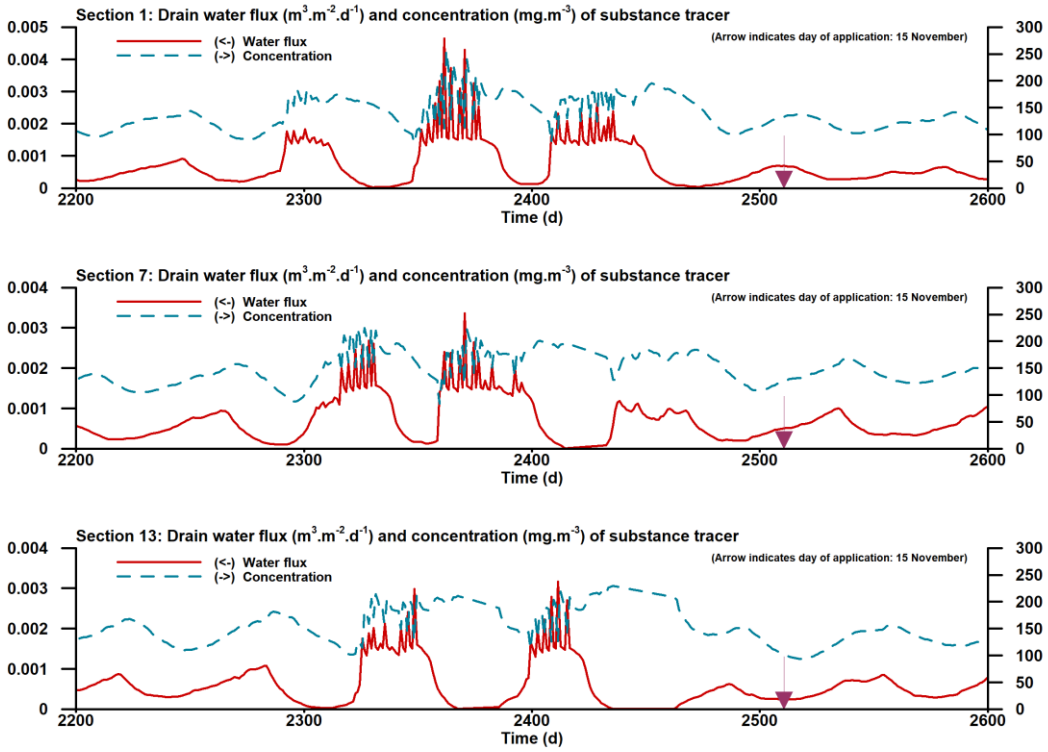

Figure 7.14 *Drain water flux and concentration of tracer in drain water. Application date 15 November. Time 2200.0 corresponds to 10-Jan-2000 0h00*

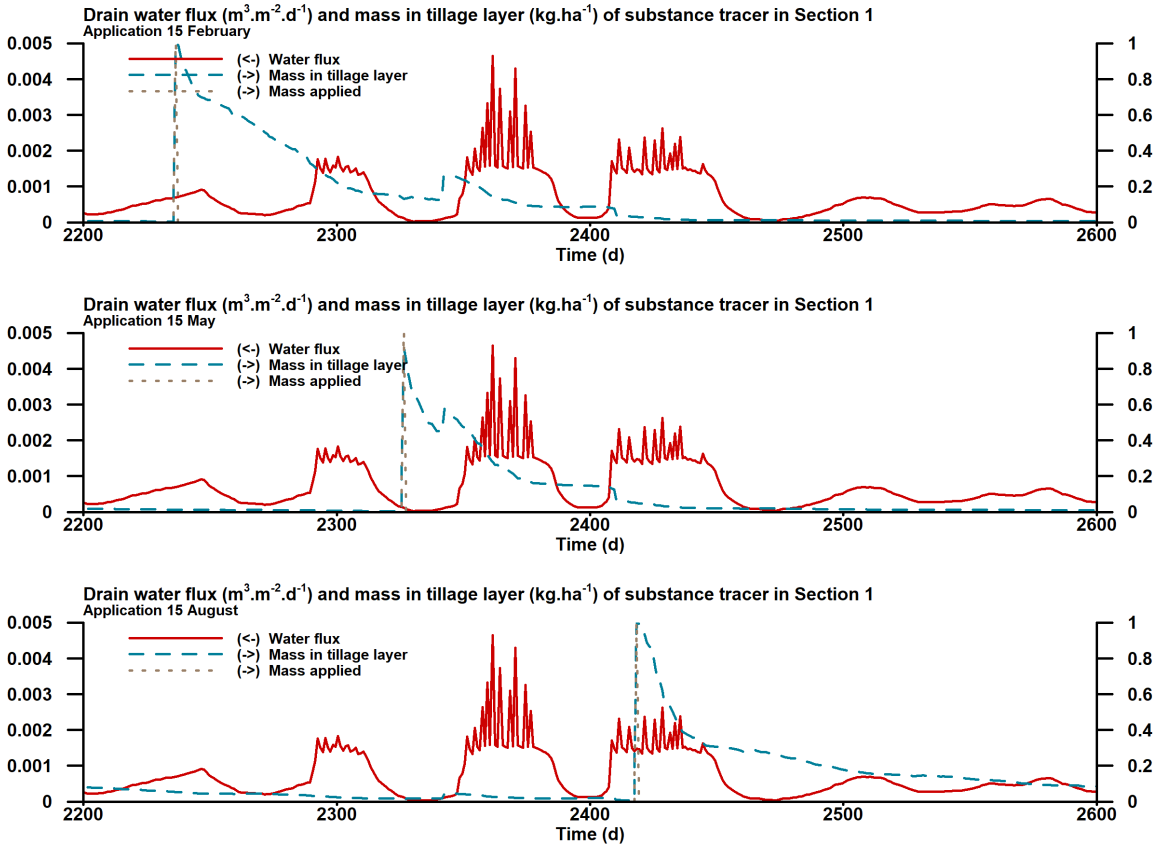

Figure 7.15 *Drain water flux and mass of tracer in tillage layer of Cultivation Section 1. Time 2200.0 corresponds to 10-Jan-2000 0h00*

7.3 Comparison of calculations using the revised surface water scenario with monitoring data

In their report on exposure scenarios of aquatic organisms resulting from the use of plant protection products in soil-bound crops in greenhouses, Wipfler et al. (2014) compared the 90th percentile PEC calculated with the newly-developed scenario for the active substance tolclophos-methyl (fungicide 2 in Wipfler et al., 2014) with results from a monitoring study. This monitoring study has been done in the Bommelerwaard, an area in the Meuse catchment in the Eastern part of the Netherlands. The data on tolclophos-methyl are shown in Figure 7.16. The monitored concentrations in surface water (from the waterboard 'Rivierenland') were used as a benchmark to test the scenario, because the expectation is that the measured concentrations should be lower than the 90th percentile PEC calculated. Such a comparison is also done for the revised surface water scenario presented in this report.

The calculations were made for the substance tolclophos-methyl, which is a fungicide that is applied at the start of a new crop cycle, so for the current comparison it was set at 1 day before planting. The application rate was set at 16 kg ha^{-1} and the application method selected was application to the soil surface. Data on the substance properties were obtained from field studies included in the registration dossier. The half-life of tolclofos-methyl in soil was set to 5.4 d and the K_{om} set to 2099 L kg^{-1}.

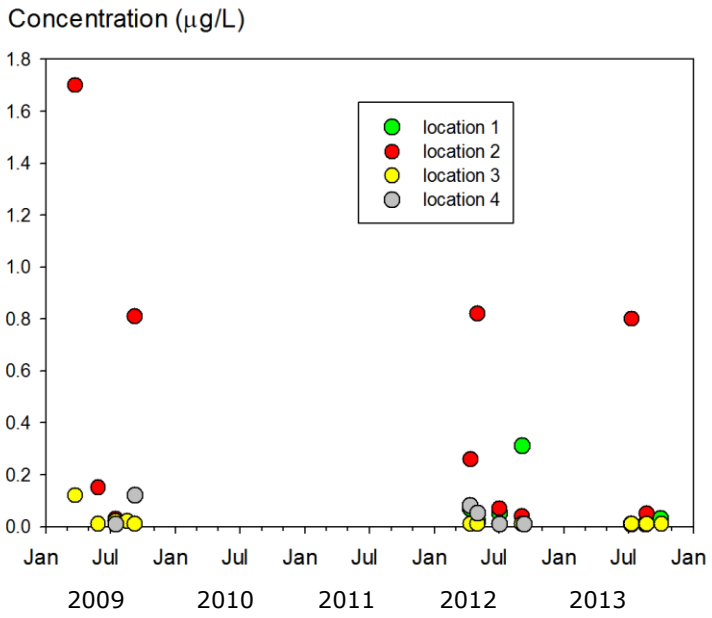

Figure 7.16 *Concentrations of tolclophos-methyl in surface water in the Bommelerwaard (source: Waterboard 'Rivierenland')*

The 90th percentile concentration in the ditch for tolclophos-methyl with a DT50 of 5.4 d for an application on 1 April at a rate of 16 kg ha^{-1} was calculated to be 0.00650 µg L^{-1}. This is almost the same value as that reported by Wipfler et al. (2014, see Table 9.2 of the report) for the same substance - application combination, i.e. 0.007 µg L^{-1}. The concentration calculated is much lower than that measured in the monitoring study in the Bommelerwaard. However, the DT50 value of 5.4 has been derived from studies with field soils. Matser et al. (1996) measured the rate of transformation of tolclophos-methyl in four greenhouse soils. The geomean value for the half-life of this substance was calculated to be 108 d. Using a value of the DT50 of 108 d, the PEC90 for tolclophos-methyl was calculated to be much higher: 1.593 µg L^{-1}. This value is of the same order of magnitude as the highest concentration measured in the monitoring study. As mentioned by Wiplfer et al. (2014) the use of DT50 values obtained from field studies are not representative for greenhouse soils. For cultivations of soil-bound crops in greenhouses sterilisation of the soil occurs once a year and this results in a reduction of microbial activity and as a consequence to a slower transformation rate. Therefore, a DT50 value as obtained from measurements in greenhouse soils had better be used to calculate the exposure of aquatic organisms due to the discharge of water from the greenhouse via the drains.

7.4 Comparison with GEM version 3.3.2

7.4.1 Groundwater scenario

The results of the assessments using the revised ground water scenario in GEM 4.4.3 were compared with those obtained using the groundwater scenario in GEM version 3.3.2. Computations were done for FOCUS Groundwater example compounds B and C. The application method selected was spraying to the soil surface and the runs were done for a single application on the 15th of each month. The results are shown in Table 7.1.

The results of the comparison show that the 90th percentile leaching concentrations using the revised groundwater scenario of GEM 4.4.3 are about an order of magnitude higher than those obtained using the groundwater scenario of GEM 3.3.2. The larger part of this difference is due to the ploughing events as part of the revised scenario. Between two consecutive crop cycles the top 15 cm is ploughed and once a year the top 25 cm is ploughed by rototillage. Consequently, the mass of plant protection product is mixed over this layer, which increases the transport downward to the groundwater.

The average yearly irrigation amount is about 50 mm lower in the new scenario. Because the total evapotranspiration is similar in both scenario's, the percolation from the target layer is also about 50 mm less.

Another factor that contributes to the difference in the leaching concentration is the difference in uptake by plant roots. In the old scenario the rooting depth is 30 cm throughout the assessment period, but it is variable in the revised scenario and the development of the crop during the cultivation period is taken into account. Therefore, the passive uptake of substance by the plant roots is less in the revised scenario, so the fraction of the remaining mass in the soil that is subject to leaching is higher.

Table 7.1 *The PEC90 concentration in groundwater for FOCUS Groundwater example compound C and its metabolite using the groundwater scenarios of GEM 3.3.2 and GEM 4.4.3*

Application date	**Compounds**			
	FOCUS C		**FOCUS MetC**	
	GEM 332	**GEM 443**	**GEM 332**	**GEM 443**
15-Jan	0.000000	0.000000	0.089924	0.684145
15-Feb	0.000000	0.000000	0.086489	0.807240
15-Mar	0.000000	0.000000	0.080227	0.946963
15-Apr	0.000000	0.000000	0.068205	1.14064
15-May	0.000000	0.000000	0.060691	1.352594
15-Jun	0.000000	0.000000	0.055445	1.381854
15-Jul	0.000000	0.000000	0.064674	1.208427
15-Aug	0.000000	0.000000	0.077727	0.332906
15-Sep	0.000000	0.000000	0.080842	0.369089
15-Oct	0.000000	0.000000	0.082902	0.422964
15-Nov	0.000000	0.000000	0.086051	0.495814
15-Dec	0.000000	0.000000	0.089805	0.579859

Table 7.2 *The PEC90 concentration in groundwater for FOCUS Groundwater example compounds B using the groundwater scenarios of GEM 3.3.2 and GEM 4.4.3*

Application date	**GEM version**	
	GEM 332	**GEM 443**
15-Jan	0.00116	0.006578
15-Feb	0.001596	0.012054
15-Mar	0.002104	0.019898
15-Apr	0.001349	0.026582
15-May	0.000646	0.037637
15-Jun	0.000134	0.088236
15-Jul	0.000093	0.056586
15-Aug	0.00026	0.001972
15-Sep	0.000278	0.001314
15-Oct	0.000305	0.001212
15-Nov	0.000401	0.001781
15-Dec	0.000717	0.003147

7.4.2 Surface water scenario

For the comparison of results of assessments using the revised surface water scenario in GEM 4.4.3 with those obtained using GEM version 3.3.2 computations were done for tolclophos-methyl. The comparison was done using a DT50 in soil of 5.4 d and a DT50 in soil of 108 d. The application method selected was spraying to the soil surface and the runs were done for a range of dates in August. Dates in August were selected as the outcome using GEM 3.3.2 was very sensitive to the application date in August. The results of the comparison are shown in Table 7.3.

Table 7.3 *The PEC90 concentration in surface water for tolclophos-methyl using the surface water scenarios of GEM 3.3.2 and GEM 4.4.3*

Application date	**tolclophos-methyl**			
	DT50 5.4 d		**DT50 108 d**	
	GEM 332	**GEM 443**	**GEM 332**	**GEM 443**
1-Aug	0.04751	0.03718	0.3753	0.2822
8-Aug	0.1177	< 1e-6	0.2894	0.09503
15-Aug	0.07619	< 1e-6	0.1733	0.1011
17-Aug	0.09	< 1e-6	0.1459	0.1029
20-Aug	0.000677	< 1e-6	0.0518	0.1057
22-Aug	0.001063	< 1e-6	0.05328	0.1074
31-Aug	0.000636	< 1e-6	0.05949	0.1156

For tolclophos-methyl using a DT50 value of 5.4 d in combination with the GEM 3.3.2 surface water scenario, there is a strong fluctuation of the PEC90 concentration when the application date changes from 1 to 31 August. This is caused by the repetition of irrigation and drainage events occurring on the same day every year. Using the revised surface water scenario, there is no longer such a strong fluctuation, but there is a strong decrease when the application date changes from 1 to 8 August. This strong decrease can be explained by the rototillage event in the period from 2 to 7 August. When the application is on 1 August, the subsequent tillage result in mixing the applied substance over the entire top layer, so transport of substance into the main bypass domain into the subsoil can occur faster. For tolclophos-methyl using a DT50 value of 108 d there is less variation.

8 Sensitivity of the revised surface water scenario to the application date

The PEC90 in the ditch adjacent to the greenhouse as calculated using the surface water scenario as implemented in GEM version 3.3.2 turned out to be very sensitive to the application date of the substance. As the irrigation scheme was repeated every year, the days with substantial drainage events from the main bypass domain occurred on the same day every year. As the planting and harvesting dates differ from year to year, the issue of repetition of drainage events occurring on the same date every simulation year was remedied by specifying the planting and harvest dates as well as the development of the crop for all cultivations in the simulation period. Consequently, the irrigation scheme also changed from year to year. A further change was introduced in the parameterisation of the soil profile. For cut-flowers ploughing of the topsoil occurs between two consecutive cultivations. The consequence of this ploughing is that no macropores are present in the top 0.25 m layer, but only in the subsoil, so below a depth of 0.25 m. To check the sensitivity of the revised surface water scenario to the selection of the application date, a series of runs were done using this scenario for an absolute application at a date (specified as day-month) covering the entire calendar year and for a relative application date (expressed as number of days before or after planting or harvest) covering the full cultivation period.

8.1 Procedure

A first series of runs were prepared with a different absolute application date for every run. In total 52 runs were created, one for the 3rd day of every week of the year. Using this option the application occurs at the same calendar day every year. The substances selected were substance E, F and the tracer. The applied dose was set at 1 kg.ha^{-1} and the application method was spraying to the soil surface. A second series of runs were prepared by selecting a date relative to the date of planting. Runs were done with a relative date ranging from 1 to 65 d after planting, covering the entire cultivation period. As the simulation period contains a series of cultivations (up to 70 for the surface water scenario), the application in a run occurs at the same date relative to the date of planting for all cultivations of the simulation period.

8.2 Results

The results of the runs for applications of substances E, F and the tracer at different days-in-year numbers are presented in Figure 8.1. The 90th percentile concentration (PEC90) in surface water is calculated from the 7 annual maximum concentrations in the water layer of the adjacent ditch. For substance E the PEC90 varies between 1 and 11 µg L^{-1}. As noted in Chapter 6, drainage mass fluxes are highest during the summer period. Because the DT50 of substance E is 100 days, substantial residues will remain throughout the year, even for an application early in the year. A decrease in the PEC90 values occur after the 1st of August. This decrease can be explained by the absence of deep-ploughing events, i.e. ploughing of the top 0.25 m layer, for the remaining part of the year after the beginning of August. Ploughing after the beginning of August is limited to the top 0.15 m layer, so no substance is added to the soil compartment just above the top of the macroporous part of the soil profile at a depth of 0.25 m. Therefore, less transport of substance occurs via the main bypass and internal catchment domains of the macroporous subsoil for applications that occur after the day on which the soil is ploughed to a depth of 0.25 m.

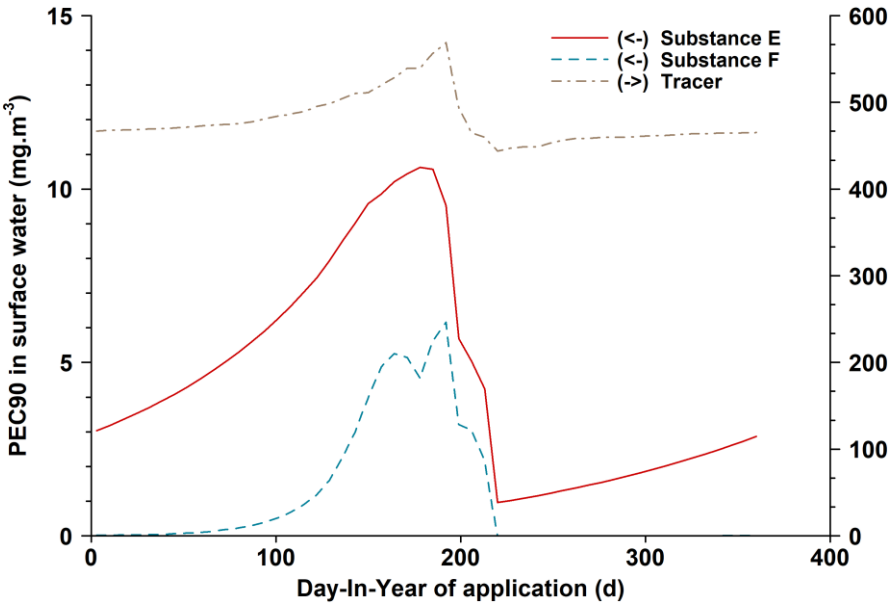

Figure 8.1 *PEC90 of substances E and F in surface water at different days-in-year. Application method: spraying of the soil surface*

The PEC 90 concentrations of substance F in surface water are highest during the summer period. This can be explained by the fact that drain water fluxes are highest during this period. For applications outside the summer months the concentrations are calculated to be lower than 0.1 µg $L^{-}1$. As the DT50 of substance F is comparatively low, i.e. 20 days, no substantial residue remains in the top soil at the start of the period with high drain water fluxes for applications in the autumn and winter period.

The PEC90 concentration of the tracer in the surface water is at a level of 500 mg m^{-3} for all applications at a specific day-of-the year. As no transformation and sorption occurs the transport through the soil is fast and does not depend predominantly on large drainage events in the summer period.

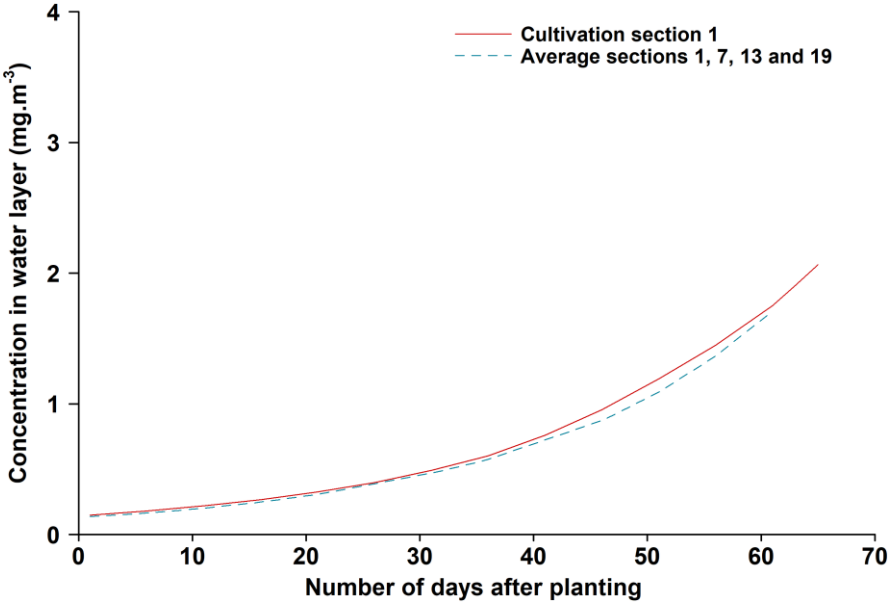

Figure 8.2 *PEC90 of substance F in surface water at different day after planting. Application method: spraying of the soil surface*

In Figure 8.2 the PEC90 concentration in the water layer is plotted against the number of days after planting as specified in the application scheme. It should be noted that for each run the application is repeated at the

same time interval after planting for each cultivation. In this Figure, the results are plotted for the PEC90 concentration in surface water based on the output of only cultivation Section 1 as well as the flux-weighted average of cultivation sections 1,7,13 and 19. Both lines are very similar with only minor differences.

As shown in Figure 8.2, there is a continuous increase in the 90th percentile concentration in surface water with an increase in the time interval between planting date and date of application. As no irrigations occur during the last week of the cultivation of cut-flowers, no increase in the PEC90 would be expected when the time interval between planting and application approaches the duration of the crop cycle. Therefore, a more detailed analysis was done to find an explanation for this behaviour. Figure 8.3 shows the pattern of the drain water flux and the concentration in drain water over time for the full 7 year evaluation period for a time interval of 1 day between planting and application. The application times are also shown in this Figure; it is clear that the application time precedes the period in the cultivation period with the highest irrigation amounts. Furthermore, the highest water fluxes and concentrations in drain water occur during the years 2000 and 2006.

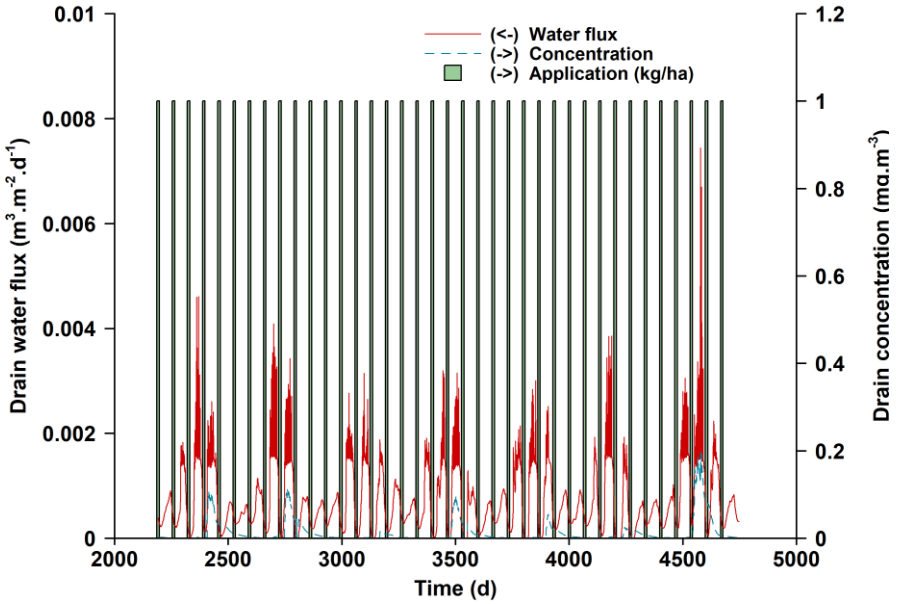

Figure 8.3 *Drain water flux and concentration of substance F in drain water for cultivation Section 1. Application at 1 day after planting of for each cultivation. Application method: spraying of the soil surface. Time 2200.0 corresponds to 10-Jan-2000 0h00*

Next a more detailed comparison was done on the pattern of the drain concentrations and water fluxes over time for time intervals between planting and application of 1, 31 and 61 days. For this comparison the year 2000 was selected as during this year relatively high yearly maximum concentrations were calculated. The data for a comparison of these 3 time intervals are presented in Figure 8.4. In this figure the application data are indicated as well as the date the topsoil is ploughed to a depth of 0.25 m. As mentioned in Section 2.2 the soil is ploughed by rototillage over a depth of 0.15 m between two consecutive cultivations, except before the yearly disinfection that occurs some time during the summer period, when the soil is ploughed over a depth of 0.25 m.

For an application of 1 day after planting, the highest concentrations of about 0.1 mg m^{-1} in the drain are calculated to occur in August (see Figure 8.4, top graph). The concentrations calculated in the preceding period with high drain water fluxes are lower, because of a longer time interval between the application and the start of the period for that cultivation with high drain water fluxes. It should be noted the date of ploughing is only a few days prior to the application date.

For an application of 31 days after planting, the highest concentrations of about 0.4 mg m^{-1} in the drain are calculated to occur in August again (see Figure 8.4, centre graph). In this case the time period between the preceding application date and the date of ploughing to a depth of 0.25 m is about half of the period for the

corresponding period for an application of 1 day after planting. Because of this shorter period, the ploughing results in higher contents of substance in the lowest soil compartment of the top layer, which is adjacent to the first compartment of the macroporous subsoil.

The effect of the time interval between ploughing to 0.25 m and the consecutive application is even more pronounced in case the application is 61 days after planting, as is shown in the bottom graph of Figure 8.4. Now there are only a few days between the date of ploughing and the immediate preceding application. This results practically in a redistribution of the dosage over the top 0.25 m, so significant fluxes into the macropores are calculated during the subsequent period with high drain water fluxes. So the continuous increase in PEC90, when increasing the interval between planting an application is due to the corresponding decrease between the date of ploughing to 0.25 m and the preceding application.

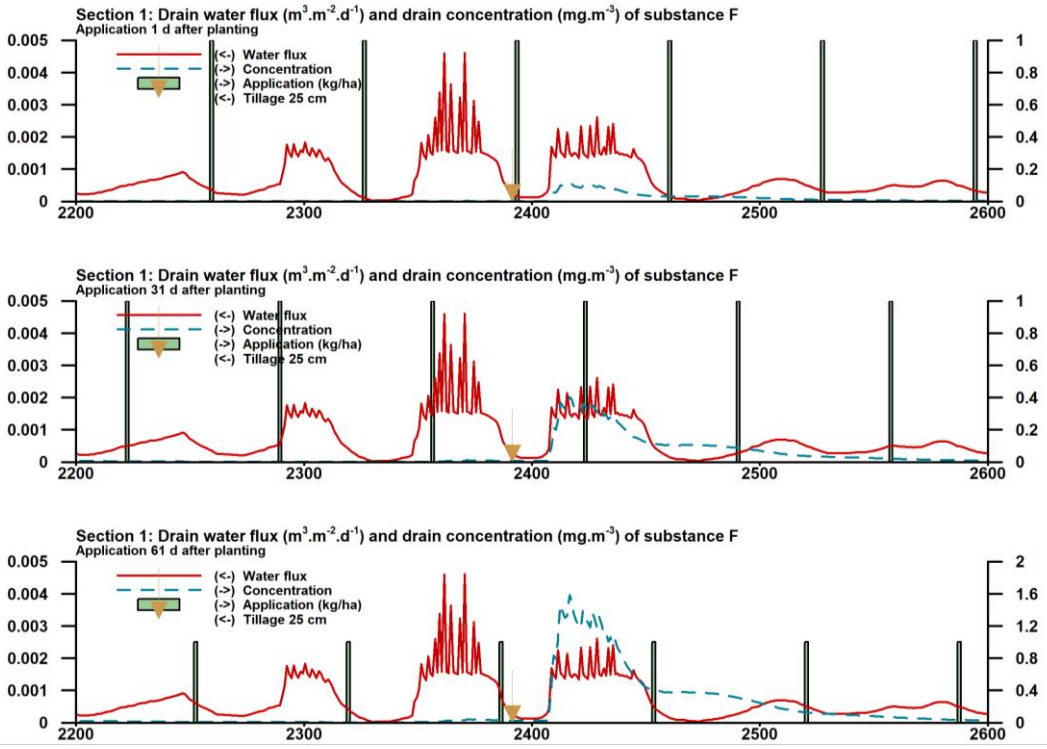

Figure 8.4 *Drain water flux and concentration of substance F in drain water for cultivation Section 1. Application at 1 day (top), 31 (centre) and 61 d (bottom) after planting of for each cultivation. Application method: spraying of the soil surface. Time 2200.0 corresponds to 10-Jan-2000 0h00*

Based on the results of the calculations presented above, it is clear that for a single application of a substance with a DT50 of up to a few tens of days at a specific date the highest values of the 90th percentile concentration in surface water are calculated for an application during the summer months. For substances with a higher value of the DT50 substantial values for this PEC90 are also calculated for applications in the autumn or winter period. This can be explained by the higher residues of these substances in the topsoil during the summer period with high drain water fluxes.

For repeated applications at a specific interval after the date of planting, the highest PEC90 concentrations in surface water are calculated for the latest possible time for this application to occur, possibly during the last week prior to the harvest.

9 General discussion

The results of the calculations using the revised surface water scenario showed that strong fluctuations in the PEC90 concentration in surface water no longer occur for different absolute application dates within a limited time window, so of the order of days or weeks. When using the application option of an absolute date it may occur that the application is shortly before the rototillage of the top 25 cm layer. As substantial drainage into the main bypass domain occurs mostly during the summer period, a comparatively high discharge of substance may enter the surface water and result in a comparatively high concentration in the surface water.

Comparison of the results using the revised groundwater scenario showed that the 90th percentile leaching concentrations were roughly a factor 10 higher than those computed using the groundwater scenario of GEM 3.3.2. This increase is mainly due to the fact that ploughing of the top soil between two consecutive cultivations has been taken into account in the new scenario. With ploughing downward transport of the plant protection product occurs more rapidly than without ploughing. It should be noted that the 90th percentile leaching concentrations of the FOCUS example compounds calculated using the revised groundwater scenario of GEM 4.4.3 are still much lower than those obtained using the FOCUS Kremsmuenster scenario for winter cereals. This lower concentration for the GEM scenario is due to higher organic matter content in the greenhouse soil compared to the Kremsmuenster soil, i.e. 12.1 vs. 3.6%, respectively.

The revised irrigation scheme is based on a surplus irrigation of 25%. It should be noted that the discharge via the drains can be expected to decrease if measures are taken to reduce this surplus irrigation. The impact of lower surplus irrigation could be accounted by the model by introducing a scaling factor for the irrigation amounts, as specified in the input file with meteorological data. However, further study is needed on whether such measures are feasible in practice before this mitigation option could be considered in the exposure assessment.

The applications for registration of a plant protection product in soil-bound cultivation systems in most cases concern a group of crops, including cut-flowers. If the GAP (Good Agricultural Practice) of a plant protection product specifies a number of applications per crop cycle, the relative option for application of the product as implemented in GEM version 4.4.3 should be used. If the GAP specifies a number of applications per year, the user should select the absolute application option. In that case the use of the product is needed for pest control irrespective of the growth stage and therefore the application date for the last application in the application scheme has to be set at a date around the 1st of July.

For the selection of the application date using the revised surface water scenario, an update of the SAFE (Select Application For Evaluation) tool would be helpful. This tool has been developed to support the use of the groundwater scenario in GEM version 3.3.2. It enables the user to run the model for a range of application dates and then select the application date with the highest leaching concentration. An update of this tool would make it easier to select the application date resulting in a reasonable worst-case estimate of the exposure concentration in surface water.

The revised surface water scenario has implications for the effects of formulation additives on the preferential flow fluxes into the macropores of the subsoil. Measurements on the sorption of tolclophos-methyl to greenhouse soils by Matser et al. (1996) gave a geomean K_{om} of 255 L kg^{-1}, whereas Wipfler at al. (2014) used a K_{om} of 2099 L kg^{-1} from the dossier. Probably, the low value measured by Matser et al. (1996) was caused by the formulation additives; in case of preferential flow events shortly after application, these additives are present in the mixing layer of the top soil, so it is likely that this 255 L kg^{-1} is more realistic for the preferential flow fluxes to the macropores than the value of 2099 L kg^{-1}. In the revised surface water scenario the top 0.25 m layer no longer contains macropores, which can be expected to result in a smaller effect of formulation additives on the fluxes into the macropores of the subsoil.

The most important soil property that affects the fate of an active substance in soil is the soil organic matter content. The organic matter content in the top soil of the current scenario for chrysanthemum is 0.137 kg kg^{-1}. This value represents the average of the organic matter content (n = 5) in greenhouse soils with heavy clay soils reported by Wipfler et al (2014). The soil organic matter in soils used for radish cultivation as reported by Voogt and Korsten (1996) is substantially lower, ranging from 0.023 to 0.045 kg kg^{-1}. Whether this would result in higher PEC90 concentrations in surface water, depends also on the irrigation scheme as applied for the cultivation of radish. Further research is needed to collect data on the irrigation schemes used in radish, data on the crop development, as well as data on a characterisation of the soil profile to assess the differences in PEC90 values for these two crops.

10 Conclusions and recommendations

10.1 Conclusions

The goal of the revision of the scenarios for soil-bound cultivation was to solve two major problems in the parameterisation of the surface water scenario of GEM version 3.3.2. The first problem was the extreme sensitivity of the outcome of the assessment using the surface water scenario as a result of the exact repetition of the irrigation scheme for a fully-grown chrysanthemum crop throughout the year as assumed in the scenario. The other issue was the practice of regularly ploughing of the topsoil, which was assumed to contain a well-developed macropore system. To address the first problem, the greenhouse was divided into 24 cultivation sections with a different sequence of chrysanthemum crops. The irrigation scheme for the simulation of each cultivation section is linked to the growth stage of the crop in each crop cycle in this section. The second problem was addressed by the change of the topsoil layer with a well-developed macropore system into a layer without macropores. Therefore, these two major issues as reported for GEM 3.3.2 have been solved.

The greenhouse represented in the GEM 3.3.2 surface water scenario was selected from a set of twelve representative greenhouses. The change in the description of the soil profile could have affected the greenhouse selection for the scenario, because the relative vulnerability of each greenhouse might have changed. Therefore, the selection procedure was repeated. The outcome of the selection procedure was the same as that obtained by Wipfler et al. (2014). Again greenhouse 5 was selected; this greenhouse has a heavy clay soil with a fluctuating groundwater level at around a depth of 80 cm.

The greenhouse selection procedure was also repeated to find the greenhouse meeting the requirement that the average annual concentration in groundwater for at least 90th of the population (in time and space) to be lower than 0.1 µg L^{-1}. This resulted in the selection of a different greenhouse, greenhouse 8 (in the Westland area) instead of greenhouse 11 (in the Venlo area). Both greenhouses have a light sandy clay soil, but the temporal variation in the groundwater level is somewhat less in the Westland greenhouse.

Calculations with the revised surface water scenario showed that there was no longer an extreme sensitivity of the exposure concentration to the date of application. Nevertheless, the exposure concentration is still sensitive to the date of application. This sensitivity is, however, more predictable and is primarily linked to the seasonal pattern of drainage fluxes.

The new version of GEM contains the option to specify an application day relative to the date of planting or harvest. If the GAP (Good Agricultural Practice) of a plant protection product specifies a number of applications per crop cycle, the relative application date option should be used. If the GAP specifies a number of applications per year, the application option to specify an absolute date should be selected. Given the seasonal pattern, the date of the last application in the application scheme can best be set at around the 1st of July. This would result in a reasonable worst-case estimate of the exposure concentration.

For a more accurate selection of the application date resulting in the required percentile of the PEC90 in surface water, we recommend an update of the SAFE (Select Application For Evaluation). This tool has been developed to support the use of the groundwater scenario in GEM version 3.3.2. It enables the user to run the model for a range of application dates and then select the application date with the highest leaching concentration. An update of the SAFE tool would make it easier to select the application date resulting in a reasonable worst-case estimate of the exposure concentration in surface water.

As no experimental data on soil hydrology and concentrations in soil and drainage water were available, the plausibility of the revised surface water scenario was tested using monitoring data of tolclophos-methyl collected in the Bommelerwaard. When using the DegT50 value obtained from studies with field soils the PEC90 concentration calculated was much lower than those measured in the monitoring study, but when

using the value for the DegT50 obtained from studies with greenhouse soils (Matser et al., 1996), the resulting PEC90 concentrations were of the same order as the highest values measured in the Bommelerwaard area.

The target concentration for the assessment of the exposure in surface water strongly depends on the half-life of the substance in the greenhouse soil. Therefore, it is important to use data on substance properties that are representative for greenhouse soils. Matser et al. (1996) have shown that more reliable values for DegT50 and K_{om} could be obtained when using soil samples from greenhouse soils instead from soil samples from field soils.

10.2 Recommendations

For the assessment of the exposure of aquatic organisms to the plant protection products in surface water, data on the DegT50 of the substance should preferably be obtained from measurements in greenhouse soils. If such data are not available, it is recommended to apply provisionally the same factor as included in the tiered assessment scheme proposed by Wipfler et al. (2014), i.e. multiplying the DegT50 value derived from measurements in field soils by a factor 10. This factor could be used in the surface water and groundwater exposure assessments for substances for which only DegT50 values for field soils are available. The measurement of the half-life in greenhouse soils could be part of the exposure assessment at a higher tier.

To further check the validity of the revised surface water scenario, a greenhouse experiment would be needed for an application with different substances in a chrysanthemum crop. In this experiment detailed measurements need to be collected on the hydrology in the greenhouse system as well as measurements of pesticide residues in the soil and in the waste water discharged into the ditch. It is recommended to develop a protocol first with a specification of the design of the experiment as well as a specification of all measurements to be made.

Although developed and tested for chrysanthemum (cut flowers), the revised scenarios can be used for all soil-bound crops that are grown in Dutch greenhouses. However, in the case of radish – another important soil-bound greenhouse crop in the Netherlands – the protectiveness of the scenarios can be questioned, because radish is grown in soil with a much lower organic matter content. On the other hand, irrigation amounts in radish are lower. Therefore, it is recommended to collect data on cultivation practices and to check whether the revised cut-flowers scenario is protective enough for radish.

The scenarios have been developed to assess the risk of exposure of pesticides used in Dutch greenhouses. The GEM model could be a useful tool for the assessment of the exposure of plant protection products in other crops in greenhouse systems in the EU. Therefore, it is recommended to investigate the extent and characteristics of soil-bound crops as well as the cultivation practices in other EU countries. This could help in identifying the areas where additional exposure scenarios would be needed.

References

Bouma, J., 1987. Stroming van water. In: Locher, W.P. and H. de Bakker, 1987. Bodemkunde van Nederland. Stichting voor Bodemkartering, Wageningen en Ministerie van Landbouw en Visserij, Den Haag. (in Dutch).

Bronswijk, J.J.B., 1988. Effect of swelling and shrinkage on the calculation of water balance and water transport in clay soils. Agricultural Water Management 14 (1988): 185-193.

EFSA, 2005. Conclusion regarding the peer review of the pesticide risk assessment of the active substance tolclofos-methyl. EFSA Scientific Report 32: 1-65.

Ernst, L.F., 1962. Groundwater flow in the saturated zone and its calculation when parallel open conduits are present. Thesis (Dutch with English summary), University of Utrecht, 189 pp

Fenoll, J., Ruiz, E., Flores, P., Hellín, P. and Navarro S., 2011. Reduction of the movement and persistence of pesticides in soil through common agronomic practices. Chemosphere 85: 1375-1382.

Graaf, R. de, 1981. Transpiration and evapotranspiration of glasshouse crops. Acta Hort. 119:147-158.

Jarvis, N. 2008. Near-Saturated Hydraulic Properties of Macroporous Soils. Vadose Zone J. 7:1302-1310.

Jarvis, N.J., and I. Messing. 1995. Near-saturated hydraulic conductivity in soils of contrasting texture as measured by tension infiltrometers. Soil Sci. Soc. Am. J. (59):27-34.

Leistra, M., Dekker, A., van der Burg, A.M.M., 1984a. Leaching of oxidation products of aldicarb from greenhouse soils to water courses. Arch. Environ. Contam. Toxicol. 13: 327-334.

Leistra M., Dekker, A. and van der Burg, A.M.M., 1984b. Computed and measured leaching of the insecticide methomyl from greenhouse soils into water courses. Water, Air and Soil Pollution 23: 155-167.

Matser, A.M., Leistra, M., Pellikaan-van Harten, H.A.J., van den Berg, F. and Runia, W.T., 1996. Uitspoeling van bestrijdingsmiddelen uit kasgronden naar waterlopen. Gegevens over de kasteeltsystemen. Rapport 481.1, DLO-Staring Centrum, Wageningen, 66 pp.

Rijtema, P. E., 1969. Soil moisture forecasting. Instituut voor Cultuurtechniek en Waterhuishouding, Nota 513, Wageningen.

Schaap, M.G. and Van Genuchten M. Th., 2006. A Modified Mualem–van Genuchten Formulation for Improved Description of the Hydraulic Conductivity Near Saturation. In: Vadose Zone Journal 5:27–34.

Smelt, J.H., Leistra, M., Houx, N.W.H. and Dekker, A., 1978. Conversion rates of aldicarb and its oxidation products in soils. II. Aldicarb sulphoxide. Pestic. Sci. 9: 286-292.

Swinkels, G.L.A.M., 2006. Software for calculating the effect of energy saving investments on greenhouses. Acta Hortic. 718, 233-242. DOI: 10.17660/ActaHortic.2006.718.25

Tiktak, A., Boesten, J.J.T.I, Hendriks R.F.A. and van der Linden, A.M.A., 2012. Leaching of plant protection products to field ditches in the Netherlands: development of a drainpipe scenario for arable land. RIVM report 607407003/2012, RIVM, Bilthoven.

Visser, J. and Linders, J.B.H.J., 1992. Tolclofos-methyl. Milieufiche. Adviesrapport 90/670101/018, RIVM, Bilthoven.

Voogt, W., Kipp, J.A., Graaf, R. de and Spaans, L., 2000. A fertigation model for glasshouse crops grown in soil. Acta Hort, 537, 495-502.

Voogt W. and Korsten P., 1996. Mineral balances for radish crops grown under glass. Acta Hort. 428, 53 - 64.

Wipfler, E.L., Cornelese, A.A., Tiktak, A., Vermeulen, T. and Voogt, W., 2014. Scenarios for exposure of aquatic organisms to plant protection products in the Netherlands. Alterra report 2388.

Wösten, J.H.M., Veerman, G.J., de Groot, W.J.M. and Stolte, J., 2001. Water retention and hydraulic conductivity functions of top- and subsoils in The Netherlands: The Staring Series. Alterra report 153, Alterra, Wageningen, the Netherlands.

List of Abbreviations

Ctgb	Board for the authorisation of plant protection products and biocides
EFSA	European Food Safety Authority
EU	European Union
FOCUS	Forum for Co-ordination of pesticide fate models and their use
GAP	Good Agricultural Practice
GEM	Greenhouse Emission Model
KASPRO	Greenhouse Process model
PBL	Netherlands Environmental Assessment Agency
PEARL	Pesticide Emission At Regional and Local Scales
PEC	Predicted Environmental Concentration
RIVM	National Institute of Public Health and the Environment
SAFE	Select Application For Evaluation
SWAP	Soil Water Atmosphere Plant
TOXSWA	Toxic Substances in Water. Model that simulates

Annex 1 Parameterisation of revised macropore system

Section Macropores

OptMacropore *[SWMACRO]*	Option for macropore flow simulations	Set to 1, so macropores are considered.
OptMacroporePTF	Option for use of pedotransfer functions	Set at 'Yes'
ZAHor *[Z_AH]*	Depth bottom A-horizon (m)	0.30 m
ZIca *[Z_IC]*	Depth bottom Internal Catchment (IC) domain (m)	0.6959 m (from ptf function based on GLG)
ZSta *[Z_ST]*	Depth bottom Static macropores (m)	1.3919 m (from ptf function based on GLG)
VolStaTop *[VLMPSTSS]*	Volume of Static Macropores at Soil Surface (m3/m3)	0.0779 m3/m3 (from ptf function using COLE)
FraIcaTop *[PPICSS]*	Proportion of IC domain at Soil Surface (-)	0.9
NumIcaDom *[NUMSBDM]*	Number of Subdomains in IC domain (-)	Set to 10. Fixed value in PEARL
PowMac *[POWM]*	Exponent M for frequency distribut. curve IC domain (-)	Set to 1
[SWPOWM]	Switch for double convex/concave freq. distr. curve	0
FraZAHor *[RZAH]*	Fraction macropores ended at bottom A-horizon (-)	0.0
SPOINT *[SPOINT]*	Symmetry Point for freq. distr. curve	1.00
DiaPolMin *[DIPOMI]*	Minimal diameter soil polygones (shallow) (m)	0.02
DiaPolMax *[DIPOMA]*	Maximal diameter soil polygones (deep) (m)	0.10
[Z_MB50]	Depth at which MB domain width is 50% of max (m)	1.0439
ZPndMacMax *[PNDMXMP]*	Threshold of ponding for overland flow into macropores (m)	0.0
table shrinkage option *[SWSoilShr]*	Table with shrinkage option for each soil horizon: horizon number and option (0 = no shrinkage)	Set to 0 for each horizon in SWAP input file; option not supported by PEARL. *[ISOILLAY3] [SWSoilShr]* 1 0 2 1 3 1 4 1 5 1 6 1 7 1 8 1 9 1
table sorptivity option *[ISOILLAY4]* *[SwSorp]* *[SorpFacParl]*	Table with sorptivity option for each soil horizon: horizon number and option (1 = calculated from hydraulic functions) and reduction factor sorpt. (-)	Set to 1 for each horizon in SWAP input file; option not supported by PEARL. Hor SwSorp SorpFacParl SorpMaxParl SorpAlphaParl 1 1 1 1.0 0.5 2 1 1 1.0 0.5 3 1 1 1.0 0.5 4 1 1 1.0 0.5 5 1 1 1.0 0.5 6 1 1 1.0 0.5 7 1 1 1.0 0.5 8 1 1 1.0 0.5 Source: default

[SWDARCY]	Switch for using Darcy flow for infiltration out of macropores (1=Yes)	Set to 1. Fixed value in PEARL
ShaFacMac *[ShapeFacMp]*	Shape factor macropores	0.1
RstDraRapRef *[RapDraResRef]*	Reference rapid drainage resistance (d)	10
RstDraRapExp *[RapDraReaExp]*	exponent for reaction drainage to dynamic crack width	Set to 1.0. Fixed value in PEARL
CritUndSatVol *[CritUndSatVol]*		Set to 0.1. Fixed value in PEARL

Annex 2 Some details of model revision

A2.1 Derivation of geometry factor ω_{cl}

The numerical expression of the water balance for the compartment that covers the top of the macro-pores in the heavy clay soil reads as:

$$\frac{\theta_i^{j+1}-\theta_i^j}{\Delta t^j}=\frac{1}{\Delta z_i}\left[K_{i-\frac{1}{2}}^{j+k}\left(\frac{h_{i-1}^{j+1}-h_i^{j+1}}{\frac{1}{2}(\Delta z_{i-1}+\Delta z_i)}+1\right)-K_{i+\frac{1}{2}}^{j+k}\left(\frac{h_i^{j+1}-h_{i+1}^{j+1}}{\frac{1}{2}(\Delta z_i+\Delta z_{i+1})}+1\right)-\omega\,K_i^{j+k}\left(\frac{h_i^{j+1}}{\frac{1}{2}\Delta z_i}+1\right)\right]-S_{a,i}^j-S_{d,i}^j$$

Where *i* is the index of the layer and $-\omega\,K_i^{j+k}\left(\frac{h_i^{j+1}}{\frac{1}{2}\Delta z_i}+1\right)$ is the flux to the macro pores.

The multiplicative factor ω accounts for the influence of non-vertical flow and is based on a consideration of the reciprocals of flow resistances. The derivation goes as follows.

In hydrological models, the flow resistance is often calculated as the ratio of a distance between two points and the conductivity of the medium between the two points. In our case the flow resistance between a node and the bottom of the corresponding compartment reads as:

$$\frac{1}{2}\frac{\Delta z_i}{K_i}$$

The flow from the middle of the compartment, with uniformly distributed inflow from above, to the macropores leads to longer flow paths. Therefore this type of flow leads to a greater value of the distance variable in the resistance expression. The enlargement of the flow resistance is expressed by a factor ξ. So the adjusted flow resistance reads as:

$$\xi\ \frac{1}{2}\frac{\Delta z_i}{K_i^{j+k}}$$

For design of drainage systems and for the calculation of drainage flow rates in hydrological model, the Ernst equation is often used (Ernst, 1962). The total flow resistance between a top boundary with uniformly distributed input to a line sink is expressed by:

$$\frac{1}{2}\frac{\Delta z_i}{K_i}+\frac{L}{\pi\,K_i}ln\left(\frac{L}{\pi r_0}\right)+\frac{L^2}{12K_i\ \Delta z_i}$$

Where $\frac{1}{2}\Delta z_i$ is the thickness of the flow layer, K_i is the conductivity, *L* is the distance between the line sinks and $r_0$is the radius of the line sink. $\frac{1}{2}\frac{\Delta z_i}{K_i}$ expresses the vertical flow resistance, $\frac{L}{\pi\,K_i}ln\left(\frac{L}{\pi r_0}\right)$ is and expression for the radial flow resistance and $\frac{L^2}{12K_i\ \Delta z_i}$ for the horizontal flow resistance.

The factor 12 in the denominator is used instead of 8, as originally postulated by Ernst (1982), to account for the shape of the pressure course with distance (shape factor=2/3). In our case we sum the vertical, radial and horizontal flow resistance and use $\xi\ \frac{1}{2}\frac{\Delta z_i}{K_i^{j+k}}$ for the total flow resistance:

$$\xi\ \frac{1}{2}\frac{\Delta z_i}{K_i}=\frac{1}{2}\frac{\Delta z_i}{K_i}+\frac{L}{\pi\,K_i}ln\left(\frac{L}{\pi r_0}\right)+\frac{L^2}{12K_i\ \Delta z_i}$$

Rearranging yields:

$$\xi = 1 + \frac{L}{\pi ½ \Delta z_i} ln\left(\frac{L}{\pi r_0}\right) + \frac{L^2}{6(\Delta z_i)^2}$$

The flux to the macro pores, for the situation where the convergence and divergence of streamlines is accounted for, is written as:

$$-K_i \left(\frac{h_i^{j+1}}{\frac{1}{2}\Delta z_i} + 1\right)$$

Rewriting this equation gives:

$$-\left(\frac{h_i^{j+1}}{\frac{\frac{1}{2}\Delta z_i}{K_i}} + \frac{\frac{1}{2}\Delta z_i}{\frac{\frac{1}{2}\Delta z_i}{K_i}}\right)$$

Accounting for the factor ξ implies the multiplication of $\frac{1}{2}\frac{\Delta z_i}{K_i}$ with ξ

$$-\left(\frac{h_i^{j+1}}{\frac{\frac{1}{2}\Delta z_i}{\xi\frac{\frac{1}{2}\Delta z_i}{K_i}}} + \frac{\frac{1}{2}\Delta z_i}{\frac{\frac{1}{2}\Delta z_i}{\xi\frac{\frac{1}{2}\Delta z_i}{K_i}}}\right)$$

Further rearrangement gives:

$$-\frac{K_i}{\xi}\left(\frac{h_i^{j+1}}{\frac{1}{2}\Delta z_i} + 1\right)$$

In this equation we can see that ξ equals the reciprocal value of ω, thus:

$$\omega = \frac{1}{\xi} = \frac{1}{1 + \frac{L}{\pi\frac{1}{2}\Delta z_i} ln\left(\frac{L}{\pi r_0}\right) + \frac{L^2}{6\Delta {z_i}^2}}$$

A2.2 Revised calculation of groundwater level

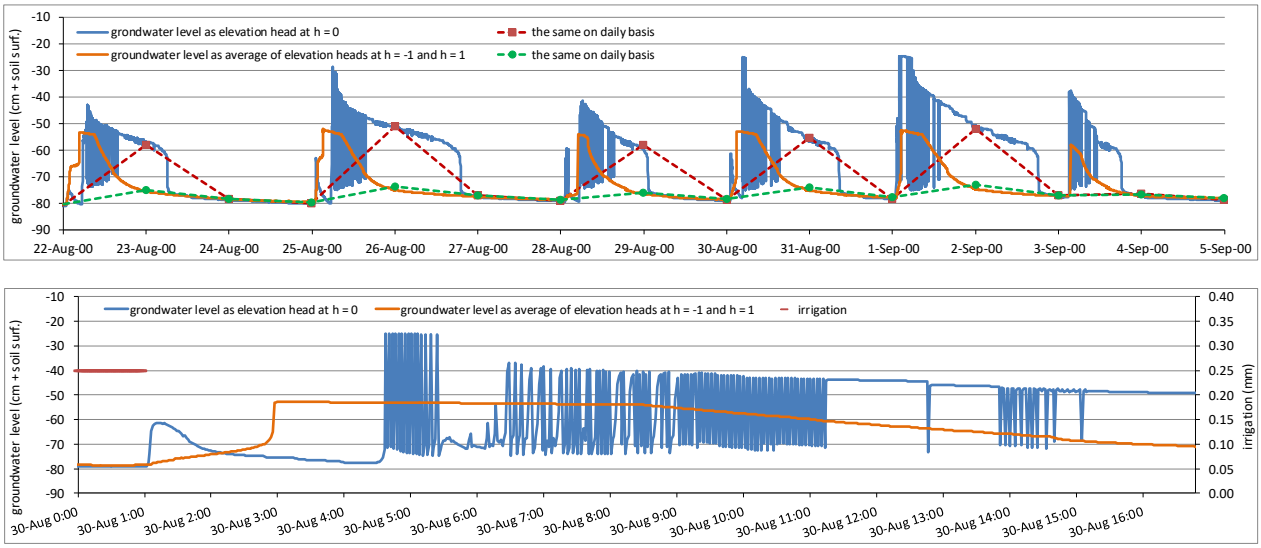

Figure A2.1 *Comparison of the results of two ways of simulation of groundwater levels with SWAP for Cultivation Section 1 in 2000: the original way as groundwater level equals elevation head at pressure head h = 0 and an adapted way where groundwater level is calculated as the average of the elevation heads at pressure heads h = -1 cm and h = 1 cm*
Top: for the period August 22 until September 5. The groundwater level at daily basis applies at the end of the day
Bottom: in more detail for the day of Augustus 30. The irrigation is applied in the first 0.04 part of the day

Annex 3 Revised interface between SWAP and PEARL

The changes in the interface file *.bfo between SWAP and PEARL are indicated in green in the table below with description of output from SWAP to PEARL. Both changes concern the inflow into the top of the macropores of both domains. The name of parameter IQInTop**Pre**Dm1/2 for direct precipitation into macropores is changed into IQInTop**Vrt**Dm1/2 which is a more general name for vertical inflow into the top of the macropores. In the new version this name is used for both options: with and without a covering layer. In the version with covering layer parameter IQInTopLatDm1/2 has no meaning and is treated as a dummy; its value is not relevant.

Description of variable	Unit	Range	R	DT	Mnemonic
Dynamic part for macropores, domain 1 (Main Bypass Flow domain)					
Water level at end of time-interval	m-surf.	[0.0 ...]	*	R	WaLevDm1
Areic volume at end of time-interval	$m^3\ m^{-2}$	[0.0 ...]	-	R	VlMpDm1
Areic volume of water stored at end of time-interval	$m^3\ m^{-2}$	[0.0 ...]	-	R	WaSrDm1
Infiltration flux **in top of macropores from covering layer without macropores** ~~at soil surface directly by precipitation~~	$m\ d^{-1}$	[0.0 ...]	-	R	**IQInTopVrtDm1** ~~IQInTopPreDm1~~
Dummy ~~Infiltration flux at soil surface indirectly by lateral overland flow (runoff)~~	$m\ d^{-1}$	**[0.0]**	-	R	IQInTopLatDm1
Exchange flux with soil matrix per compartment 1-numnod (positive: from macropores into matrix)	m d-1	[...]	*	R	InQExcMtxDm1Cp(numnod)
Rapid drainage flux towards drain tube per compartment 1-numnod	$m\ d^{-1}$	[0.0 ...]	*	R	InQOutDrRapCp(numnod)
Average fraction of macropore wall in contact with macropore water during timestep per comp. 1-numnod	$m\ d^{-1}$	[0.0 ...]	*	R	FrMpWalWetDm1(numnod)
Dynamic part for macropores, domain 2 (Internal Catchment domain)					
Areic volume at end of time-interval	$m^3\ m^{-2}$	[0. 0 ...]	*	R	VlMpDm2
Areic volume of water stored at end of time-interval	$m^3\ m^{-2}$	[0. 0 ...]	-	R	WaSrDm2
Infiltration flux **in top of macropores from covering layer without macropores** ~~at soil surface directly by precipitation~~	$m\ d^{-1}$	[0. 0 ...]	-	R	**IQInTopVrtDm2** ~~IQInTopPreDm2~~
Dummy ~~Infiltration flux at soil surface indirectly by lateral overland flow (runoff)~~	$m\ d^{-1}$	**[0. 0]**	-	R	IQInTopLatDm2
Exchange flux with soil matrix per compartment 1-numnod (positive: from macropores into matrix)	$m\ d^{-1}$	[...]	*	R	InQExcMtxDm2Cp(numnod)
Average fraction of macropore wall in contact with macropore water during timestep per comp. 1-numnod	$m\ d^{-1}$	[0.0 ...]	*	R	FrMpWalWetDm2(numnod)

Annex 4 Some details of the parameterisation

A4.1 Hydraulic curves with imposed boundary entry pressure value

In the GEM scenarios the hydraulic functions of the heavy clay subsoil are described with the Mualem-VanGenuchten (MVG) parameter values of Staring Series unit O13. The saturated conductivity K_s of this unit amounts to 4.37 cm d^{-1}. This is very high for a heavy clay soil matrix. Values smaller than 1 cm d^{-1} are more realistic (e.g. Rijtema, 1969; Bouma, 1987; Bronswijk, 1988). Although Wösten et al. (2001) suggest that the Staring Series' K_s is a fitting parameter of the MVG hydraulic conductivity function and as such does not reflect the macropore conductivity in the field, it is very likely that the underlying undisturbed field samples of 10.2 cm diameter and 8 cm height did contain very small structural cracks. According to Poiseuille's law even tiny cracks strongly increase saturated hydraulic conductivity.

The small cracks will be fully drained at a certain negative pressure head. This 'boundary pressure head' h_e resembles the macropore air entry value that marks the boundary capillary height below which macropores can no longer retain water. Typical values are between -1 and -10 cm (Jarvis and Messing, 1995). Schaap and Van Genuchten (2006) found a soil-independent value of -4 cm for h_e in their modified MVG model. This modMVG model can be used to describe macropore flow in an implicit way. It was already implemented in SWAP. It yields saturated conditions in the soil matrix for the pressure head range of 0 to h_e. In this range, capillary pressure is high enough to retain saturation in the micropores of the soil matrix. Therefore, using this modMVG model in simulations with the explicit macropore concept in SWAP is more consistent than using the original MVG model.

In the GEM scenarios, a value of -5 cm is used for the boundary pressure head h_e. For the Staring Series unit O13 this value yields a hydraulic conductivity K of 0.168 cm d^{-1} and a volumetric water content θ of 0.5664 cm^3 cm^{-3}. In the modMVG model these values are the input values for K_s and θ_s (volumetric water content at saturation). In combination with h_e = -5 cm and the original values of the remaining MVG parameters of unit O13 this yields the hydraulic curves of Figure A4.1. The complete set of used modMVG parameter values is listed in Table A4.1.

Table A4.1 *Parameters values of the modified Mualem-VanGenuchten functions for the heavy clay subsoil in the GEM scenarios. Compared to the original parameterisation of Staring Series unit O13, Ks and θs are modified and he is added*

Description	Layer depth (cm)	θ_r (cm^3/cm^3)	θ_{sat} (cm^3/cm^3)	α (1/cm)	n (-)	Ksat,fit (cm/d)	l (-)	α_w (1/cm)	h_e (cm)
Subsoil	25-500	0.08	0.5664	0.0194	1.089	0.168	-5.955	0.0194	-5.0

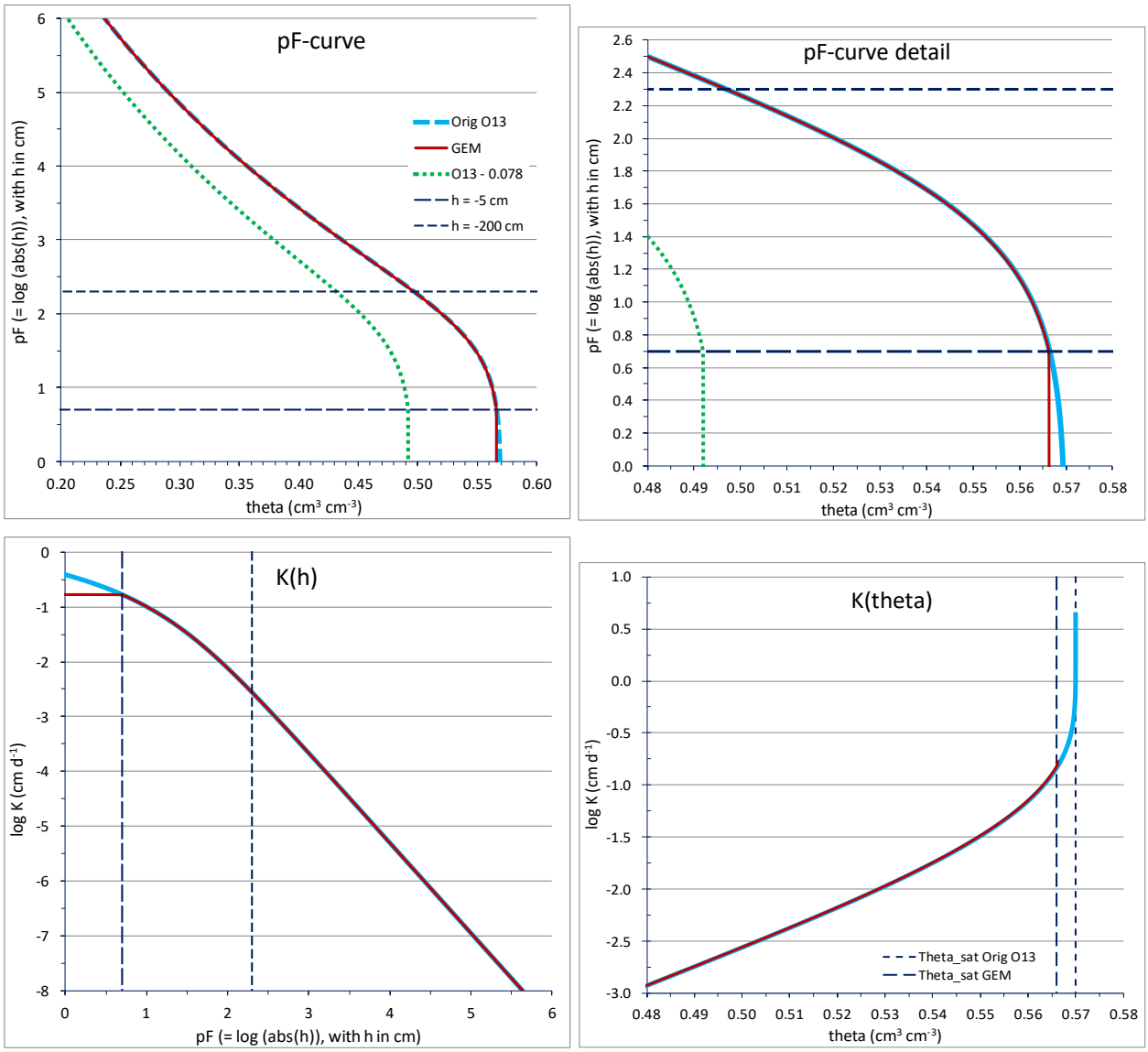

Figure A4.1 *Top: original water retention curve (pF) of Staring Series Unit O13 (heavy clay), adapted curve used in GEM (red line) with boundary pressure head h_e = -5 cm and θ_s = 0.5663 and θ_s based on Staring Series Unit O13 and macropore volume of 0.078 cm³ cm⁻³ (green dotted line). Bottom: original hydraulic conductivity curves (K(h) and K(theta)) of Staring Series Unit O13 and adapted curve used in GEM with boundary pressure head h_e = -5 cm and K_s = 0.168 cm d⁻¹. The dashed straight lines mark the pressure head values of -5 and -200 cm (except bottom right)*

The curves of Figure A4.1 show that at pressure heads below -5 cm (pF-values above 0.699) both the pF-curve and the K(h)-curve modified for GEM scenario NewTopLayer are similar to the original O13-curves. This indicates that refitting of the MVG curves is not required if in the modMVG model the $K(h_e)$ and $\theta(h_e)$ values of the original curves are used as input for K_s and θ_s.

As the boundary pressure head h_e of -5 cm marks the division of pore volume between macropores and micropores (soil matrix) a value for macropore volume can be read from the x-axes of the pF-curve as the distance between the red line and the blue line. This volume amounts to 0.57 – 0.5664 = 0.0036 cm³ cm⁻³ which is much less than the inputted value for macropore volume of 0.078 cm³ cm⁻³ (Table 4.3 in main text). This implies that the GEM scenario suggests that most of the macropore volume originates from large structural features like ripening cracks and not only from small structural cracks that are captured in an undisturbed soil sample with diameter of 10.2 cm like the samples on which unit O13 is based. These large structures were not present in these samples.

To illustrate the latter suggestion: if we calculate the matrix θ_s of the modMVG model in a similar way as in the former section on the basis of the total pore volume of unit O13 but now with the GEM macropore volume of 0.078 $cm^3\ cm^{-3}$ we get 0.57 - 0.078 = 0.492 $cm^3\ cm^{-3}$. This value yields the green pF-curve in Figure A4.1-top. This curve is far off from the original pF-curve for the unsaturated soil matrix and thus it cannot represent the matrix retention characteristics. Therefore, another approach is applied in SWAP: the permanent macropore volume V_{mp} is taken apart from the matrix volume by considering the fraction of horizontal matrix area FrArMtrx = 1 - V_{mp} / Δz (layer thickness) and multiplying θ of the matrix (and the vertical fluxes in the matrix) with this fraction. For the GEM pF-curve of Figure A4.1 with a macropore volume of 7.8% this yields a matrix pore volume of 0.922 * 0.5664 = 0.522 and a volume of solid matrix parts of 0.400. As the ratio between the volumes of pores and solids of the matrix is not changed, the original pF-curve of unit O13 is still valid for the unsaturated matrix.

A4.2 Sensitivity analyses to determine optimal DTMAX value

In the original and the ptf corrected GEM 332 scenario the value of the maximum time step DTMAX in SWAP is set at the default value of 0.2 day. SWAP uses this relatively large time step if the model is able to reach a numerical solution in solving the Richards' equation with this step size. If not, SWAP starts decreasing the time step until a solution is reached. If time series of variables are input to the model the smallest time interval of the input dictates the maximum time step of that moment.

Flow processes in macroporous soils are most of the time relatively rapid processes, because of the high potential of macropores for conducting water compared to the soil matrix. Particularly inflow into the top of the macropores at the soil surface or from a covering layer without macropores is a rapid process as it is triggered by exceeding thresholds like the infiltration capacity of the soil matrix at soil surface or the matrix pressure head at saturation. If this exceedance is due to high intensity precipitation – rainfall or irrigation – SWAP adapts the time step accordingly to this intensity. But when precipitation ends, flow processes like inflow and rapid drainage are often still very dynamical. Then SWAP could choose a too large time step that yields less realistic results.

To investigate the effect of the size of the time step on the SWAP results, simulations of four values of DTMAX are compared: 0.2, 0.1, 0.01 and 0.001 day. From the results an optimal time step size is chosen. Where 'optimal' is defined according to two criteria:

1. small enough to yield results that differ only little from the results obtained with an one order of magnitude smaller time step;
2. as large as is allowed by the first criterion in order to reduce computing time.

The analyses are conducted for the New Top Layer ptf corrected scenario and the year 2005. Figure A4.2 shows the results for the annual water balance terms 'inflow at the top of the macropores', 'rapid drainage (from the macropores)', 'drainage from the matrix' and 'upward seepage', and for the computing time (cpu).

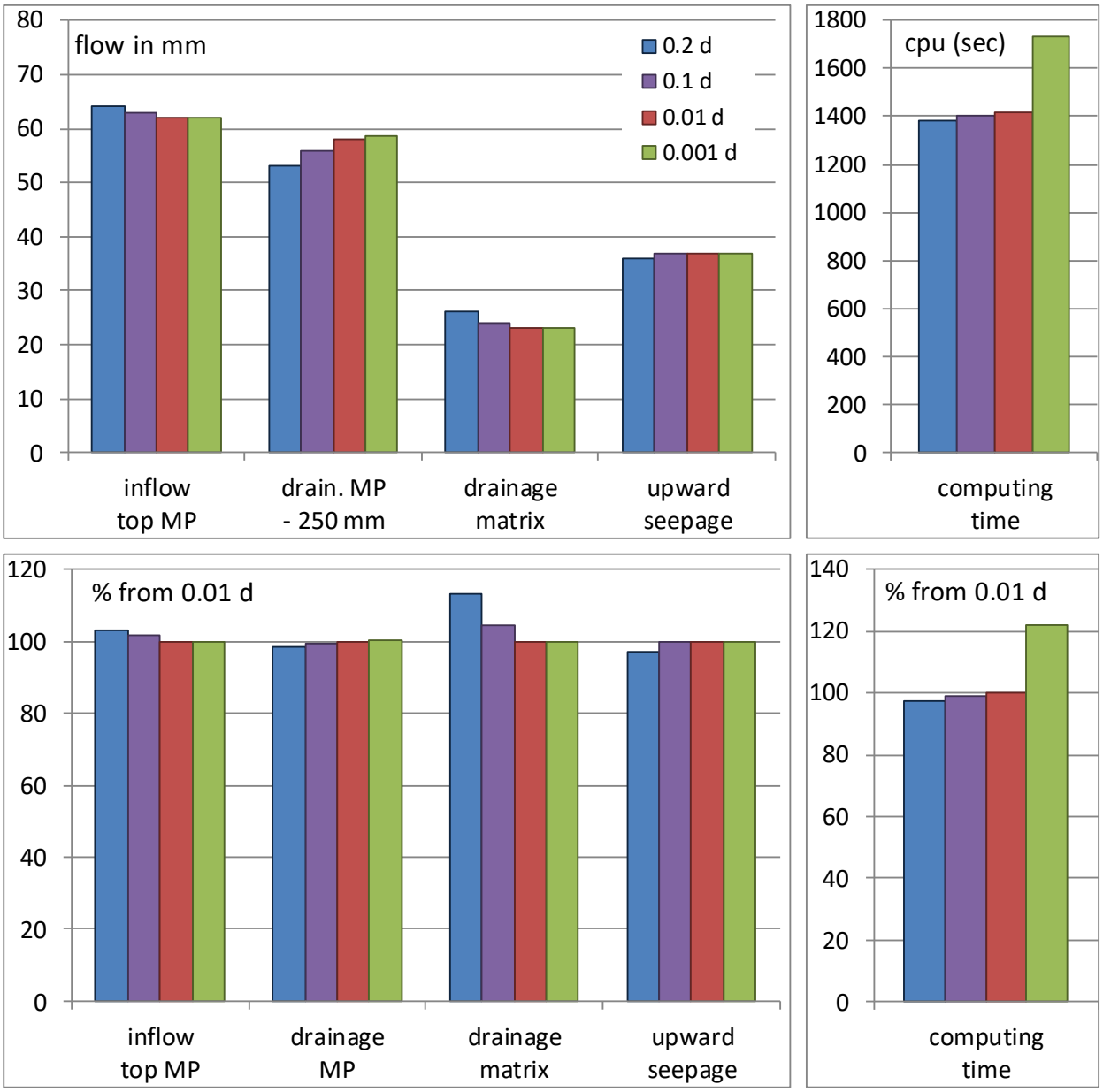

Figure A4.2 *Results of the sensitivity analyses for four values of the maximum time step DTMAX in SWAP, i.e. 0.2, 0.1, 0.01 and 0.001 day. Top: absolute values in mm per year and in seconds; bottom: values in percentages relative to the chosen optimal time step of 0.01 day*

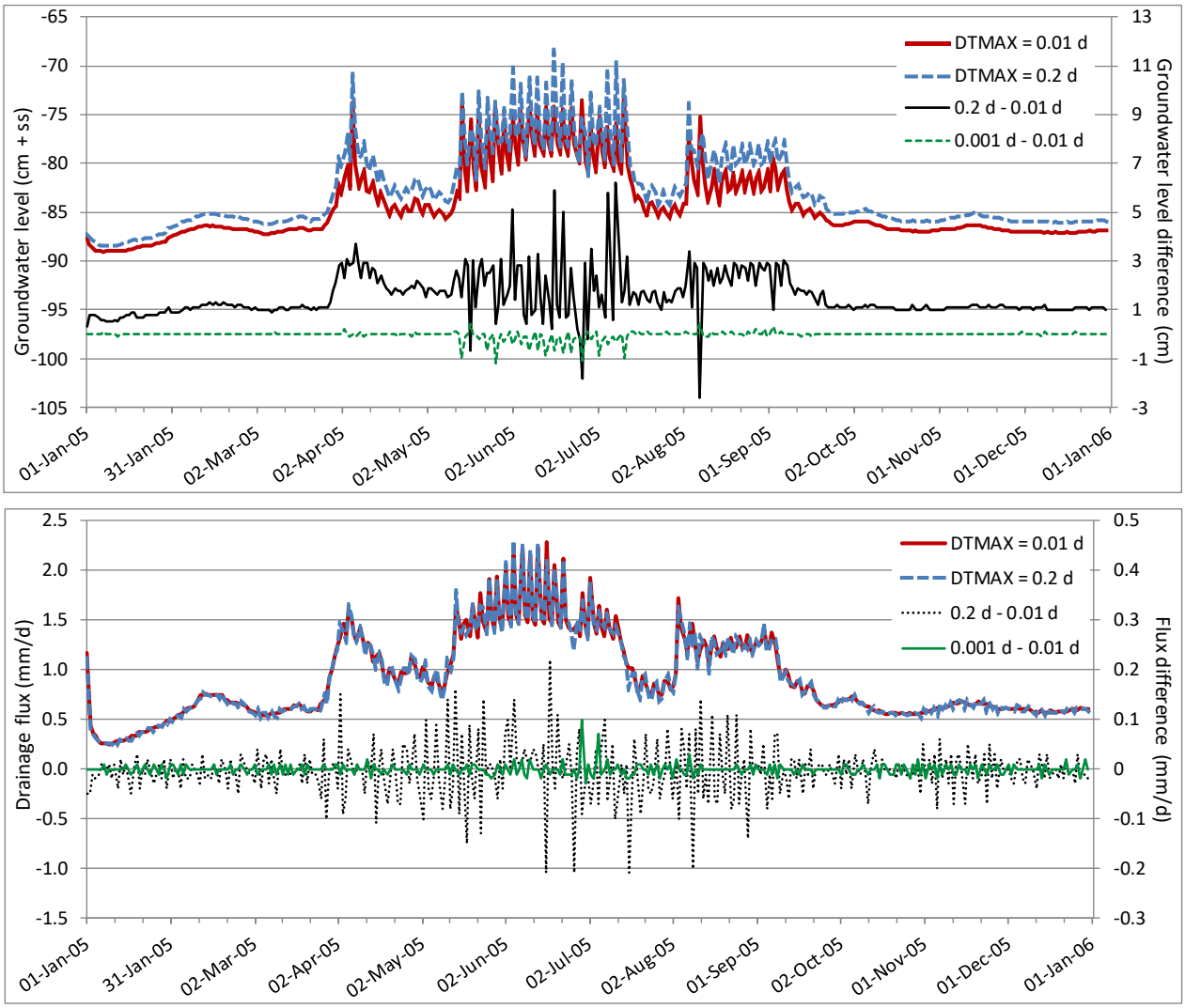

Figure A4.3 *As in Figure A4.2 but results as time series of groundwater level (top) and drainage fluxes (bottom). Time series of DTMAX = 0.2 and 0.01 day are shown. Time series of DTMAX = 0.1 and 0.001 day are not shown (see main text). Also shown are time series of differences between DTMAX = 0.2 and 0.01 day and between DTMAX = 0.001 and 0.01 day (right y-axes).*

Figure A4.3 shows time series of the two most dynamic output parameters: groundwater level and drain flux. Only the results of the default time step value of 0.2 d and the chosen optimal value of 0.01 d are shown. Results of 0.1 d are in between those of 0.2 and 0.01 d, and results of 0.001 d are more or less on top of those of 0.01 d.

From the results of Figures A.4.2 and A.4.3 the value of 0.01 day is chosen as optimal value of the time step. For the computing time this value only differs little from the maximum allowed value of 0.2 day, while the difference with the ten times lower value of 0.001 day is substantial: 314 sec or 22% (second criterion). The differences in annual balance terms are relatively small, even between the maximum and the optimal time step. Exception is drainage from the matrix, but there absolute differences are small. Values of the optimal time step and the one order smaller time step hardly differ which meets the first criterion.

The choice for the optimal time step value of 0.01 d is mainly based on the differences in time series dynamics. Differences between 0.2 (and also 0.1) day and the optimal value are substantial, while differences between 0.001 and the optimal value are only minor.

Wageningen Environmental Research
P.O. Box 47
6700 AA Wageningen
The Netherlands
T 0317 48 07 00
wur.eu/environmental-research

Report 3151
ISSN 1566-7197

To explore the potential of nature to improve the quality of life

Wageningen Environmental Research
P.O. Box 47
6700 AB Wageningen
The Netherlands
T +31 (0) 317 48 07 00
wur.eu/environmental-research

Report 3151
ISSN 1566-7197

The mission of Wageningen University & Research is "To explore the potential of nature to improve the quality of life". Under the banner Wageningen University & Research, Wageningen University and the specialised research institutes of the Wageningen Research Foundation have joined forces in contributing to finding solutions to important questions in the domain of healthy food and living environment. With its roughly 30 branches, 6,800 employees (6,000 fte) and 12,900 students, Wageningen University & Research is one of the leading organisations in its domain. The unique Wageningen approach lies in its integrated approach to issues and the collaboration between different disciplines.